This Page Is Inserted by IFW Operations
and is not a part of the Official Record

BEST AVAILABLE IMAGES

Defective images within this document are accurate representations of the original documents submitted by the applicant.

Defects in the images may include (but are not limited to):

- BLACK BORDERS
- TEXT CUT OFF AT TOP, BOTTOM OR SIDES
- FADED TEXT
- ILLEGIBLE TEXT
- SKEWED/SLANTED IMAGES
- COLORED PHOTOS
- BLACK OR VERY BLACK AND WHITE DARK PHOTOS
- GRAY SCALE DOCUMENTS

IMAGES ARE BEST AVAILABLE COPY.

As rescanning documents *will not* correct images, please do not report the images to the Problem Image Mailbox.

THIN FILM PROCESSES

Edited by

JOHN L. VOSSEN *WERNER KERN*

RCA Laboratories
David Sarnoff Research Center
Princeton, New Jersey

ACADEMIC PRESS New York San Francisco London 1978

A Subsidiary of Harcourt Brace Jovanovich, Publishers

ACADEMIC PRESS, INC.
111 Fifth Avenue, New York, New York 10003

United Kingdom Edition published by
ACADEMIC PRESS, INC. (LONDON) LTD.
24/28 Oval Road, London NW1 7DX

Library of Congress Cataloging in Publication Data

Main entry under title:

Thin film processes.

Includes bibliographical references.
1. Thin films. I. Vossen, John L. II. Kern, Werner, Date
TK7871.15.F5T43 621.381'73 78-3348
ISBN 0-12-728250-5

PRINTED IN THE UNITED STATES OF AMERICA

80 81 82 9 8 7 6 5 4 3

Contents

List of Contributors

Numbers in parentheses indicate the pages on which the authors' contributions begin.

VLADIMIR S. BAN (257), RCA Laboratories, Princeton, New Jersey 08540

J. J. CUOMO (11), IBM Thomas J. Watson Research Center, Yorktown Heights, New York 10598

CHERYL A. DECKERT (401), RCA Laboratories, Princeton, New Jersey 08540

DAVID B. FRASER (115), Bell Telephone Laboratories, Murray Hill, New Jersey 07974

JAMES M. E. HARPER, (175), IBM Thomas J. Watson Research Center, Yorktown Heights, New York 10598

J. R. HOLLAHAN (335), Applied Materials Incorporated, Santa Clara, California 95051

WERNER KERN (257, 401), RCA Laboratories, Princeton, New Jersey 08540

FREDERICK A. LOWENHEIM (209), 637 West 7th Street, Plainfield, New Jersey 07060

C. M. MELLIAR-SMITH (497), Bell Telephone Laboratories, Murray Hill, New Jersey 07974

C. J. MOGAB (497), Bell Telephone Laboratories, Murray Hill, New Jersey 07974

ALAN S. PENFOLD (75), Telic Corporation, Santa Monica, California 90404

R.S. ROSLER* (335), Applied Materials Incorporated, Santa Clara, California 95051

* Present address: Motorola, Inc., Phoenix, Arizona 85002

II-1

Glow Discharge Sputter Deposition

J. L. VOSSEN

RCA Laboratories
Princeton, New Jersey

J. J. CUOMO

IBM Thomas J. Watson Research Center
Yorktown Heights, New York

ISBN 0-12-728250-5

I. INTRODUCTION

Over the past 20 years or so there have been numerous reviews of sputtering and sputtering processes for film deposition [1–15]. In this chapter we shall take a somewhat different viewpoint than those of most earlier reviewers. We shall attempt to treat this very complex subject from a process viewpoint. That is, we shall discuss the interactions of the process parameters to expose the many permutations and combinations that are available to control the properties of thin films.

Because there are so many interactions among parameters in sputtering systems, it is impossible to separate them completely. Thus, there are necessary, but regrettable references made to later sections throughout the chapter. In an attempt to minimize any confusion that this may cause, we shall give a brief, simple overview of the subject in this section before going to the more detailed discussions.

Figure 1 represents a greatly simplified cross section of a sputtering system. Typically, the target (a plate of the material to be deposited or the material from which a film is to be synthesized) is connected to a negative voltage supply (dc or rf). The substrate holder faces the target. The holder may be grounded, floating, biased, heated, cooled, or some combination of these. A gas is introduced to provide a medium in which a glow discharge can be initiated and maintained. Gas pressures ranging from a few millitorr to about 100 mTorr are used. The most common sputtering gas is argon.

When the glow discharge is started, positive ions strike the target plate and remove mainly neutral target atoms by momentum transfer, and these

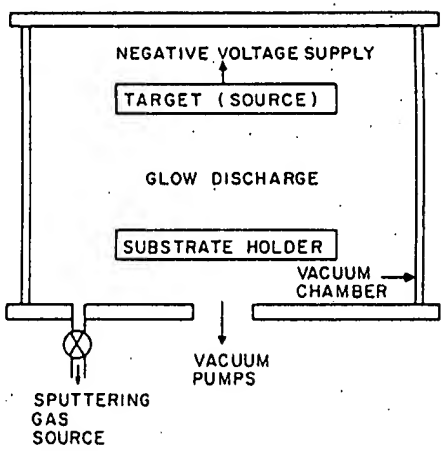

Fig. 1. Simplified cross section of a sputtering system.

condense into thin films. There are, in addition, other particles and radiation produced at the target, all of which may affect film properties (secondary electrons and ions, desorbed gases, x rays, and photons). The electrons and negative ions are accelerated toward the substrate platform and bombard it and the growing film. In some instances, a bias potential (usually negative) is applied to the substrate holder, so that the growing film is subject to positive ion bombardment. This is known variously as *bias sputtering* or *ion plating*. Initially, the term "ion plating" referred to a process in which the deposition source was a thermal evaporation filament instead of a sputtering target and the substrates were connected to a dc sputtering target [16], but it has sometimes been applied to any process in which the substrate is subjected to purposeful ion bombardment during film growth in a glow discharge environment [17].

In some cases, gases or gas mixtures other than Ar are used. Usually this involves some sort of *reactive sputtering* process in which a compound is synthesized by sputtering a metal target (e.g., Ti) in a reactive gas (e.g., O_2 or Ar–O_2 mixtures) to form a compound of the metal and the reactive gas species (e.g., TiO_2). Reactive sputtering is also used to replenish constituents of compound targets lost by dissociation. The reactive version of ion plating is sometimes known as *activated reactive evaporation* [18], but this terminology is more often applied to processes in which an evaporant passes through a glow discharge in transit to an electrically floating or grounded substrate. Reactive sputtering should not be confused with *chemical sputtering* in which the reactive gas (e.g., O_2) reacts with the target surface (e.g., C) to form volatile compounds (e.g.,

CO) that are pumped away [1]. Chemical sputtering is more properly related to ion etching processes (see Chapter V-2).

We shall consider in detail the complex interplay among target kinetics, glow discharge phenomena, substrate conditions, equipment configuration, etc. that bear on the ability to control the properties of thin films.

II. PHYSICAL AND CHEMICAL EFFECTS OF ION BOMBARDMENT ON SURFACES

In sputter deposition, surfaces subject to ion bombardment are usually considered as the source of material from which films are grown. In addition to the neutral (sputtered) material liberated from the bombarded surface which eventually condenses as a film, there are numerous other events that can occur at the target surface which may influence the growth of films profoundly. These include: secondary electron emission, secondary positive and/or negative ion emission, emission of radiation (photons, x rays), reflection of incident particles, heating, chemical dissociation or reaction, bulk diffusion, crystallographic changes, and reflection of some of the emitted particles back to the bombarded surface (backscattering). It should be noted that all of these same phenomena apply to sputter-etching processes (Chapter V-2) in which the workpiece *is* a sputtering target and to *substrates in most glow discharge deposition processes.* (As will be shown later, any material body immersed in a glow discharge acquires a negative potential with respect to its surroundings and must be considered a sputtering target.)

There have been several recent comprehensive reviews of the kinetics involved when a surface is ion bombarded [3, 6, 8, 12]. Therefore, we shall review them only briefly, emphasizing those target effects that can affect the way in which films grow.

A. Emission of Neutral Particles—The Sputtering Yield

The sputtering yield is defined as the number of atoms ejected from a target surface per incident ion. It is the most fundamental parameter of sputtering processes. Yet all of the surface interaction phenomena involved that contribute to the yield of a given surface are not completely understood. Despite this, an impressive body of literature exists showing the yield to be related to momentum transfer from energetic particles to target surface atoms. There is a threshold for sputtering that is approximately equal to the heat of sublimation. In the energy range of practical interest for sputtering processes (10–5000 eV), the yield increases with

incident ion energy, and with the mass and d-shell filling of the incident ion [19, 20].

The sputtering yield determines the erosion rate of sputtering targets; and largely, but not completely, determines the deposition rate of sputtered films. Several compilations of experimental sputtering yield and related data have been published [3, 5, 6, 21, 22]. All sputtering yields and related data should be used with caution. In glow discharge systems, bombarding ions are by no means monoenergetic, and it is not necessarily valid to use yield values for pure metals when alloys, compounds, or mixtures are sputtered. As will be shown, the sputtering yield of material A from a matrix of A + B is often very different from the sputtering yield of A from a matrix of A. Also, when sputtering yields of compounds are given, dissociation reactions are often ignored. Despite this, tabulations of sputtering yields are useful, if only to give a rough indication of the deposition or etch rate that might be expected for a given material. Tables I–III give a compilation of sputtering yields and relative film deposition

Table I

Sputtering Yield of Elements at 500 eV

Gas	He	Ne	Ar	Kr	Xe	Reference
Element						
Be	0.24	0.42	0.51	0.48	0.35	[23]
C	0.07	—	0.12	0.13	0.17	[23]
Al	0.16	0.73	1.05	0.96	0.82	[23]
Si	0.13	0.48	0.50	0.50	0.42	[23]
Ti	0.07	0.43	0.51	0.48	0.43	[23]
V	0.06	0.48	0.65	0.62	0.63	[23]
Cr	0.17	0.99	1.18	1.39	1.55	[23]
Mn	—	—	—	1.39	1.43	[23]
Mn	—	—	1.90	—	—	[24]
Bi	—	—	6.64	—	—	[24]
Fe	0.15	0.88	1.10	1.07	1.00	[23]
Fe	—	0.63	0.84	0.77	0.88	[25]
Co	0.13	0.90	1.22	1.08	1.08	[23]
Ni	0.16	1.10	1.45	1.30	1.22	[23]
Ni	—	0.99	1.33	1.06	1.22	[25]
Cu	0.24	1.80	2.35	2.35	2.05	[23]
Cu	—	1.35	2.0	1.91	1.91	[25]
Cu (111)	—	2.1	—	2.50	3.9	[26]
Cu	—	—	1.2	—	—	[27]
Ge	0.08	0.68	1.1	1.12	1.04	[23]
Y	0.05	0.46	0.68	0.66	0.48	[23]
Zr	0.02	0.38	0.65	0.51	0.58	[23]

Table I (*Continued*)

Gas	He	Ne	Ar	Kr	Xe	Reference
Nb	0.03	0.33	0.60	0.55	0.53	[23]
Mo	0.03	0.48	0.80	0.87	0.87	[23]
Mo	—	0.24	0.64	0.59	0.72	[25]
Ru	—	0.57	1.15	1.27	1.20	[23]
Rh	0.06	0.70	1.30	1.43	1.38	[23]
Pd	0.13	1.15	2.08	2.22	2.23	[23]
Ag	0.20	1.77	3.12	3.27	3.32	[23]
Ag	1.0	1.70	2.4	3.1	—	[27]
Ag	—	—	3.06	—	—	[28]
Sm	0.05	0.69	0.80	1.09	1.28	[23]
Gd	0.03	0.48	0.83	1.12	1.20	[23]
Dy	0.03	0.55	0.88	1.15	1.29	[23]
Er	0.03	0.52	0.77	1.07	1.07	[23]
Hf	0.01	0.32	0.70	0.80	—	[23]
Ta	0.01	0.28	0.57	0.87	0.88	[23]
W	0.01	0.28	0.57	0.91	1.01	[23]
Re	0.01	0.37	0.87	1.25	—	[23]
Os	0.01	0.37	0.87	1.27	1.33	[23]
Ir	0.01	0.43	1.01	1.35	1.56	[23]
Pt	0.03	0.63	1.40	1.82	1.93	[23]
Au	0.07	1.08	2.40	3.06	3.01	[23]
Au	0.10	1.3	2.5	—	7.7	[29]
Pb	1.1	—	2.7	—	—	[27]
Th	0.0	0.28	0.62	0.96	1.05	[23]
U	—	0.45	0.85	1.30	0.81	[23]
Sb	—	—	2.83	—	—	[24]
Sn (solid)	—	—	1.2	—	—	[30]
Sn (liquid)	—	—	1.4	—	—	[30]

rates. The latter have been normalized to the sputtering yields of pure metals [21]. All target materials are polycrystalline unless otherwise indicated.

B. Emission of Other Particles

1. Secondary Electrons

Since sputtering targets are held at high negative potentials, secondary electrons are accelerated away from the target surface with an initial energy equal to the target potential. As will be shown in Section III.A, these electrons help to sustain the glow discharge by ionization of neutral sputtering gas atoms which in turn bombard the target and release more secondary electrons in an avalanche process. Upon arrival at the substrate, such energy as they retain after collisions in the gas is liberated in the form of heat [38–43]. Many of the secondary electrons are thermalized by collisions in the gas, but even at high gas pressures, a substantial number of electrons retain full target potential upon impact at the substrates [41, 42].

Table II

Sputtering Yield of Elements at 1 keV

Gas	He	N	Ne	N_2	Ar	Kr	Xe	Reference
Element								
Fe	—	—	0.85	—	1.33	1.42	1.82	[25]
Fe	—	0.55	—	0.78	—	—	—	[3]
Ni	—	—	1.22	—	2.21	1.76	2.26	[25]
Ni	—	0.74	—	1.05	—	—	—	[3]
Ni	—	—	—	—	2.0	2.0	2.0	[26]
Cu	—	—	1.88	—	2.85	3.42	3.6	[25]
Cu	—	1.5	—	—	—	—	—	[3]
Cu	—	—	—	—	3.2	2.5	—	[27]
Cu (111)	—	—	2.75	—	4.5	4.65	6.05	[26]
Cu	—	—	—	1.95	—	—	—	[31]
Mo	—	—	0.49	—	1.13	1.27	1.60	[25]
Mo	—	0.16	—	0.3	—	—	—	[3]
Ag	1.8	—	2.4	—	3.8	4.7	—	[27]
Sn	—	—	—	—	0.8	—	—	[32]
W	—	0.18	—	0.2	—	—	—	[3]
Au	—	—	—	—	1.0	—	—	[32]
Au	0.3	—	2.1	—	4.9	—	—	[29]
Pb	1.5	—	—	—	3.0	—	—	[27]
Sn (liquid)	—	—	—	—	1.7	—	—	[30]
Au (111)	—	—	—	—	3.7	—	—	[33]
Au (100)	—	—	—	—	3.0	—	—	[33]
Au (110)	—	—	—	—	2.0	—	—	[33]
Au	—	—	—	—	3.6	—	—	[33]
Al (111)	—	—	—	—	1.0	—	—	[33]

2. Secondary Ions

Most of the data on ion emission from solids due to primary ion bombardment is to be found in the literature of secondary ion mass spectroscopy (SIMS). Most of this literature deals with the formation and emission of positive ions. However, in glow discharge sputtering, it is highly

Table III

Miscellaneous Sputtering Yields

Material	Gas	Energy (keV)	Yield	Reference
Fe	Ar	10	1.0	[32]
Cu	Ne	10	3.2	[34, 35]
Cu	Ar	10	6.25	[34, 35]
Cu	Kr	10	8.0	[35]
Cu	Xe	10	10.2	[35]
Ag	Ar	10	10.4	[36]
Ag	Kr	10	14.8	[36]
Ag	Xe	10	15.5	[35, 36]
Au	Ne	10	3.7	[35]
Au	Ar	10	8.5	[32, 35]
Au	Kr	10	14.6	[35]
Au	Xe	10	20.3	[35]
Sn	Ar	10	2.1	[32]
Mg (0001)	Ar	5	3.13	[37]
Mg ($10\bar{1}0$)	Ar	5	2.70	[37]
Mg ($11\bar{2}0$)	Ar	5	1.64	[37]
Zn (0001)	Ar	3	11.22	[37]
Zn (0001)	Ar	4	11.43	[37]
Zn (0001)	Ar	5	12.65	[37]
Zn ($11\bar{2}0$)	Ar	3	9.19	[37]
Zn ($11\bar{2}0$)	Ar	4	10.07	[37]
Zn ($11\bar{2}0$)	Ar	5	9.35	[37]
Zr (0001)	Ar	5	1.12	[37]
Zr ($10\bar{1}0$)	Ar	5	1.56	[37]
Zr ($11\bar{2}0$)	Ar	4	0.74	[37]
Zr ($11\bar{2}0$)	Ar	5	0.64	[37]
Zr ($11\bar{2}0$)	Ar	10	0.65	[37]
Cd (0001)	Ar	4	19.01	[37]
Cd (0001)	Ar	5	21.25	[37]
Cd ($10\bar{1}0$)	Ar	4	15.86	[37]
Cd ($10\bar{1}0$)	Ar	5	17.86	[37]
Cd ($11\bar{2}0$)	Ar	5	13.58	[37]
PbTe (111)	Ar	0.5	1.4	[28]
GaAs (110)	Ar	0.5	0.9	[28]
GaP (111)	Ar	0.5	0.95	[28]
CdS ($10\bar{1}0$)	Ar	0.5	1.12	[28]
SiC (0001)	Ar	0.5	0.41	[28]
InSb	Ar	0.5	0.55	[28]
TaC	Ar	0.6	0.13	[21]
Mo_2C	Ar	0.6	0.15	[21]

improbable that a positive ion generated at the target surface could escape the negative target field, so these are of little interest. Negative ions have been studied by SIMS to a lesser extent [44–53]. Negative ions result mainly from the sputtering of the anionic species of compounds [48–51] and high-electron-affinity constituents of alloys [53a,b]. Virtually no secondary negative ions are produced during inert gas ion bombardment of pure metal surfaces. Negative ions, like electrons, are accelerated away from the target toward the substrates, thus representing another source of substrate bombardment. Experimental evidence [54] shows that these ions actually arrive at the substrates as energetic neutrals, having suffered electron-stripping collisions in transit through the glow discharge.

3. *Reflected Incident Particles*

Some of the primary bombarding particles are reflected from the target surface. The literature of ion scattering spectroscopy (ISS) [55–62] contains most of the pertinent literature related to this effect. These reflected particles are neutralized and reflected as atoms, not ions. The amount of reflection is an inverse function of primary bombarding energy because this effect competes with ion implantation. As low primary energies, reflection fractions as high as 0.4 have been observed [56], whereas at high primary bombarding energies (>1000 eV) typical reflection fractions are of the order of 0.05. These particles represent still another source of substrate bombardment during film growth [43].

4. *Desorption of Gases*

Desorption of gases occurs even for very dense target materials. Initially, adsorbed gas layers on target surfaces are sputtered away, and then, depending on the nature of the target material, chemisorbed gases, occluded gases, and gases generated by decomposition of target compounds are released in that order [63–66]. For adsorbed gases there are marked peaks in the desorption rate at low energies (generally <200 eV) which have been attributed to local heating of the lattice in a radius of the order of 10 Å. Chemisorbed gases are truly sputtered [66]. It is these gases that usually leave the target initially as negative ions as noted above. Occluded gases are both sputtered and thermally desorbed. This is especially a problem with hot-pressed targets [67] and powder targets [68]. The effect of massive gas desorption from porous targets is to contaminate the sputtering gas and, hence, the deposited film. In addition, depending on the nature of the gas, it will have an effect on the film deposition rate (Section VIII.B).

C. Emission of Radiation

In this section, we consider the emission of radiation due to the sputtering process alone at the target surface—not to that contributed by the glow discharge.

1. Photons

Both ultraviolet (UV) and visible radiation are emitted from sputtering targets [69–76]. Sputtered metal and elemental semiconductor atoms leaving the target in an excited or ionized state undergo resonance- and Auger-type electronic transitions with subsequent photon emission characteristic of the metal being sputtered. Electronic transitions do not apply to compounds or glasses. In these cases the radiative process is simply due to the excited species of the sputtered atoms. Only semiquantitative data on this phenomenon have been reported, but the heirarchy of emission proceeds from low to high in the sequence: elemental targets, binary compounds, ternary compounds, etc., glasses. In the context of sputter deposition, this effect is mainly related to radiation damage to surface-sensitive substrates by energetic UV photons. However, it has been used to advantage to monitor sputter deposition and etching rates (Section IV.C).

2. X rays

X rays characteristic of the target material are emitted from the target surface at energies up to that of the primary bombarding ions. These x rays also can damage surface-sensitive substrates. Also energetic secondary electrons originating at the target which arrive at substrates can generate x-rays at the substrate surface. Tables of x-ray energies and excitation potentials [77] can sometimes be used to estimate the degree of damage that may be introduced by this effect.

D. Ion Implantation

Primary bombarding particles can embed into the target surface, become neutralized and trapped. A large body of literature exists on ion-surface interactions particularly those dealing with first-wall problems in fusion reactors. Even at relatively low bombarding energies [78–81] substantial implantation of the primary bombarding ions occurs (Fig. 2). When these ions lose their energy, they contribute to target heating and do not give rise to sputtering.

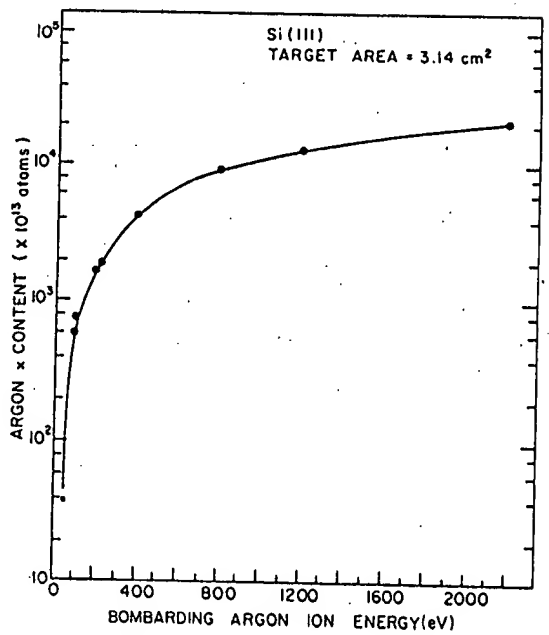

Fig. 2. Argon content of Si versus incident ion energy (after Comas and Carosella [78], with permission of The Electrochemical Society).

E. Altered Surface Layers and Diffusion

1. Multicomponent Targets

The bombardment of a multicomponent solid surface with ions or neutral atoms alters the chemical composition of the surface due to the difference in the sputter yield of the constituents [82]. The region of change is known as the altered layer. Upon initial bombardment of the surface the constituent with highest sputter yield is preferentially removed from the surface, enriching the surface layer in the lower sputter yield material until a steady state is reached. At steady state, the sputtered composition is that of the bulk target composition and the altered layer will recede uniformly with continued sputtering as long as the steady state conditions are maintained. Data on altered layers come from several areas: sputter deposition [83, 84], surface analysis [85, 86], and ion beam alteration of surface properties [86]. Empirical data were generated in attempts to quantify surface analysis techniques [86–91].

2. Yield

The surface composition alteration generally assumes yields of the components as in the elemental form [88], although it is has been shown [87] that some alloys have yields that are greater than those of either element by itself. For example, the yield of Cu from ⟨100⟩ Cu_3Au was found to be higher than from ⟨100⟩ single crystal Cu.

3. Steady State

The thickness of the altered layer has been explored in some detail for a variety of targets [83–85, 92–94]. Estimates for metal alloys have been a few tens of angstroms. For oxides the layer is much thicker (~1000 Å) [94].

4. Diffusion

Diffusion severely affects the altered layer thickness and the time to reach steady state. These can be due to ion-induced diffusion [87, 91, 94, 95], the ion mean range [93, 94], temperature driven surface diffusion [88], and enhanced diffusion due to the surface implantation of sputter-gas species [93, 95]. As noted in the previous section, surface diffusion will be affected by the phases present, grain size, and the nature of the species in the target. The temperature dependence of diffusion of the two phase Ag–Cu system was examined at 80 and 270°C [96]. Forty minutes sputtering time was required to reach steady state for the 80°C target while the 270°C target required about 200 min to reach steady state. In the 270°C experiment the target showed a definite reddish cast, the altered layer thickness was estimated to be about 1 μm, and the films deposited were enriched in Ag. The difference in sputter yield ratios of Ni/Cu of 1.9 at room temperature [88] to that of 1.6 [96] at 300°C was attributed to diffusion in the target at 300°C.

5. Models

There have been numerous phenomenological models for the altered layer [83–85, 92, 93]. Due to the relationship between multicomponent sputter deposition and altered layer formation [96a] these will be considered in the section on multicomponent sputtering.

F. Dissociation Processes

1. Sublimation

Most of the energy of the incident ions at a sputtering target is transferred to the target surface as heat. When one or more of the target constituents is volatile this can lead to sublimation from the target [97–99]. Even though the back surface of the target is directly cooled, substantial thermal gradients can arise with materials of low thermal diffusivity. This effect can lead to stoichiometric differences between the target and the deposited film. For fixed sputtering conditions, it is possible to compensate for this effect by purposely enriching the target in the volatile material [98].

2. Chemical Dissociation

Since most compounds have dissociation energies in the 10–100 eV range, it is not surprising that sputtering with keV ions results in chemical dissociation. Numerous studies in sputter-deposition systems have shown this by indirection [21, 97–104], but there is also a significant body of literature related to electron spectroscopy for chemical analysis (ESCA) that gives direct, quantitative evidence of this effect [105–107]. What is less obvious is the relationship between film stoichiometry and target bombarding potential. For example, in the case of binary oxide targets, films are, in general, less deficient in oxygen if the target potential is high than if it is low [11, 108–110]. This is because higher target potentials sputter more secondary oxygen ions that are accelerated toward the substrate where they can recombine to form the original compound. At low target potentials, these secondary ions have insufficient energy to survive the collisions encountered between the target and the substrate, and are lost to the vacuum pumps. If truly stoichiometric oxides, nitrides, sulfides, etc. are desired in the film, it is virtually always required to add O_2, N_2, H_2S, etc. to the sputtering gas to ensure stoichiometry by reactive sputtering. In some cases, sputtering with 100% reactive gas will still not result in stoichiometric films [100] because it is probable with weakly bonded compounds that reactive gas bombardment of the substrate will lead to preferential sputtering of the reactive gas rather than incorporation of it in a film [102, 106].

G. Chemical Sputtering

Chemical sputtering involves the reaction of an excited neutral or ionized gas with a surface to form volatile compounds [1, 111, 112]. This technique is mainly used for plasma treatment of organic surfaces and for etching in plasmas (Chapter V-2). However, it is sometimes a factor in film deposition [113]. When targets containing reactive anions (e.g., F^-, Cl^-) are sputtered, some of these anions are sputtered as secondary ions and accelerated toward the substrates where chemical etching reactions can occur. Etching of glass substrates, rather than film deposition, has

been observed during "sputter deposition" from targets of TbF_3 and $TbCl_3$ [113].

III. GLOW DISCHARGES

In this section, we give a brief account of glow discharge phenomena relevant to diode sputtering. The treatment of magnetron glow discharges is not included here; (see Chapters II-2–II-4). The effects of these glow discharge phenomena on substrates are described in Section VII.

A. DC Glow Discharges

Figure 3 illustrates the manner in which a glow discharge is formed in a low-pressure gas with a high-impedence dc power supply. When a voltage is first applied, a very small current flows. This is due to the presence of a small number of ions and electrons resulting from a variety of sources (e.g., cosmic radiation). Initially, the current is nearly constant, because all of the charge present is moving. As the voltage is increased, sufficient energy is imparted to the charged particles so that they produce more charged particles by collisions with the electrodes (secondary electron emission) and with neutral gas atoms. As more charge is created the current increases steadily, but the voltage is limited by the output impedence of the power supply. This region is known as the Townsend discharge.

Eventually, an avalanche occurs. Ions strike the cathode, release secondary electrons which form more ions by collision with neutral gas atoms. These ions then return to cathode, produce more electrons that, in turn produce more ions. When the number of electrons generated is just sufficient to produce enough ions to regenerate the same number of electrons, the discharge is self-sustaining. The gas begins to glow, the voltage drops, and the current rises abruptly. At this point, the mode is called the "normal glow." Since the secondary electron emission ratio of most materials is of the order of 0.1, more than one ion must strike a given area of the cathode to produce another secondary electron. The bombardment of the cathode in the normal glow region self-adjusts in area to accomplish this. Initially, the bombardment is not uniform, but is concentrated near the edges of the cathode or at other irregularities on the surface. As more power is supplied, the bombardment increasingly covers the cathode surface until a nearly uniform current density is achieved. (This region of the glow discharge is used for voltage regulator tubes.)

After the bombardment covers the whole cathode surface, further increases in power produce both increased voltage and current density in

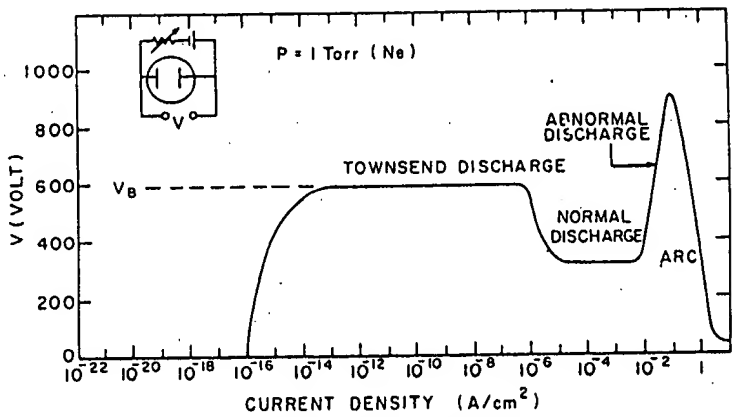

Fig. 3. The formation of a dc glow discharge.

the discharge. This region, the "abnormal glow," is the mode used in sputtering and virtually all other glow discharge processes. If the cathode is not cooled, when the current density reaches about 0.1 A/cm^2, thermionic electrons are emitted in addition to secondary electrons, followed by a further avalanche. The output impedance of the power supply limits the voltage, and the low-voltage high-current arc discharge forms.

The foregoing represents a qualitative description of the various dc discharge modes. Several more quantitative reviews have appeared [114–117].

Crucial to the formation of an abnormal glow is the breakdown voltage V_B (Fig. 3). This voltage is mainly dependent upon the mean-free-path of secondary electrons and the distance between the anode and cathode. Each secondary electron must produce about 10–20 ions for the original avalanche to occur. If the gas pressure is too low or the cathode–anode separation too small, the secondaries cannot undergo a sufficient number of ionizing collisions before they strike the anode. If the pressure and/or separation are too large, ions generated in the gas are slowed by inelastic collisions so that they strike the cathode with insufficient energy to produce secondary electrons. This is a qualitative statement of Paschen's law which relates V_B to the product of gas pressure and electrode separation (Fig. 4). In most sputtering glow discharges, the pressure-separation product is well to the left of the minimum, thus requiring relatively high discharge starting voltages. In close-spaced electrode configurations it is often necessary to increase the gas pressure momentarily to start the discharge. Alternatively, an external ionizing source may be used (e.g., a Tesla coil connected into the chamber by a high-voltage feedthrough).

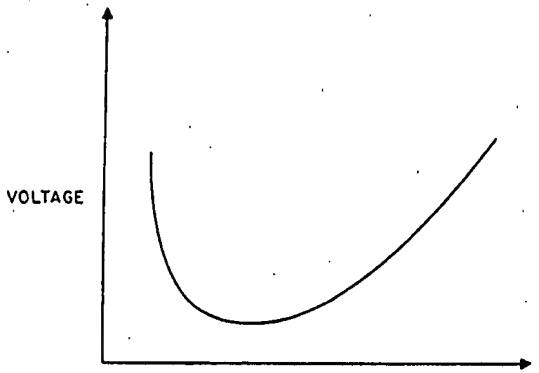

Fig. 4. Paschen's Law.

Figure 5 illustrates the luminous regions of a dc glow discharge, the voltage distribution, and the net space charge as a function of distance from cathode to anode. Adjacent to the cathode, there is a brilliant luminous layer known as the cathode glow. This is the region in which incoming discharge ions and positive ions produced at the cathode are neutralized by a variety of processes. This is also the region in which secondary electrons begin to accelerate away from the cathode. The light emitted is characteristic of both the cathode material and the incident ion.

Secondary electrons are repelled at high velocity from the cathode and start to make collisions with neutral gas atoms at a distance away from the cathode corresponding to their mean free path. This leaves a dark space which is very well defined. Since the electrons rapidly lose their energy by collisions, nearly all of the applied voltage appears across this dark space. The dark space is also the region in which positive ions are accelerated toward the cathode. Since the mobility of ions is very much less than that of electrons, the predominant species in the dark space are ions [118]. Acceleration of secondary electrons from the cathode results in ionizing collisions in the negative glow region.

The Faraday dark space and positive column are nearly field-free regions whose sole function is to connect electrically the negative glow to the anode. They are not at all essential to the operation of a glow discharge. In most sputtering systems, the anode is located in the negative glow and these other regions do not exist. The length of an unobstructed negative glow is exactly equal to the range of electrons that have been accelerated from the cathode [119]. When the negative glow is truncated,

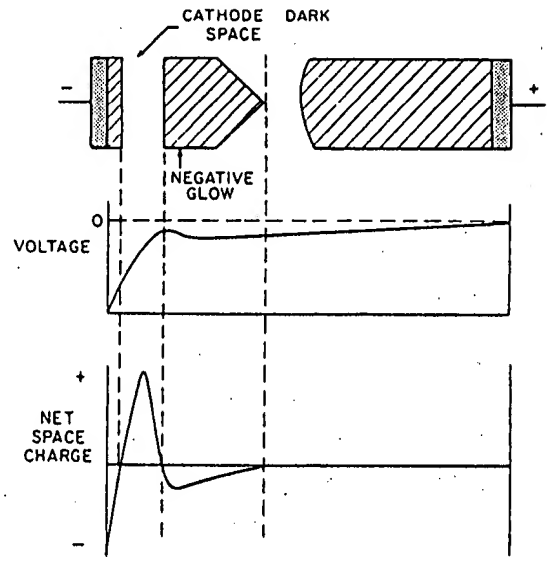

Fig. 5. Luminous regions, voltage and net space charge versus position in a dc glow discharge.

higher voltages must be applied to make up for the ions that would have been generated in the part of it that is blocked by the anode. In general, for uniform cathode bombardment, the anode should be located at least 3–4 times the thickness of the dark space away from the cathode. This distance, of course, is inversely related to gas pressure.

B. Low-Frequency AC Glow Discharges

Low-frequency ac glow discharges are not often used for sputtering. At frequencies up to about 50 kHz, ions are mobile enough so that there is ample time for a complete dc discharge to form on each electrode on each half-cycle. Thus, the discharge is basically the same as a dc discharge, except that both electrodes are alternatively cathode and anode (i.e., both are sputtered).

C. RF Glow Discharges

As the frequency of an applied ac signal is increased above 50 kHz, two important effects occur. First electrons oscillating in the glow space acquire sufficient energy to cause ionizing collisions, thus reducing the

dependence of the discharge on secondary electrons and lowering the breakdown voltage [120]. Second, the electrodes are no longer required to be electrical conductors since rf voltages can be coupled through any kind of impedance. Thus, it is literally possible to sputter anything. However, this does not imply that the films deposited will necessarily resemble the target (Section VII).

At typical rf frequencies used for sputtering (5–30 MHz), most ions are sufficiently immobile that one would expect negligible ion bombardment of the electrodes. In fact this is not the case. If one or both of the electrodes is coupled to the rf generator through a series capacitor, a pulsating, negative voltage will be developed on the electrode [121]. Owing to the difference in mobility between electrons and ions, the I–V characteristics of a glow discharge resemble those of a leaky rectifier (Fig. 6). Upon application of an rf voltage through the capacitor, a high initial electron current flows to the electrode. On the second half of the cycle, only a relatively small ion current can flow. Since no charge can be transferred *through* the capacitor, the voltage on the electrode surface must self-bias negatively until the net current (averaged over each cycle) is zero. This results in the pulsating negative potential shown in Fig. 6 [122]. The average dc value of this potential (V_s) is nearly equal to the peak voltage applied [123].

To obtain sputtering from only one electrode in an rf system, it has been shown [120] that the electrode which is to be the sputtering target must be an insulator or must be capacitively coupled to the rf generator and that the area of that electrode must be small compared to that of the directly coupled electrode. Also the ratio of the voltage between the glow space and the small capacitively coupled electrode (V_c) to the voltage between the glow space and the large directly coupled electrode (V_d) is

$$V_c/V_d = (A_d/A_c)^4, \tag{1}$$

where A_d and A_c are the areas of the directly and capacitively coupled electrodes, respectively. In practice, the directly coupled electrode is the system ground, including baseplates, walls, etc., and is quite large with respect to A_c. Thus, the average sheath potential (V_s) varies between the target electrode and ground as shown in Fig. 7. Clearly, to minimize bombardment of grounded fixtures, the area of all grounded parts should be very large by comparison to that of the target. We shall expand on this point further in Section VII.A.

Recently, Logan *et al.* [124] have described a total model for an rf sputtering system in which externally measured parameters can be put into a computer program to predict ionization levels, sputtering, material transport, and other bombardment effects in the system.

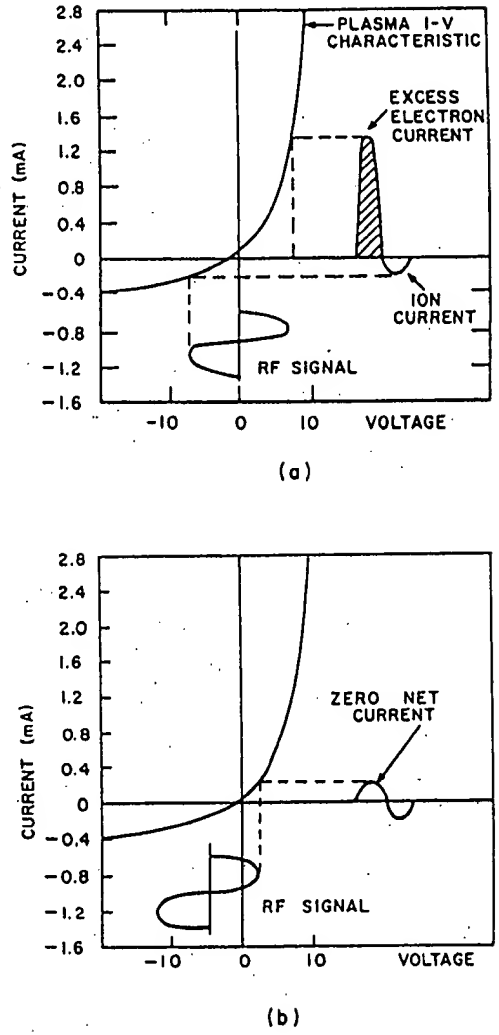

Fig. 6. The formation of a pulsating negative sheath on a capacitively coupled surface in an rf glow discharge (after Butler and Kino [121]).

D. Discharge Supporting Modes

Glow discharges are relatively inefficient ion sources. Only a few percent of the gas atoms in a glow discharge are ionized. Several techniques have been developed for increasing the ionization efficiency somewhat.

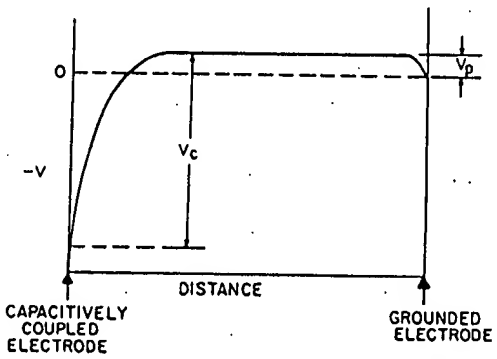

Fig. 7. Distribution of voltage in an rf glow discharge from a small, capacitively coupled electrode (target) to a large, directly coupled electrode.

These include axial and transverse magnetic fields, thermionic additions of electrons, and rf coils. The transverse magnetic field devices are described in Chapters II-2–II-4.

1. Axial Magnetic Field

A magnetic field normal to the target surface constrains secondary electrons to follow a helical, rather than straight-line path, the radius of which is given by

$$r = (mv \sin \theta)/eB, \tag{2}$$

where m is the electron mass, v the velocity, θ the angle of emission, e the electron charge, and B the magnetic flux density. The effect is to give electrons a longer path length for a fixed mean free path, thus increasing the probability of ionizing collisions before the electron reaches the anode. The magnetic field pinches the discharge in toward the center of the target, resulting in nonuniformity of film thickness. For relatively small targets (<20-cm diameter) the judicious use of low magnetic fields (10–50 G) can be used to improve uniformity by compensating for excessive edge bombardment (Section VII.F). For targets >20 cm in diameter, axial magnetic fields should be avoided.

2. Thermionic Support (Triode Sputtering)

In this technique, ions are generated in a low-voltage (~50 V), high-current (5–20 A) arc discharge between a thermionic filament and a main anode. The sputtering target is located in this main discharge and ions are extracted from it toward the target which can be powered either by a dc or

capacitively coupled rf source. This technique produces a very high ion density, allows operation at much lower pressures than a two-terminal glow discharge, and allows control of the target current density independent of the target voltage. However, it is not necessarily good practice to operate a sputtering system at low gas pressures (Section VI.A). The use of triode sputtering is mainly advantageous for sputter etching (Chapter V-2).

The main limitation of this technique is that it is difficult to scale up to very large sizes because of the difficulties involved in producing a large, uniform thermionic arc discharge. Numerous configurations have been described in the literature [125–132] and a complete analysis of such systems has been published by Tisone and co-workers [133–137].

3. RF Coil

Radio-frequency coils are sometimes employed in ion plating systems to increase the ionization efficiency at low gas pressure [138]. The evaporant passes through the coil in transit to substrates attached to a dc sputtering target. This increases the level of ionization of both the evaporant and the sputtering gas.

IV. EQUIPMENT CONFIGURATION

A. Target Assemblies

Electrodes to which the target material is attached and the counter electrodes to which substrates are attached have been designed in a variety of configurations [5, 9, 10, 16, 39, 97, 139–141]. For bias sputtering and ion plating, the counter electrode is a sputtering target assembly similar to the type used as deposition sources. There are four essential considerations in the design of target assemblies: heat dissipation, electrical isolation and contact, ground shielding, and materials of construction. A versatile assembly suitable for research is shown in Fig. 8. Several multitarget arrangements have been described which are useful in sequential deposition of several materials (see, e.g., Cambey [141]).

1. Heat Dissipation

It is estimated [8, 9] that 1% of the energy incident on a target surface goes into ejection of sputtered particles, 75% into heating of the target, and the remainder is dissipated by secondary electrons that bombard and heat the substrates. The heat generated is usually removed by water cool-

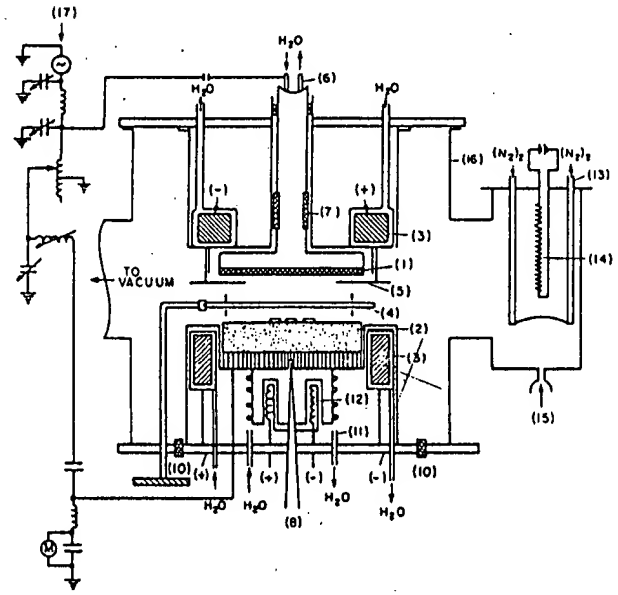

Fig. 8. Schematic of an rf sputtering apparatus. The components are listed as follows: (1) cathode target, (2) anode substrate holder, (3) cathode and anode magnets (water cooled), (4) shutter (SS), (5) cathode shield (SS), (6) cathode water cooling, (7) cathode isolation insulator, (8) substrate thermocouple, (9) substrates, (10) anode isolation insulator, (11) substrate cooling, (12) substrate heating, (13) liquid nitrogen cooled SS shroud, (14) Ti sublimation filaments, (15) sputter gas, (16) SS vacuum chamber, and (17) rf power supply matching network and substrate bias supply.

ing the backing plates to which the target or substrates are attached. Since targets are often soldered or epoxy bonded to the backing plates, the water-cooling channels should be designed so that water is forced through convolutions machined in the material. In this way, no hot spots can develop.

Substrates merely resting on a water-cooled plate are not in good thermal contact, and will be heated almost as much as if the plate were not cooled at all. In cases where substrate heating must be minimized, the substrates must be bonded to the cooled plate (Section IV.D) [142].

2. *Electrical Isolation and Contacts*

Isolation of the target assembly from grounded parts of the system usually involves a ceramic-to-metal seal with a sufficiently thick ceramic to minimize capacitive losses. Water lines must be isolated from ground by putting several meters of insulating tubing in series with both inlet and outlet connections. Electrical connection from the power supply or matching network is made conveniently by bolting a strap to the water line on the back of the target assembly.

3. *Ground Shields*

To prevent sputtering of the target assembly itself, a ground shield is contoured around all surfaces at a distance less than that of the cathode dark space. In some cases, shields are placed over the outer rim of the target surface (e.g., to prevent clamping screws from sputtering). In these cases, focusing effects near the ground shield result in excessive erosion of the target [9].

4. *Materials of Construction*

Many materials have been used to construct sputtering target assemblies, the most common being stainless steel and copper. Stainless steel is highly corrosion resistant, but has very poor thermal conductivity. Copper usually must be gold plated for corrosion protection and is difficult to machine, but it is a good choice. Aluminum, unless it is perfectly protected from corrosion in the presence of water, is a very poor choice.

B. Power Supplies

1. *DC*

There are many requirements imposed on power supplies used for glow discharge sputtering. The output rating is determined by the size of the target and should be capable of delivering up to 10 W/cm² at voltages up to about 5 kV. (Note that this does not apply to magnetron sputtering which generally requires higher output power and current but lower voltage. See Chapters II-2, II-3, and II-5.) The actual power drawn from the supply depends on the process operating parameters (voltage, gas, and gas pressure) and on the secondary electron yield of the target surface. For most metals, the secondary electron yield is initially high and then decreases as surface oxides and other contaminants are sputtered away. Insulating surface contaminants give rise to arcing due to local dielectric breakdown. The power supply must be capable of withstanding these arcs without shutting down, but must be able to distinguish between these small arcs and catastrophic ones such as may happen if a flake of metal shorts the target to ground.

For relatively small targets (up to about 300 cm²), the most commonly used type of dc supply involves an autotransformer-controlled high-volt-

age transformer that is magnetically shunted followed by a full-wave bridge rectifier. No smoothing filters are employed, but rf chokes should be used in series with the output to prevent high-frequency spikes (due to arcing) from damaging the bridge rectifier. Magnetic shunting of the power transformer leads to a high output impedance. In the event of a serious arc, the short circuit output current is limited by circulating the current in the transformer and the output voltage drops to zero [143]. This type of supply is limited in that the maximum usable voltage decreases rapidly as the rated output current is approached (Fig. 9).

For larger targets, saturable reactor power supplies are preferred because these are tolerant of arcs, even when operated with very high output currents [143]. They are, however, unstable when the output load is small (Fig. 10).

2. *Low-Frequency AC*

Power line frequencies are generally used only in processes in which both sides of a substrate are to be coated simultaneously by two targets facing each other. The power supply problems are basically the same as those with dc, except that no rectifiers are used and it is not necessary to use rf chokes in the output circuit.

3. *RF (Crystal Controlled)*

Most rf generators used for sputtering are crystal controlled to one of the "Industrial, Scientific, and Medical Equipment" (ISM) frequencies allotted by international agreement for unlimited radiation [144]. The frequencies and their tolerances most often used are 13.56 ± 0.00678, 27.12 ± 0.0160, and 40.68 ± 0.020 MHz.

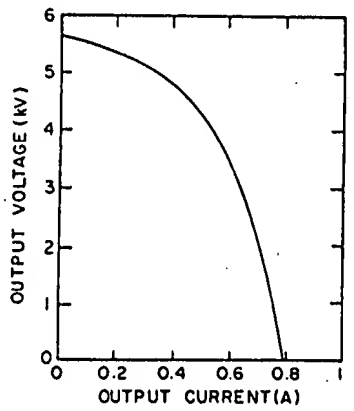

Fig. 9. Typical maximum output voltage and current for a magnetically shunted dc power supply rated at 2 kW.

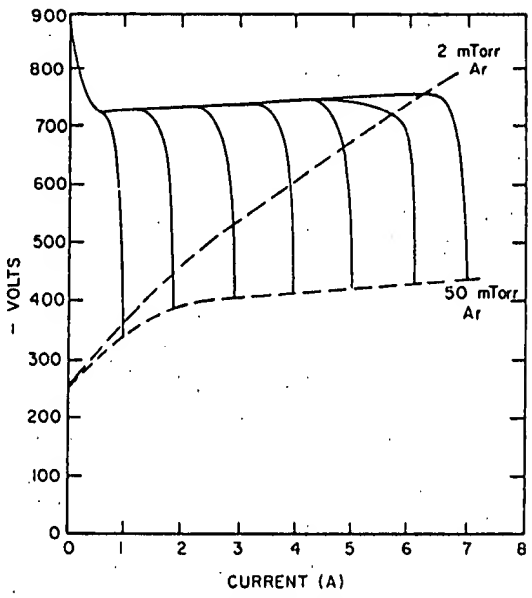

Fig. 10. Typical operating characteristics of a saturable-reactor dc power supply.

Since the output impedance of these generators must be held constant (usually 50 Ω), and since the glow discharge impedance is much higher than this, a matching network must be situated physically close to the target assembly. A typical matching network for a single-ended sputtering system includes a variable-shunt capacitor, a variable-series capacitor, and a fixed inductor. The design of such matching networks are the same as for antenna matching to transmitters [145]. When bias sputtering is contemplated, the situation is more complex. Several manual and automatic circuits have been described for splitting the rf power from a single supply to control voltages and phase at two interacting targets in the same glow discharge [124, 146–151]. In some cases, the substrate target is directly driven, while in others substrate power is coupled through the discharge either by substrate tuning (i.e., inserting a matching network between the substrate target and ground) or by adjusting the system geometry and glow discharge to produce a high plasma potential (Section VII.A).

To prevent damage to the power supply (e.g., during an arc), the

power output tubes should be triodes rather than pentodes or tetrodes so that reflected power appears on the plate rather than the grids of the tubes.

4. RF (Self-Excited)

While crystal-controlled rf generators are most commonly used, variable-frequency, self-excited oscillators have advantages in some applications and have been used extensively [97, 152–157]. For output power up to about 1.5 kW, the usual circuit is a Hartley class-C oscillator. For higher power and/or for bias sputtering, in which the rf power must be split between the deposition and substrate targets, push–pull circuits are preferred. The output circuit is usually transformer coupled, and tuning is accomplished by varying the frequency with a capacitor across the primary of the transformer. If the output circuit is slightly over-critically coupled, one observes a very broad, flat-topped tuning peak as compared to the very high-Q output of crystal-controlled oscillators [157]. As a result of this, these generators are much more tolerant of arcs and other disturbances in the glow discharge. For bias sputtering, the secondary of the transformer is center tapped to ground and a series capacitor is inserted in both target legs. These capacitors act as voltage dividers and can vary the two target voltages independently and in a very smooth fashion. The major disadvantage of self-excited oscillators relates to the fact that their output impedance is quite high. Thus, flexible coaxial cables cannot be used to make electrical connection. Instead the generator must be physically close to the target(s) and connections must be made using rigid, air-dielectric coaxial pipes or some other kind of high-impedance connection, which often complicates the mechanical design of the system. As with all kinds of rf equipment, precautions such as shielding, power line filters, etc. should be taken to minimize radio frequency interference.

C. Instrumentation and Control

Depending on the application, one must be able to monitor voltage, current (dc), power (rf), and sputtering gas pressure. In rf glow discharges it is often useful to measure both the average dc self-bias voltage, the peak-to-peak voltage, the waveform, and the phase angle. Pressure measurements can be especially difficult. Thermocouple, Pirani, and high-pressure ion gauges can sometimes be used, but they are easily contaminated by reactive gases (leading to erroneous readings and drift), are not tolerant of rf fields if the output impedance of the sensing head is high, and are difficult to use when gas mixtures are employed (e.g., in reactive sputtering). The most suitable gauges for critical work are low-impedance capacitance manometers with temperature-controlled heads [158]. The membranes in these gauge heads suffer from mechanical hysteresis if they must be cycled from atmosphere to vacuum frequently, so it is advisable to include a shutoff valve between the head and the vacuum chamber to keep them under vacuum at all times.

Many processes are affected by gas flow throughput, which determines how fast impurities are flushed out of the system. In such cases, mass-flow meters should be included in the gas feed supply.

Langmuir probes are especially helpful in calibrating a system to determine plasma and floating potentials (Section VII.A), but they perturb and contaminate the discharge [159] so they should not be used for *in situ* monitoring.

Temperature measurements of anything in a vacuum system are difficult at best. If properly attached and of sufficiently low thermal mass, thermocouples or thermisters can be used [160], but they can also contaminate the system, and the pyrometer or potentiometer must be isolated from ground. Infrared pyrometers are quite useful [161]. Their main advantage is that no material must contact the substrates. However, they must be carefully calibrated for optical losses in the light path (windows, etc.), infrared emission from the glow discharge, and the emissivity of the coated and uncoated substrate surface.

If a given sputtering process is stable and relatively slow, deposition rates can be monitored by controlling conditions and deposition time. In-vacuum monitors (e.g., quartz microbalance) simply do not work because resputtering processes are different on the head than on substrates. Also, they are intolerant of rf fields (high impedance). The most successful techniques for rate monitoring have been optical emission and absorption spectroscopies [162–168], but they must be independently calibrated. These same spectroscopies along with mass spectroscopy are also useful for diagnosing glow discharge species of all kinds (ions, neutrals, molecular fragments, etc.) [169–181]. These techniques are especially useful in reactive sputtering.

D. Substrate Heaters

Given the fact that there is heat input to substrates from the glow discharge, control of substrate temperatures above ambient can be quite difficult. Both resistance (Fig. 8) and radiant heating (Fig. 11) have been used. The resistance heater is relatively massive and has a relatively slow thermal response time. The radiant heater can be used either to heat substrates in the holder shown directly or to heat a solid plate which has a

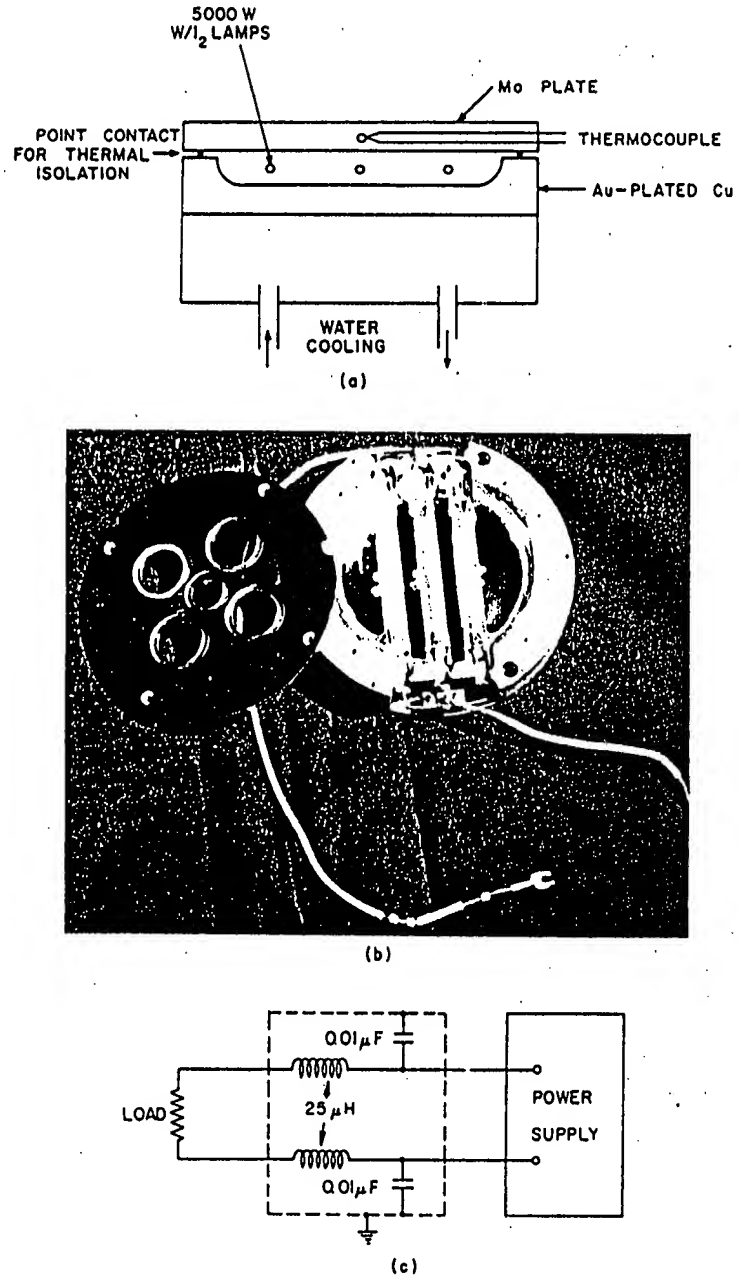

Fig. 11. Radiant substrate heater. (a) Cross section, (b) photograph, (c) rf decoupling network (courtesy of Silano and Leary [142]).

thermocouple embedded in it. Because of its machinability, high-thermal conductivity and resistance to warping, molybdenum is the preferred material of construction for the heated surface (plate or substrate holder). When rf is used, a decoupling network must be employed to prevent rf interference with the thermocouple controls and heat-input circuits (Fig. 11c).

As with substrate cooling, it is essential to make a good thermal contact between the substrate and heated holder. Ga or In–Ga eutectic can be used up to about 450°C if the substrate holder is made of molybdenum. At higher temperatures there are reactions of Ga or In–Ga with Mo. The Ga or In–Ga is best used at a temperature at which it is molten. Upon solidification the thermal mismatch between it, the substrate and substrate holder sometimes can crack the substrate or break the bond. For lower temperatures a thermally conductive grease has been employed which is a mixture of alumina powder and high vacuum grease [142].

E. Wall Losses

"Wall losses" is a generic term for any material body in a glow discharge which can act as a point of neutralization for ions. Ions cannot be neutralized in the gas phase because there is no mechanism which can dissipate the heat of the neutralization to conserve both momentum and energy. This can only happen at a surface. Thus, to obtain a uniform ion density across a target surface, all extraneous solid objects (e.g., vacuum chamber walls, support posts, etc.) should be kept well away from the target edges. How far away is far enough depends inversely upon the glow discharge gas pressure. For typical gas pressures (5–50 mTorr) a safe distance is about 10 cm.

F. Shields and Shutters

Dark-space shields around targets and shutters used for preconditioning targets and/or substrates are necessary objects which must be near the target. To minimize their effect on ion neutralization, they should be made as symmetric as possible with respect to the target. As will be shown in Section V.D, the materials from which shields and shutters are constructed are also important to avoid contamination of targets and/or films.

G. Deposition Sources for Bias Sputtering and Ion Plating

Bias sputtering or ion plating are film deposition processes in which substrates are ion bombarded (sputter etched) prior to and/or during dep-

osition from a vapor source. Thus, the substrate holder is a sputtering target assembly which is usually the same type of assembly as a deposition target. However, depending upon the vapor source used, modifications to the substrate target assembly may be required. Vapor sources that can be used include dc or rf sputtering targets, magnetron sputtering targets of all types, resistance-heated filament, rf-heated or electron-beam evaporation sources, or gaseous reagents of the type normally used for chemical vapor deposition. Problems arise mainly with those vapor sources that require that the substrate target be up and the vapor source down in the system. When the reverse is true, the substrates merely rest on an appropriate backing plate, but if the substrates have to be supported against gravity, the substrate holders become a major problem because of contamination (Section V.D), and the nonuniform bombardment that occurs near sharp edges due to fringing fields. This is mainly a problem with thermal evaporation vapor sources in which the molten evaporant must be contained (as, e.g., in the hearth of an electron beam gun). Numerous inverted target assemblies for holding various kinds of substrates have been reported [182–187], all of which probably suffer from these problems to some extent.

H. Scale-Up Problems

Scaling up any deposition process from small laboratory equipment to large production is a very major problem. There are several examples in the literature [188–198a] of laboratory to production scale ups that range from larger bell jars to very large continuous machines. It is almost axiomatic to state that each production application must be treated as a special case, so it would be futile to present a detailed discussion of such systems here.

Most of the problems with large systems arise if they are not designed around the process. That is, if the deposition process is subordinated to a mechanical design, pumping considerations, etc., the process inevitably suffers. The major process-related factor in large sputtering systems is sputtering gas uniformity across large target surfaces to maintain uniform levels of target ion bombardment. Because of implantation of gases into the target and, in some cases, getting of sputtering gas by the target and/or growing films (e.g., in reactive sputtering), sputtering systems must be considered as vacuum pumps. In general, the sputtering gas must be introduced in several locations, and the main vacuum pumps must be located sufficiently far from the active sputtering region that uniform gas flow across large target surfaces is achieved. Particular attention must also be paid to other effects described earlier (wall losses, target shielding, etc.). Systems intended for long operation between cleaning of fixtures must be carefully designed to assure that buildup of film material on system parts will not result in short circuits, arcs (due to flaking material), or jamming of moving parts (e.g., substrate carriers).

It is especially helpful if sputtering targets can be built into one of the walls of vacuum chamber, so that electrical and water-cooling connections can be made at atmospheric pressure. Otherwise one must face the formidable task of ensuring that high-voltage leads and water lines inside the vacuum chamber do not become part of the glow discharge.

V. PRECONDITIONING OF TARGETS, SUBSTRATES, AND SYSTEMS FOR FILM DEPOSITION

As a general rule, the best way to prepare a system for sputter deposition is to run the system first without substrates in exactly the way in which it will be run during the deposition. A preconditioning run of this sort may have one or more of several beneficial effects: (1) the target altered surface layer is established, (2) fixtures are outgassed by bombardment, and (3) fixtures are coated with the material to be deposited, minimizing subsequent contamination.

A. Target Materials

While it is possible to use virtually any kind of material as a sputtering target, for high purity work very dense targets are preferred. Sputtering can and has been done successfully from sintered, hot-pressed, powder, and liquid targets, but the highest purity work has been done with very dense targets (e.g., vacuum-cast or arc-melted materials). Hot-pressed and powder targets have been shown to be nearly limitless sources of gaseous contamination [67]. The major contaminant appears to be oxygen sorbed onto the raw powder surface prior to hot pressing. For oxides this is not a problem, but it can be severe for other materials depending upon the intended application and the tolerance of the desired film properties to oxygen contamination. Even getter sputtering cannot eliminate gaseous contaminants from films if they originate in the target because a large fraction of the contaminant is sputtered as negative ions, accelerated toward the substrate, and implanted in the growing film.

Targets are usually bonded to some kind of water-cooled backing plate. Target bonding must be done with great care to avoid contamination from the bonding material and/or failure of the bond due to nonuniformity and thermal fatigue. In general, epoxy bonds are not recom-

mended because of their poor thermal transfer properties and brittleness. Epoxy bonds usually lead to large amounts of organic contamination. Solder bonds with appropriate plating layers on the back of the target and the front of the backing plate are generally preferred [199].

B. Presputtering of Targets

Presputtering of targets is done to clean and equilibrate target surfaces prior to film deposition with a shutter usually located close to the substrates. For pure metal targets surface oxides are removed, the target surface is brought to thermal equilibrium, and the system is outgassed. The discharge current can be used as a monitor to determine when the system is equilibrated [200]. Initially, oxides with high secondary electron emission ratio are sputtered and background gaseous contaminants (especially H_2O) are being broken down, leading to high discharge current which gradually decreases as the contaminants are removed from the system and/or covered up with film material. When the discharge current falls to a constant value, presputtering can be terminated. Alternatively, glow discharge optical spectroscopy or mass spectroscopy can be used to determine the endpoint (Section IV.C).

When alloy or compound targets are used, one must establish the altered surface layer in addition to the phenomena noted above. The amount of time needed for this must be established empirically. Since there will be inevitably some resputtering of material deposited onto the shutter and subsequent return of some of this material to the target, the shutter must be kept at the same potential as that which the substrate will have when the shutter is removed. This means that shutters should not be grounded, and in some cases they should be biased. If this is not done, there will be a transient in resputtering as the shutter is removed which can change the composition of the first few monolayers of the film [83]. In general, all discharge conditions (voltages, pressure, etc.) should be the same as those used during the subsequent deposition.

C. Sputter Etching of Substrates

Practical methods for cleaning substrates prior to film deposition have been reviewed by Mattox [201, 202]. In this section, we shall restrict our discussion to sputter etching of substrates prior to film deposition, and assume that gross surface contaminants have been removed chemically or otherwise prior to putting the substrates into the vacuum chamber. If it is not done properly, sputter etching can actually produce more surface contamination than was originally present on the substrate.

With glow discharge sputter etching, it is rarely possible to obtain an atomically clean substrate surface. In general, this is only possible in an ultrahigh vacuum system using ion beams followed by high-temperature annealing [203–208].

The first problem in glow discharge sputter etching relates to organic contamination. This may be on the surface as it is put into the vacuum chamber or may be adsorbed into the surface (e.g., from backstreaming vacuum pump fluids). In either case inert gas ion bombardment will polymerize the organic material [209] and render it very difficult to remove [21].

In most cases organic contaminants can be removed by chemical sputtering in O_2 [111, 112, 210]. Clearly, this will not be adequate if there is continuous backstreaming of pump fluids. If the contaminant is a silicone, this will leave a residue of SiO_2. If the substrate is a metal, the O_2 discharge may oxidize the surface [211]. In both cases, a subsequent sputter-etch step in Ar can be used to remove these oxides.

The next problem that must be addressed is backscattering of material emitted from the target surface [11, 21, 200, 212–219]. When the substrate surface is heterogeneous (e.g., an integrated circuit consisting of Si and SiO_2 areas) and/or when the substrate rests upon a target backing plate of a material that is different from that of the substrate, some fraction of all the materials sputtered are returned to the target, forming a new composite surface consisting of all the bombarded materials. Some of the material is returned by simple collisions in the gas phase, and some is returned by being resputtered from the shutter after condensing there. The latter can be largely eliminated by using a "catcher" [213] such as that shown in Fig. 12. The former can only be minimized, but not eliminated in glow discharge sputtering [212]. The amount of material returned to the target and substrates is directly proportional to the sputtering gas pressure and the axial magnetic field applied (if any), and inversely proportional to the target voltage and to the sputtering yield of the materials involved [11, 212, 219]. Even at the lowest gas pressures at which a glow

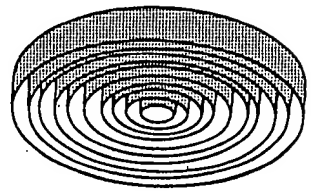

Fig. 12. Catcher (after Maissel *et al.* [213]; copyright 1972 by International Business Machines Corporation, reprinted with permission).

discharge can operate, monolayer quantities of backscattered material are found. Radio-frequency target excitation is much more efficient in minimizing backscattering than is dc, but sputter-etch voltages of 2 kV or more must be used [200, 219]. Reactive gases similar to those used for plasma etching, reactive ion etching, etc. have been shown to produce exceptionally clean substrate surfaces, even at relatively high gas pressures and low rf voltages [220]. For example, various refractory alloys have been cleaned successfully in Ar–HCl mixtures, but cleaning in Ar–CCl_4 resulted in C deposits on the substrates. With the Ar–HCl mixtures there may have been some Cl residue remaining after etching.

In some cases, it is desirable to enhance this effect to preform an interface during sputter etching prior to film deposition. For example, ohmic contacts to Si devices have been improved by sputter etching the Si substrate with a Pt backing plate to produce PtSi in the contact regions [221]. This effect has also been used to advantage in forming graded interfacial layers to promote adhesion of the subsequently deposited film [222]. It should be noted, however, that graded interfaces are sometimes detrimental to adhesion [223]. When it is desirable to eliminate this effect, it is necessary to use backing plates made of the same material as the substrate [212]. In the case of oxide dielectric substrates, it has been shown [224] that even this approach is not effective. Sodium ions (a typical contaminant) were found to migrate down from glass and SiO_2 surfaces rather than be sputter etched away. Similar effects have been observed in other systems [225].

The structure and chemistry of single crystal Si surfaces after backscattering have been studied in detail using a variety of surface analytic techniques [214, 226, 227]. In addition to backscattered material, significant amounts of Ar were found in the substrate surfaces (2–20 at. %, depending on the bombardment potential), and crystallographic damage was propagated to a depth of 40–110 Å as the sputter-etch voltage increased from 0.5–2.5 kV. The amounts of damage produced and gas incorporated increase with increasing substrate temperature [227].

In some cases, conelike features have been observed on sputter-etched surfaces subject to backscattering [11, 111, 218], or when the substrates contain certain bulk contaminants [228]. An example is shown in Fig. 13. This effect is due to the fact that the sputtering yield of the backscattered metal or other contaminant is lower than that of the substrate or matrix. Thus, the islands of backscattered material or contaminant, act as local etch masks. Once such structures are formed, the sputter-etch rate of the surface drops markedly for geometric reasons [11, 111, 229]. In selected cases, it is possible to add reactive gases that depress the backscattering rate to reduce this effect [218]. The cones continue to sharpen as sputter etching proceeds [230–246]. It should also be noted that such cones can form due to initial microtopography of a substrate surface in the absence of impurities [230–246]. Structures of this sort are not always undesirable (e.g., similar structures prepared by CVD have been used as solar absorbers) [247, 248]. Still another effect occurs if the substrates are nonplanar. Since the angular distribution of material emitted from sputtered surfaces at low voltage is under cosine (i.e., there is more sidewise than normal emission), some of the sputtered material will be deposited on substrate irregularities, and become more difficult to remove from these surfaces as the irregularity becomes more vertical. While this is considered a nuisance when clean surfaces are the desired result [217, 249–251], this effect been put to beneficial use in the coating of the inside walls of through holes in substrates [252], and in enabling one to cover severe substrate topographic features by bias sputtering.

In general, all of these effects and their implications to film–substrate interfaces must be considered carefully in the design of a process involving sputter etching prior to film deposition.

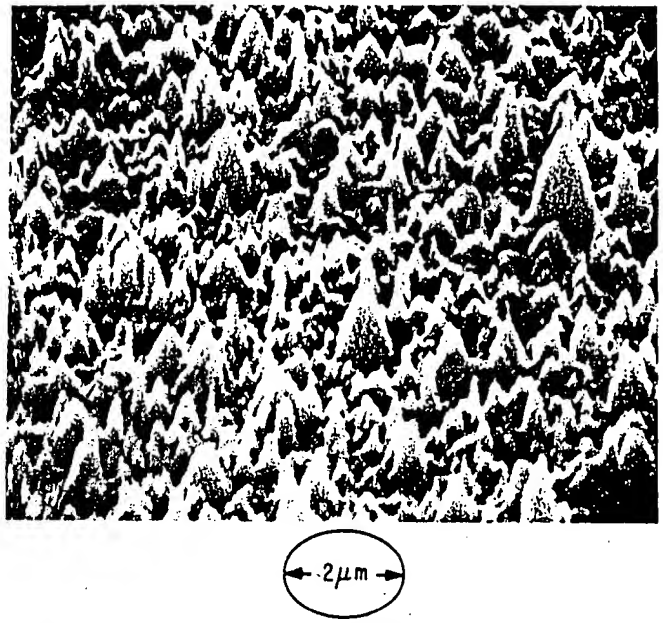

Fig. 13. Cones produced on a Si surface sputtered in contact with a Pd backing plate.

VI. THE SPUTTERING GAS

A. Effects f Gas Species, Pressure, and Flow

The effects of increasing sputtering gas pressure are to increase discharge current, increase backscattering, and to slow energetic particles by inelastic collisions. The first two effects compete and largely determine deposition rates (Section VIII.B). The third effect can be used to maximize or minimize the energy of particles incident on substrates.

In general, it is desirable to use the highest possible gas flow so that impurities are constantly swept out of the sputtering chamber. Numerous workers have found that this improves the properties of thin films (e.g., Fraser and Cook [253]). This implies that the pumping system used must be operated to obtain maximum pumping speed for the gases used.

One must also be careful to ensure that no pressure gradients occur in the vicinity of the sputtering targets. Otherwise such gradients produce nonuniform bombardment and film deposition. Local pressure gradients can occur at the target surface (because of gettering), near the pumping port, or at points of high or low temperature relative to the rest of the system (e.g., near vacuum gauges with hot elements, titanium sublimation pumps, or Meissner traps). To offset these problems it is often necessary to introduce the gas at more than one point in the system. This is especially a problem in reactive sputtering and in very large systems.

As noted in Section II.A, the nature of the sputtering gas largely determines the sputtering yield, and hence, the deposition rate. In addition to that, excited metastable neutrals of the sputtering gas are formed by collisions of electrons with ground-state gas atoms. The potentials required to raise some common sputtering gases from the ground state to the lowest excited state along with the lifetimes of the excited states are given in Table IV [254, 255]. It is well established [172] that sputtered neutral atoms can be ionized by the Penning mechanism (the collision of a metastable neutral with a ground-state neutral to produce an ion and return the metastable neutral to the ground state) when the first ionization potential of the sputtered atom is less than that of the metastable energy. Since the metastable energies of the noble gases are greater than the first ionization potential of most elements, this mechanism can produce a copious supply of ions which can bombard substrate surfaces and/or return to the target to cause self sputtering [212]. It is possible that some sputtered atoms can be doubly ionized by this process [256]. The amount of Penning ionization that occurs increases with increasing gas pressure.

Table IV

Metastable Neutral Energies and Lifetimes

Species	Metastable energy (eV)	Lifetime (sec)
H	10.20	0.12
H_2	11.86	Long
He	19.82	Very long
He	20.61	Long
N	2.38	6×10^1
N	3.58	13
N_2	6.16	0.9
N_2	8.54	1.7×10^{-4}
O	1.97	110
O	4.17	0.78
O_2	0.98	Very long
Ne	16.62, 16.71	Long
Ar	11.55, 11.72	Long
Kr	9.91, 9.99	—
Xe	8.31, 8.44	—

B. Sources of Gas Contamination

The major sources of gaseous impurities in sputtering systems are residual gases (mainly H_2O) left after initial pumpout, wall desorption due to bombardment, the surface of the target (gases adsorbed when the system is vented), occluded gases in the sputtering target, backstreaming of pump fluids, leaks (real or virtual), and impurities in the gas supply itself. Many of these can be eliminated by a combination of good vacuum practice and extensive presputtering before film deposition. For example, to minimize condensation onto the target surface during venting, the cooling water should be shut off or hot water should be valved into the cooling lines to keep the target a few degrees above room temperature. Reactive impurities in inert gas sources can be reduced by passing the gas through hot Ti sponge before introducing it into the process chamber. If the pumping system must be throttled, it is preferable to put the cold trap on the chamber side of the throttling valve so that condensable gases (e.g., H_2O) can be pumped at full efficiency [257].

C. Getter Sputtering

Getter sputtering is a technique sometimes used to reduce the amount of background contamination in the vicinity of sputtering targets and substrates [257a–262]. This technique involves enclosing the target–substrate region of the vacuum system with a rather close-fitting, cooled cylinder. With a shutter closed, the target is presputtered extensively. Films

deposited onto the cylindrical enclosure and the shutter getter reactive gases and bury them; and the cylindrical enclosure acts as a conductance-limiting baffle, retarding the entry of more contaminating gases into the active region of the discharge. After all of the reactive gases are gettered, the shutter is opened and deposition proceeds.

This procedure does not eliminate inert gas incorporation in films, but does eliminate most reactive gas incorporation. The main disadvantage of this technique is that the cylindrical enclosure acts as "wall," giving rise to wall losses and excessive nonuniformity in film deposition near the target edges. If the target itself contains dissolved or occluded reactive gases in the bulk, these gases will still be incorporated into the films because they will be sputtered as negative ions and accelerated toward the substrate.

A variant of getter sputtering has been described [263], in which the solid cylindrical container is replaced by a reactive gas (e.g., SiH_4), which decomposes in the diffuse discharge region surrounding the sputtering target. The cation of the reactive gas (e.g., Si) is capable of chemically gettering reactive gases if its free energy of formation of compounds with the reactive gases is more negative than that of the target material. This eliminates the wall problem, but the reactive gas must be introduced far enough from the substrate to exclude the possibility that some of the cations of the gas are incorporated into the growing film.

D. Reactive Sputtering

There have been numerous theoretical treatments and reviews of reactive sputtering processes [264–274]. For purposes of discussion, this topic should be subdivided. In one form of reactive sputtering, the target is a nominally pure metal, alloy, or mixture of species which one desires to synthesize into a compound by sputtering in a pure reactive gas or an inert gas–reactive gas mixture. The reactive gas either is, or contains the ingredient required to synthesize the desired compound. The second type of reactive sputtering involves a compound target that chemically decomposes substantially during inert gas ion bombardment, resulting in a film deficient in one or more constituents of the target. In this case, a reactive gas is added to make up for the lost constituent. The main difference between these two types of reactive sputtering has to do with the deposition rate dependence on partial pressure of the reactive gas.

A large number of reactive gases have been used to synthesize compounds from metal targets or to maintain stoichiometry in the face of decomposition: Air, O_2, or H_2O (oxides), N_2 or NH_3 (nitrides), $O_2 + N_2$ (oxynitrides), H_2S (sulfides), C_2H_2 or CH_4 (carbides), SiH_4 (silicides), HF or

CF_4 (fluorides), As (arsenides), etc. There are obvious safety problems with some of these gases.

The question of where compounds are synthesized (at the target, in the gas, or at the substrate) is central to an understanding of reactive sputtering [264]. Reactions in the gas phase can for the most part be ruled out for much the same reasons that ions cannot be neutralized in the gas phase. The heat liberated in the chemical reaction canot be dissipated in a two body collision. Simultaneous conservation of energy and momentum requires the reaction to occur at a surface—either the target or the substrate. At very low reactive gas partial pressure and high target sputtering rate, it is well established that virtually all of the compound synthesis occurs at the substrate and that the stoichiometry of the film depends on the relative rates of arrival at the substrate of metal vapor and reactive gas. Under these conditions, the rate of removal and/or decomposition of compounds at the target surface is far faster than the rate of compound formation at the target surface. However, as the reactive gas partial pressure is increased and/or the target sputtering rate is decreased, a threshold is reached at which the rate of target-compound formation exceeds the removal rate of compounds. For metal targets, this threshold is usually accompanied by a sharp decrease in the sputtering rate. This decrease is due partly to the fact that compounds have generally lower sputtering rates than metals and partly that compounds have higher secondary-electron emission yields than metals. As a result, more of the energy of incoming ions is used to produce and accelerate secondary electrons. With constant-current power supplies, the increased secondary electron current automatically decreases the target voltage for a fixed power setting. A third cause of the drop in sputtering rate is simply due to less efficient sputtering by reactive gas ions than by inert gas ions.

The net effect of all of this is illustrated in Fig. 14. If instead of main-

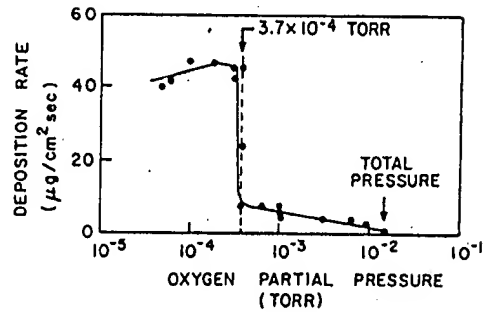

Fig. 14. Deposition rate versus oxygen partial pressure for an iron target in an Ar–O_2 mixture (after Heller [269]).

taining constant power one maintains constant voltage, the abrupt decrease in rate is smoothed out considerably. Likewise, for compound targets there is a much more gradual decrease in sputtering rate with increasing partial pressure of reactive gas which is mainly related to the less efficient sputtering ion concentration.

Clearly, the critical partial pressure depends not only on the glow discharge conditions, but on the kinetics of compound formation of the target surface itself. For example, target materials that do not oxidize readily do not show abrupt rate decrease as oxygen partial pressure increases.

It is impossible for us to review in detail all of the reactive sputtering processes that have been described in the literature. Instead, we present a bibliography of reactive sputtering and reactive ion plating processes in Table V. This table includes only processes in which the target (or evaporant in reactive ion plating) is a metal, and the desired compounds are wholly synthesized in the deposition process. Reactive sputtering of compounds to maintain stoichiometry is not included. The table is organized alphabetically by source material with elemental sources first, then binary sources, ternary sources, etc. For multielement sources, the elements are listed according to their abundance in the source.

VII. DEPOSITION WITH SIMULTANEOUS ION BOMBARDMENT OF THE SUBSTRATE AND GROWING FILM

A. Plasma, Floating, and Bias Potentials

The true potentials on substrates in glow discharge sputtering have been studied extensively [124, 147, 454–459]. The luminous region of a glow discharge is not a true plasma in that the concentrations of electrons and ions are not equal, but plasma conditions are roughly approximated. The substrates in a glow discharge may be treated as floating-plane probes. Figure 15 shows the I–V characteristics of such a probe in somewhat idealized fashion. Any material body immersed in a glow discharge, unless it is grounded, will acquire a potential with respect to ground that is slightly negative. This is known as the floating potential V_f. This potential arises because of the higher mobility of electrons, as opposed to ions, in the discharge so that more electrons reach the surface than ions. It can be shown [460] that the floating potential is related to the electron temperature T_e and the masses of the electron m and ion M involved in the discharge:

$$V_f = -(1/2e)kT_e \ln(\pi m/2M), \qquad (3)$$

where e is the electron charge and k is Boltzmann's constant.

Table V

Bibliography of Reactive Sputtering and Reactive Ion Plating

Source	Gases	References
Ag	Air	[275]
Ag	Ar + N_2	[272]
Ag	Ar + O_2	[272, 273, 276, 277]
Al	Ar + N_2	[278, 279]
Al	Ar + O_2	[18, 261, 273, 280]
Al	O_2	[281]
Au	Air	[275]
Au	Ar + O_2	[276]
Bi	Ar + O_2	[276, 277, 282]
C	N_2	[283]
Cd	Ar + H_2O	[266]
Cd	Ar + H_2S	[266, 284, 285]
Cd	Ar + O_2	[266, 276, 277, 286–294]
Cr	Ar + CH_4	[295]
Co	Ar + O_2	[269, 296, 297]
Cu	Ar + H_2S	[284, 285]
Cu	Ar + O_2	[264, 298–303]
Cu	Ne + O_2	[302]
Fe	Ar + CH_4	[295]
Fe	Ar + O_2	[269, 273, 276, 304–306]
Ga	Ar + As	[307]
Ge	Ar + N_2	[308]
Hf	Ar + C_2H_2	[18]
Hf	Ar + N_2	[309]
Hf	Ar + O_2	[309–311]
In	Ar + O_2	[266, 286, 288, 312–318]
Mg	Ar + O_2	[319]
Mn	Ar + O_2	[296, 320, 321]
Mo	Ar + CH_4	[295]
Mo	Ar + H_2S	[303]
Mo	Ar + N_2	[322]
Mo	Ar + O_2	[272, 323]
Nb	Ar + CH_4	[324]
Nb	Ar + C_2H_2	[18]
Nb	Ar + N_2	[325–327]
Nb	Ar + O_2	[310]
Nb	Ar + N_2 + CH_4	[326]
Nb	Ar + N_2 + O_2	[328]
Ni	Ar + CH_4	[295]
Ni	Ar + O_2	[277, 296, 329–331]
Pb	Ar + H_2O	[266]
Pb	Ar + H_2S	[303]
Pb	Ar + N_2	[308]

Table V (*Continued*)

Source	Gases	References
Pb	Ar + O_2	[266, 277, 332–334]
Pb	O_2	[334]
Pt	Air	[275]
Pt	Ar + O_2	[276, 335]
Sb	Ar + O_2	[276, 277]
Si	Ar + C_2H_2	[336]
Si	Ar + N_2	[280, 319, 337–350]
Si	Ar + NH_3	[268]
Si	Ar + O_2	[273, 276, 277, 351–358]
Si	C_2H_2	[359]
Si	N_2	[67, 360, 360a]
Si	NH_3	[360]
Si	NH_3 + SiH_4	[360]
Si	O_2	[360b]
Si	Ar + N_2 + O_2	[357, 361]
Sn	Air	[312]
Sn	Ar + H_2S	[303]
Sn	Ar + N_2	[308]
Sn	Ar + O_2	[276, 277, 286, 288, 362–364]
Ta	Ar + CH_4	[295, 365, 366]
Ta	Ar + C_2H_2	[18, 367]
Ta	Ar + CO	[264]
Ta	Ar + H_2	[366]
Ta	Ar + H_2O	[266, 368–370]
Ta	Ar + N_2	[264, 325, 365, 366, 371–379]
Ta	Ar + O_2	[261, 266, 267, 273, 277, 310, 325, 351, 365, 369, 380–395]
Ta	Ar + O_2 + N_2	[396–400]
Ta	Ar + SiH_4	[330]
Te	Ar + O_2	[277, 282]
Ti	Ar + CH_4	[401]
Ti	Ar + C_2H_2	[18, 402]
Ti	Ar + H_2O	[266]
Ti	Ar + N_2	[18, 272, 325, 371, 401, 403]
Ti	Ar + NH_3	[18]
Ti	Ar + O_2	[266, 270, 272, 274, 276, 310, 319, 323, 325, 351, 383, 401, 404–407]
V	Ar + C_2H_2	[18]
V	Ar + O_2	[408]
W	Ar + CH_4	[295]
W	Ar + O_2	[276, 277, 310,]
Y	Ar + O_2	[18, 408, 409]
Zn	Ar + H_2O	[264]

Table V (*Continued*)

Source	Gases	References
Zn	Ar + H_2S	[284]
Zn	Ar + O_2	[264, 268, 410–414]
Zr	Ar + N_2	[271, 325]
Zr	Ar + O_2	[310, 325, 351, 415, 416]
Al–Si	Ar + O_2	[354, 355]
Au–Ta	Ar + O_2	[417, 418]
Au–W	Ar + O_2	[417]
Ba–Ti	Ar + O_2	[419, 420]
Bi–Ta	Ar + O_2	[421]
Bi–Ti	Ar + O_2	[421]
Cd–Cu	Ar + H_2S	[303]
Cd–Cu	Ar + O_2	[287]
Cd–In	Ar + H_2S	[303]
Cd–In	Ar + O_2	[287]
Cd–Zn	Ar + H_2S	[422]
Cr–Mo	Ar + O_2	[423]
Cu–Fe	Ar + O_2	[424]
Ga–Al	Ar + As	[307]
Gd–Fe	Ar + O_2	[425]
Hf–Ta	Ar + N_2	[426–429]
In–Sn	Ar + O_2	[286, 294, 371, 403, 430–437]
Li–Nb	Ar + O_2	[438]
Nb–C	Ar + N_2	[326]
Ni–Fe	Ar + O_2	[424, 439]
Ni–Ti	Ar + C_2H_2	[440]
Pb–Te	Ar + O_2	[354]
Pb–Ti	Ar + O_2	[415, 441, 442]
Pt–Ta	Ar + O_2	[417]
Pt–W	Ar + O_2	[417]
Si–Al	Ar + N_2	[443]
Sn–In	Ar + O_2	[286, 362]
Sn–Sb	Ar + O_2	[28, 362, 437, 444]
Ta–Si	Ar + O_2	[445]
Ta–Ti	Ar + N_2	[446]
Ti–C	Ar + O_2	[447]
Ti–Ni	C_2H_2	[448]
Zn–Cu	Ar + H_2S	[449]
Cd–Cu–In	Ar + H_2S	[303]
Fe–Cr–Ni	Ar + CH_4	[295, 450]
Mg–Mn–Zn	Ar + O_2	[451]
Ti–Al–V	Ar + C_2H_2	[452]
Pb–Nb–Zr–Fe–Bi–La	Ar + O_2	[453]

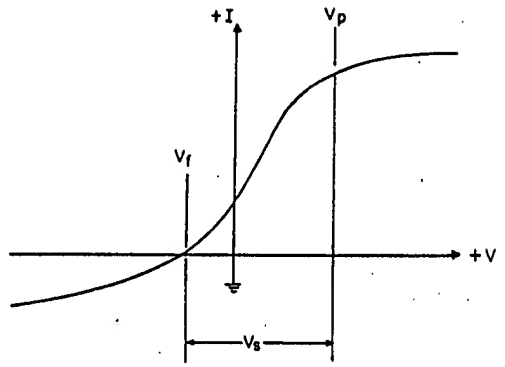

Fig. 15. Idealized *I–V* characteristics of a Langmuir probe in a glow discharge.

At the point V_p, the probe is at the same potential as the plasma. Ideally, there are no electric fields at this point, and the charged particles migrate to the probe because of their thermal velocities. Again, because electrons are more mobile than ions, what is collected by the probe is predominantly electron current. Under ideal conditions, the plasma potential is given by

$$V_p = kT_i \ln 2/q_i, \tag{4}$$

where T_i and q_i are the temperature and charge of the ions involved [460].

The assumptions made in the derivations of these equations are by no means strictly valid in glow discharges (especially in the presence of magnetic fields), but they may be used to estimate the electron and ion temperatures in the discharge.

There are three major practical consequences to be drawn from Fig. 15. First, substrates (even if they are grounded) are at a potential that is negative with respect to the plasma. This is shown for a floating substrate in Fig. 15 as V_s. If the substrates are grounded, V_s is reduced by an amount equal to V_f. The second consequence is that *substrates in sputtering systems should rarely be grounded.* If an insulating substrate is attached to a grounded substrate support, the surface of the substrate acquires the potential V_s while its surroundings acquire the lower potential $V_s - V_f$. This leads to nonuniformity of bombardment near the edges of the substrate which, in turn, leads to variable thickness, composition or other properties as a function of distance from the edge of the substrate. The only exception to this rule is in the case of a conducting substrate onto which a conducting film is to be deposited. Finally, since target voltages and substrate voltages (in the case of bias sputtering or ion plating) are measured relative to ground, the existence of the plasma potential introduces a systematic error since the true potential is the sum of the measured voltage and V_p. In some cases the error can be large.

The variation of the floating potential (V_f) with various dc glow discharge parameters is shown in Fig. 16. For rf glow discharges, the behavior is similar, except the magnitudes of the voltages involved are generally

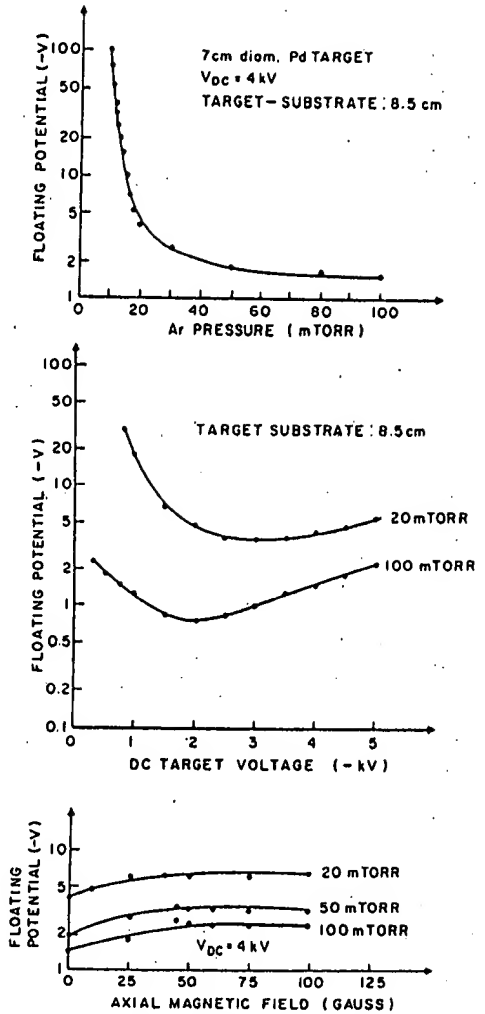

Fig. 16. The variation of the floating potential with Ar pressure, target voltage, and axial magnetic field in a dc sputtering system.

higher because the electron temperatures are higher for otherwise equivalent conditions.

The variation of the plasma potential (V_p) with dc glow discharge conditions is similar to the variation of the floating potential because parameters that increase electron temperature generally increase ion temperatures as well. For example, as the pressure is decreased, V_f and V_p, respectively, become more negative and more positive with respect to ground, leading to higher substrate potentials V_s.

The situation with rf glow discharges is somewhat more complicated because the geometry of the system becomes a major factor. As was pointed out (Eq. (1)), the ratio of the average potential on the capacitively coupled electrode (target) to that of the grounded electrode with respect to the plasma is given by $(A_g/A_c)^4$, where A_c and A_g are the areas of the capacitively coupled and grounded electrodes, respectively. These areas refer to the areas actually in contact with the glow discharge. If the discharge is confined (e.g., by placing a cylinder around the target), a limited portion of the total grounded area is actually in contact with the discharge. This has been done [454], and the plasma potentials have been measured for various confining ratios, R = target area/grounded area versus the sum of the applied target potential to ground and the plasma potential (i.e., the total target potential) as shown in Fig. 17. These effects can be used to impose a negative bias on a substrate without the necessity for making a direct electrical contact, but it is clearly difficult to control.

It should be noted that the potentials described so far are *average* dc potentials. This does not imply that all ions striking substrate surfaces arrive with these potentials. In both dc and rf glow discharges, the thickness of the ion sheath at the substrates is greater than the ionic mean free paths, leading to inelastic collisions which slow many of the ions as they traverse the sheath. For this reason alone, ions reach the surface at all energies from zero up to that corresponding to eV_s [118]. In rf glow discharges, the potential of the ion sheath is time dependent. This leads to modulation of the ion energies depending upon exactly when the ions reach the outer edge of the ion sheath. In this case, incident ions can arrive with potentials ranging from zero to almost $2eV_s$ [123].

Negative substrate bias voltages can be applied from an external power source. If the substrate is electrically conducting, this may be accomplished with a dc power supply [461]. For insulating substrates and/or for the deposition of insulating films on conducting substrates, rf-induced substrate bias is preferred [11, 147, 462–463]. When this is done, the applied bias voltage, V_b, in effect takes the place of the floating potential, and the plasma potential remains unchanged [454]. Thus, the total negative substrate bias is $-(V_p - V_b)$.

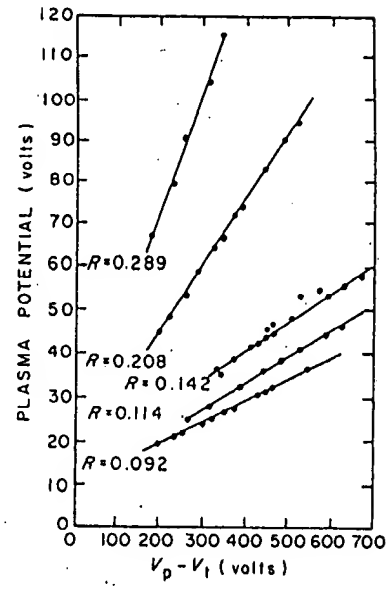

Fig. 17. Plasma potential versus total target potential for various confining ratios, R (see text) in an rf glow discharge (after Coburn and Kay [454]).

If a positive bias is applied to a substrate in a dc glow discharge, the substrate simply becomes a virtual anode, resulting in a very large electron current flow to the substrate. This, in turn, leads to a large amount of substrate heating and a very nonuniform current distribution [456]. For both dc and rf discharges, application of a positive bias to an independent electrode (e.g. a substrate) leads to an increase in the plasma potential to more positive values [454, 456] as shown in Fig. 18. Even for very high positive values of V_b, the effective substrate bias never exceeds the plasma potential. Thus, application of a positive bias is seen to have little effect on the effective substrate potential, but the relatively large increase in V_p leads to rather high levels of bombardment of all grounded surfaces in contact with the discharge. This can lead to rather large amounts of gas desorption from the walls of the chamber. Except in those instances where one might wish to clean up the grounded parts of a sputtering system, the application of positive substrate biases should be avoided.

It can be seen from this discussion that substrates in sputtering systems are nearly always subject to a negative bias (ion bombardment), whether externally applied or not. Consequently, substrates must be treated as sputtering targets, and all of the effects described in Section II

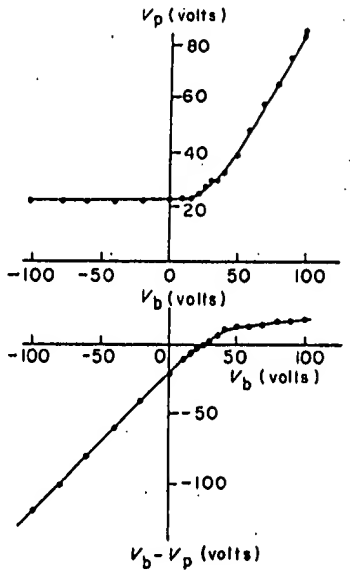

Fig. 18. The plasma potential (V_p) and total substrate potential ($V_b - V_p$) versus substrate bias in an rf glow discharge (after Coburn and Kay [454]).

apply to substrates during film growth as well as to sputtering targets. In some cases, one may wish to maximize substrate bombardment, while in other cases minimum bombardment may be desired. In all cases it should be controlled.

Bombardment of substrates is not limited to charged particles. High-energy neutrals reflected from the target and/or generated in the glow discharge by various excitation processes also bombard the substrate. Clearly these are unaffected by the substrate potential, and bombardment from this source is impossible to eliminate completely in glow discharge sputtering [464]. Recent estimates have been made of the relative contribution to substrate bombardment by ions (10%) and energetic neutrals (90%) in ion plating [465–467].

It should also be pointed out that the phenomena discussed in this section apply to substrates in *any* glow discharge. Thus, they apply not only to sputtering processes, but to all glow-discharge deposition and etching processes.

B. Gas Incorporation and Desorption

During the sputtering process, gas is incorporated in the growing film. The amount depends on target voltage [468–472], substrate bias voltage

[469–471, 473–478], target-to-substrate distance [473, 479], sputter gas pressure [471, 473, 479], inert gas atomic volume [471, 480], substrate temperature, magnetic field, and system geometry. The interplay among these parameters is responsible for the varied results found in the literature. There are two mechanisms by which gas is incorporated: ions can be neutralized at the target surface and reflected at high energy toward the substrate where they may be implanted; and ions can bombard the substrate and be implanted because of the effective substrate bias.

1. Substrate Bias

The effective substrate bias is the most important parameter in determining gas incorporation [468–488]. At very low bias voltages, there is insufficient energy to implant gas, but some thermal desorption can occur. At higher voltages, gas contents increase as V_b^2, where V_b is the substrate bias voltage. At very high bias voltages substrate heating leads to desorption of the implanted gas.

2. Target Voltage

The entrapment of energetic neutral sputter gas atoms reflected from the target surface has been amply demonstrated [468–472]. For example, in the incorporation of He in gold films [468], it was shown that at constant pressure and bias voltage, lower target voltages gave less gas incorporation than higher target voltages. Ar was found to increase in concentration for both triode and diode sputtered W films [478], and the amount of Ar that is incorporated in the film increases with the atomic number of the target material [489].

3. Substrate Temperature

As the substrate temperature is increased the sticking probability of inert sputter gas decreases [468, 473, 483, 487]. However, the rate of reaction increases in reactive sputtering.

4. Pressure

Increasing pressure decreases gas incorporation [471–473]. The increase in gas content with decreasing pressure is due to an increase in the plasma potential.

5. System Geometry

Geometric effects such as target-to-substrate distance have been shown to affect the amount of gas incorporated in films. The greater the distance of the target from the substrate the less gas will be incorporated in the growing films [472–473]. For example, in dc triode sputtering of W films [472] Ar was shown to decrease from about 15 at. % with a target–substrate separation of 9 cm to about 0.1 at. % at a separation of 18 cm.

Another geometric effect found that influences the film gas content is the target size for a fixed system geometry. Here we find seemingly conflicting results. For example, the inert gas concentration in rf sputtered amorphous films with rf bias voltage was found to vary inversely with the target electrode area [471], while in dc triode sputtered films it was found that the Ar concentration increased as the target area increased [473].

C. Stoichiometry of Films

The stoichiometry of films deposited from multicomponent targets when a substrate bias is applied has been addressed by a number of workers [83, 84, 92, 96a, 477, 483, 489–491]. Most of these treatments are theoretical. Rather than review them in detail, we summarize the practical consequences.

To control film stoichiometry, many conditions must be met. The target itself must be homogeneous. This is especially a problem with some alloys and mixtures in which constituents segregate out in patches. The altered surface layer must be established at steady state. There must be no bulk diffusion in the target. If sublimation occurs at the target, the target composition must be enriched in the subliming material. When targets with normally gaseous constituents (e.g., oxides) are used, chemical dissociation at the target must be compensated by reactive sputtering. Preferential resputtering must be compensated by adjusting the target composition and/or by reactive sputtering. Shutters should be biased to the same potential as substrates during deposition to prevent transients in resputtering which change the composition of the first few monolayers of film material.

D. Physical Film Properties

In the absence of problems with film stoichiometry, controlled resputtering in various bias modes often aids in producing films of high quality. Most of the studies of physical film properties as a function of substrate bias have been reviewed elsewhere [9, 11, 13, 147], and they will not be

covered in detail here. There have been reports of improved film density, electrical properties, magnetic properties, adhesion, and surface morphology, to name but a few. In addition, variations in grain size, preferred orientation, and crystal polymorphs have been observed in some materials. Ohmic contacts can be made to semiconductors without the need for sintering. Conformal coatings over severe topographic features on substrates can be achieved because of small-angle resputtering. In general, the judicious use of substrate biasing is one of the most powerful tools available in sputtering to tailor the properties of deposited films. To optimize some properties, high bias voltages are required, while to optimize others, substrate bombardment must be minimized.

In summary, there are three basic effects that occur at a substrate during glow discharge sputtering: (1) condensation of energetic vapor, (2) heating, and (3) bombardment by a variety of energetic species. The sum of all of these effects must be carefully controlled, and, since they are all interdependent [11], this is sometimes difficult.

VIII. RATE AND UNIFORMITY OF DEPOSITION

Most deposition rates quoted in the literature should more properly be called "accumulation rates," since they are really the difference between the arrival and resputtering rates of the film material at the substrate. Both the accumulation rate and the uniformity of film deposition have been thoroughly reviewed by Maissel [5, 9], so only a summary is presented here.

For a given target material both rate and uniformity are influenced by system geometry, target voltage, sputtering gas, gas pressure, and power. All other things being equal, rates are linearly proportional to power and decrease with increasing target–substrate separation. The sputtering gas influences deposition rate in the same way as it affects sputtering yields. As the gas pressure is increased the discharge current increases (increasing rate), but return of material to the target by backscattering also increases (decreasing rate). This is further complicated in some cases by increased Penning ionization at higher pressures which increases the rate by self-sputtering. The sum of all of this leads to a gas pressure or a small range of gas pressure at which the rate is a maximum, and this must be determined empirically for each application. The optimum pressure may be anywhere between a few mTorr and several tens of mTorr.

In general, for a given gas pressure there will be an optimum target–substrate separation to produce the best uniformity. For small targets

(<15-cm diameter) this separation is generally small (a few centimeters), while for larger targets, the optimum separation may be considerably larger (10–20 cm). The edges of the target, no matter how the dark-space shield is constructed, represent regions of gross nonuniformity. Under ideal conditions, the best uniformity that one can hope to achieve is ±2–5% over an area concentric with the deposition target, but ~5 cm smaller in diameter than the target. Often it is much worse than this.

IX. CONCLUSION

In this chapter we have attempted to review the rather complex interplay of the parameters involved in sputter deposition and to introduce some of the glow discharge aspects of related processes.

Unquestionably, the hallmark of the sputtering processes described is versatility, both in terms of materials that can be deposited and process parameters that can be adjusted to tailor the properties of thin films as desired. However, the sheer number of critical process parameters and their complex interrelationships can often make these processes difficult to control. For many applications, the advantages far outweigh the disadvantages, and "diode sputtering" and "ion plating" have been put to use in large-scale production in applications of a wide variety: electronics, optics, abrasion-resistant coatings, lubricating coatings, corrosion protection, and thermal insulation, to name but a few.

In general, these processes are found to be most useful in applications requiring rather thin films (generally <1 μm because of relatively low deposition rates) and/or in cases where the desired material simply cannot be deposited stoichiometrically any other way.

REFERENCES

1. G. K. Wehner, *Adv. Electron. Electron Phys.* 7, 239 (1955).
2. E. Kay, *Adv. Electron. Electron Phys.* 17, 245 (1962).
3. M. Kaminsky, "Atomic and Ionic Impact Phenomena on Metal Surfaces." Academic Press, New York, 1965.
4. M. H. Francombe, *in* "Basic Problems in Thin Film Physics" (R. Niedermeyer and H. Mayer, eds.), p. 52. Vanderhoeck & Ruprecht, Göttingen, 1966.
5. L. I. Maissel, *Phys. Thin Films* 3, 61 (1966).
6. G. Carter and J. S. Colligon, "Ion Bombardment of Solids." Am. Elsevier, New York, 1968.
7. K. L. Chopra, "Thin Film Phenomena." McGraw-Hill, New York, 1969.
8. G. K. Wehner and G. S. Anderson, *in* "Handbook of Thin Film Technology" (L. I. Maissel and R. Glang, eds.), Ch. 3. McGraw-Hill, New York, 1970.
9. L. I. Maissel, *in* "Handbook of Thin Film Technology" (L. I. Maissel and R. Glang, eds.), Ch. 4. McGraw-Hill, New York, 1970.

10. G. N. Jackson, *Thin Solid Films* 5, 209 (1970).
11. J. L. Vossen, *J. Vac. Sci. Technol.* 8, S12 (1971).
12. P. D. Townsend, J. C. Kelly, and N. E. W. Hartley, "Ion Implantation, Sputtering and Their Applications," Ch. 6. Academic Press, New York, 1976.
13. W. D. Westwood, *Prog. Surf. Sci.* 7, 71 (1976).
14. R. J. MacDonald, *Adv. Phys.* 19, 457 (1970).
15. I. S. T. Tsong and D. J. Barber, *J. Mater. Sci.* 8, 123 (1973).
16. D. M. Mattox, *Electrochem. Technol.* 2, 295 (1964).
17. D. M. Mattox, *J. Vac. Sci. Technol.* 10, 47 (1973).
18. R. E. Bunshah and A. C. Raghuram, *J. Vac. Sci. Technol.* 9, 1385 (1972).
19. O. Almen and G. Bruce, *Nucl. Instrum. Methods* 11, 257 (1961).
20. O. Almen and G. Bruce, *Nucl. Instrum. Methods* 11, 279 (1961).
21. J. L. Vossen and E. B. Davidson, *J. Electrochem. Soc.* 119, 1708 (1972).
22. P. D. Davidse and L. I. Maissel, *J. Vac. Sci. Technol.* 4, 33 (1967).
23. G. K. Wehner, Rep. No. 2309. General Mills, Minneapolis (1962).
24. J. L. Vossen, unpublished observations (1974).
25. C. H. Weyenfeld and A. Hoogendoorn, *Proc. Conf. Ion. Phenom. Gases, 5th, Munich* 1, 124 (1961).
26. D. McKeown and A. Y. Cabezas, *Annu. Rep. Space Sci. Lab.; General Dynamics* July (1962).
27. F. Keywell, *Phys. Rev.* 97, 1611 (1955).
28. J. Comas and C. B. Cooper, *J. Appl. Phys.* 37, 2820 (1966).
29. D. McKeown, A. Cabezas, and E. T. Mackenzie, *Annu. Rep. Low Energy Sputtering Stud.; Space Sci. Lab., General Dynamics* July (1961).
30. R. C. Krutenat and C. Panzera, *J. Appl. Phys.* 41, 4953 (1970).
31. T. W. Snouse, *NASA Tech. Note* D-2235 (1964).
32. H. Patterson and D. H. Tomlin, *Proc. R. Soc., A* 265, 474 (1962).
33. M. T. Robinson and A. L. Southern, *J. Appl. Phys.* 38, 2969 (1967).
34. P. K. Rol, J. M. Fluit, and J. Kistemaker, "Electromagnetic Separation of Radioactive Isotopes," p. 207. Springer-Verlag, Berlin and New York, 1960.
35. O. Almen and G. Bruce, *Trans. Natl. Vac. Symp., 8th, Washington, D.C.*, p. 245 (1961).
36. M. I. Guseva, *Sov. Phys.—Solid State* 1, 1410 (1959).
37. M. T. Robinson and A. L. Southern, *J. Appl. Phys.* 39, 3463 (1968).
38. P. A. B. Toombs, *J. Phys. D* 1, 662 (1968).
39. L. Holland, T. Putner, and G. N. Jackson, *J. Phys. E* 1, 32 (1968).
40. I. Brodie, L. T. Lamont, and D. O. Myers, *J. Vac. Sci. Technol.* 6, 124 (1969).
41. D. J. Ball, *J. Appl. Phys.* 43, 3047 (1972).
42. B. N. Chapman, D. Downer, and L. J. M. Guimaraes, *J. Appl. Phys.* 45, 2115 (1974).
43. Y. Shintani, K. Nakanishi, T. Takawaki, and O. Tada, *Jpn. J. Appl. Phys.* 14, 1875 (1975).
44. R. E. Honig, *J. Appl. Phys.* 29, 549 (1958).
45. R. E. Honig, *Proc. Conf. Ion. Phenom. Gases, 5th, Munich* 1, 106 (1961).
46. A. K. Ayukhanov and M. K. Abdullaeva, *Bull. Acad. Sci. USSR., Phys. Ser.* 30, 2083 (1966).
47. Y. A. Fogel, *Sov. Phys.—Usp.* 10, 17 (1967).
48. A. Benninghoven, *Z. Phys.* 220, 159 (1969).
49. A. Benninghoven, *Surf. Sci.* 28, 541 (1971).
50. A. Benninghoven, *Z. Phys.* 230, 403 (1970).
51. A. Benninghoven, *Surf. Sci.* 35, 427 (1973).
52. H. W. Werner, *Surf. Sci.* 47, 301 (1975).

IV-1

Plasma Deposition of Inorganic Thin Films

*J. R. HOLLAHAN AND R. S. ROSLER**

Applied Materials Incorporated
Santa Clara, California

I. INTRODUCTION

The technology of thin films produced by plasma deposition processes is fast outrunning the scientific understanding of their detailed properties. The physics of the deposition process, the chemical knowledge of the kinetics of formation, and the nature of film microstructural detail are just now emerging. While not a new field, plasma deposition has yet to reach the state of refinement attained in sputtering and in conventional chemical vapor deposition (CVD) processes. The production of thin film materials by electric discharge (plasma) processes has long been a laboratory study

* Present Address: Motorola, Inc. Pheonix, Arizona 85002.

ISBN 0-12-728250-5.

of interest, with published works appearing before the turn of the century. The majority of these studies relate to the formation of thin organic polymeric films, largely because of the ready availability of the organic reactant gases. Early papers on inorganic thin films produced in a plasma appeared in the 1930s. Studies and publications on both inorganic and organic films accelerated as these films became technologically important in such diverse areas as optical coatings, packaging, and in films in microelectronics.

It is the purpose here to summarize what is known about the different film materials that can be produced, to describe the probable pathways for their formation, and to note some of their general properties. A complete list of the properties found cannot be described here. Rather, reference to the original papers must be made since emphasis will be placed on the methods for film deposition and the attendant plasma conditions for the production of various types of films.

The uniqueness of the plasma to generate chemically reactive species at low temperatures is due to the nonequilibrium nature of the plasma state. By nonequilibrium, we mean a gas plasma typically sustained at 0.1 to several Torr, which exhibits temperatures of the free electrons of tens of thousands of degrees Kelvin, while the temperature of the translational and rotational modes of free atoms, radicals, or molecules will be only hundreds of degrees Kelvin. A good and concise discussion of the principles of generating low temperature plasma species, their ion and neutral balance, and their continuous loss by diffusion, attachment, and recombination may be found in Kaufman [1]. No attempt will be made here to review the general fundamentals of plasma chemistry since works are available which accomplish this in detail [2, 3].

One of the prime motivating factors in utilizing plasma deposition processes is that the substrate temperature can be kept relatively low, typically 300°C or lower. Conventional CVD processes usually require temperatures substantially higher that may be inappropriate for certain substrate materials or device structures. The films that are deposited by plasma reactions are usually amorphous in nature, with very little short-range structural ordering. The stoichiometry of the films can be made to vary in a controlled fashion by variation of dominant plasma parameters, such as reactant gas flow ratios. Because there is a range in film stoichiometry, it is to be expected, and is indeed observed, that electrical, mechanical, and chemical properties can also vary. It has been suggested by some authors that some of these materials may be referred to as "polymeric" in nature, since their structures are in most cases very likely three-dimensional networks of randomly bonded atoms and, possibly, molecular pendants. Hence, without crystalline order, structural detail

can only be inferred from optical, spectroscopic, and electrical measurements.

II. EXPERIMENTAL REQUIREMENTS AND TECHNIQUES

A. Dominant Plasma Parameters

Anyone becoming familiar with plasma thin film deposition processes will realize that there are as many deposition reactor designs and experimental conditions to consider as there are published studies describing plasma deposited thin film materials. This makes the comparison of data concerning properties and measurements of the film materials difficult, if not impossible. With the exception of production type reactors now becoming widely used, plasma reactors in which thin films have been produced are small laboratory systems with a limited usable substrate area. Obviously, it is not possible to describe or catalog here in detail all of the designs and experimental approaches that have been taken; rather, general principles and some laboratory examples will be given to exemplify the requirements and techniques of plasma thin film deposition.

The results of thin film deposition (i.e., film properties) will be subject to many variables which may be interdependent: reactor geometry, electrode configuration and separation, power level and frequency, gas composition and flow rate, gas flow direction and flow pattern, pressure, substrate temperature, and any added gas diluents. Table I categorizes the major parameters controlling plasma deposition. Of the three major groups affecting deposition, the electrical element of plasma systems is the least well understood. For example, although the literature described plasma deposition occurring under a wide variety of source frequencies, practically no published studies exist which describe film properties resulting from a systematic variation of plasma frequency for a given experimental setup and process. There are indications that the level of frequency can affect some materials properties.

B. Deposition System Requirements

1. General Requirements

Every glow discharge system for thin film production is comprised of the following basic components: (1) the reactor or deposition chamber; (2) electronics, i.e., power generation source, usually at some fixed frequency; (3) a possible impedance matching network to transfer the power more efficiently from the generator to the gas load; (4) gas flow regulators

Table I

Parameters Controlling Plasma Deposition[a]

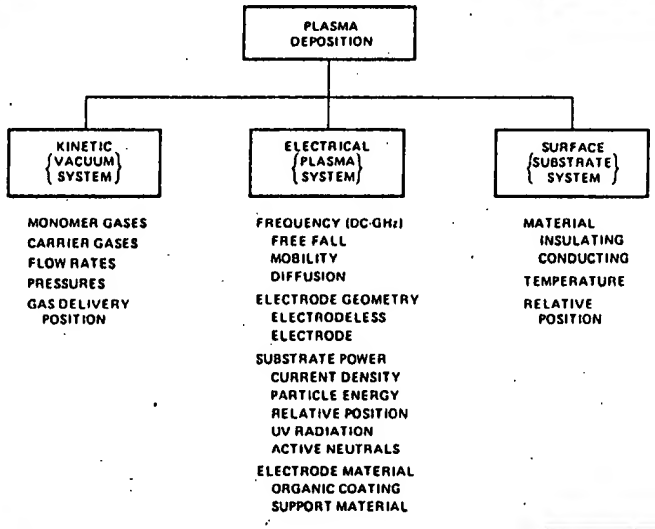

[a] After M. Hudis [3a].

(automatic or manual, such as rotameters) and gas control section; (5) pressure measurement plus other panel instrumentation. Commercial units exist for plasma dry etching and stripping or cleaning. However, those systems have, at present, no capability for inorganic thin film deposition, usually because of the barrel design approach; but they do have the above mentioned components conveniently packaged into one system.

2. *Electrode Designs*

Electrode design approaches for achieving the power to the plasma at the voltage level suitable for gas breakdown are shown in Fig. 1. Many variations are possible on these basic configurations. The electrode shown in Fig. 1a has been found suitable for larger scale production-type systems for deposition (see Section III.A.2). In the latter configuration, the substrates usually lie flat (for heating purposes), while in Figs. 1b and c, substrates normally are in the stand-up position.

While the tube design is satisfactory for photoresist stripping and some etching applications [4, 5] where the substrates typically are in the stand-up position, the requirements for thin film deposition are best met

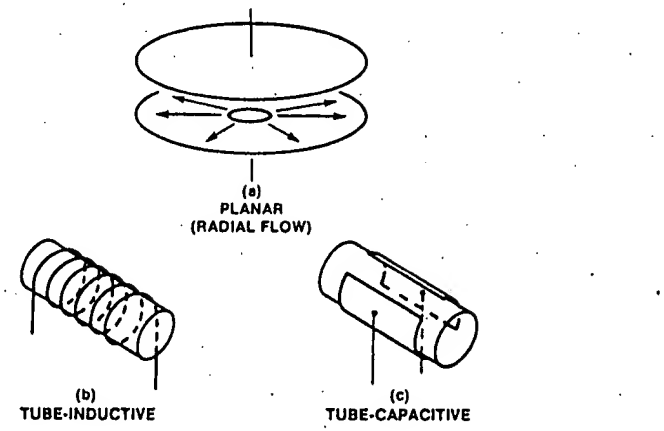

Fig. 1. Various basic types of electrode configurations. In (a) the electrodes are normally inside the reactor directly interfacing with the plasma, while in (b) and (c) the electrodes are external to the plasma process (electrodeless excitation).

by the planar reactor approach. There are various reasons for this: (1) the substrates usually lie flat for ease of heating the substrate uniformly during deposition; (2) the substrates themselves and substrate-to-substrate relative positions experience a high degree of electric field uniformity, and hence power density (watts per square centimeter) distribution. As a result, the deposition proceeds quite uniformly. In tube-type reactors, the substrates are generally difficult to heat uniformly to temperatures of 300–350°C required for proper film densities. Additionally, the tube design is usually provided with either external inductive or capacitive electrode geometries for plasma generation, and this can lead to an asymmetric electric field contour across the wafer and from front to back of the vertically standing wafers, resulting in significant radial and longitudinal thickness variations. This nonuniformity has been observed with etching processes.

3. *Power Supplies*

Power supplies, either at high or low frequency, are commercially available in a large range of power level outputs. The basic decision that has to be made is the choice of frequency, if information should exist on an optimum frequency for the particular process in question. Deposition rate does appear to be affected by the pulsing of the high frequency power instead of operating at continuous wave output. This is certainly true for organic compounds in plasma polymerization [6], and very likely holds

true for inorganic systems. In the case of organic compounds, if the power were pulsed, the polymerization rate could be either increased or decreased by as much as 100%, depending on the structure of the starting compound.

4. *Vacuum Requirements*

Most plasma systems do not require critical high vacuum or pumping components. Usually, process pressures are in the range 0.1–1.0 Torr at total gas flows of a few to several hundred cubic centimeters per minute (STP), i.e., "soft" vacuum. Thus, diffusion pumps are not necessarily required, although these have been incorporated in some experiments to establish an initial high vacuum (10^{-5}–10^{-6} Torr) prior to the start of the experiment. Often a rotary mechanical pump is all that is used. To prevent backstreaming of the high-vapor-pressure fluids used in these pumps, it is necessary to insert a trap in the vacuum line and/or gas ballast the pump so that its inlet pressure never exceeds about 150 mTorr. In addition, safety precautions are required when certain gases are used. Oxidation resistant pump fluids must be used with oxidizing gases (e.g., O_2, F_2). If the plasma reactions are expected to liberate large quantities of explosive gases (e.g., H_2), the exhaust of the pump may have to be diluted (e.g., with N_2).

In general, the choice of pumping system must be considered carefully based on considerations of pumping rate for all gases introduced and generated in the process, inlet flow rates, background contamination from residual gases outgassing and backstreaming, and safety.

5. *System Examples*

Typical systems which may be described are depicted in the following figures. In Fig. 2 [7] a straightforward vertical tube reactor is shown that is powered inductively by an rf source. In this case, silicon nitride films are produced on a small heated sample support pedestal. These smaller test reactors are usually made of quartz; they are convenient and of low cost. In Fig. 3 a vertical tube reactor is shown, again suitable for silicon nitride formation [8]. In this case, a microwave power supply is utilized with the power being delivered to the cavity out of the direct substrate region. The coil around the reactor is for the inductive heating of the substrate. The silicon-containing starting compound SiI_4, manufactured *in situ* at point C by reaction of silicon with iodine at point B, enters the reactor encountering a downward flowing nitrogen plasma produced in the cavity.

Another example is that of Fig. 4 [9], in which epitaxial silicon is being

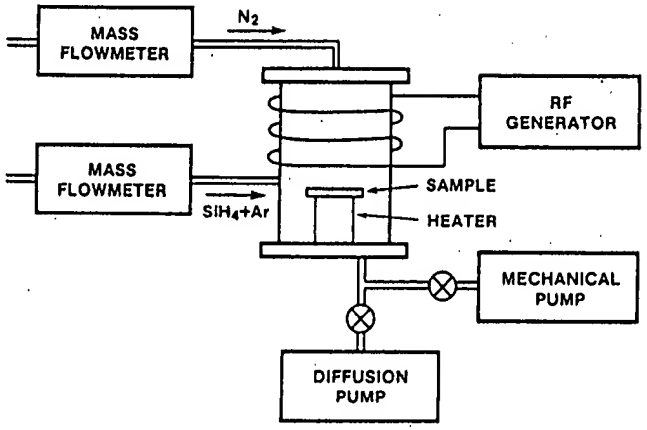

Fig. 2. Simple laboratory coil-excited vertical tube reactor with a sample support pedestal which can be heated (reprinted from Helix *et al.* by permission of the publisher, The Electrochemical Society, Inc.).

grown at several hundred degrees centigrade with substrates on a heated susceptor. At the same time, high frequency breakdown of the gas is accomplished by circular capactive band electrodes on either side of the inductive heating coil. This method couples both thermal and plasma assisted reactions at the same time to produce films of good quality.

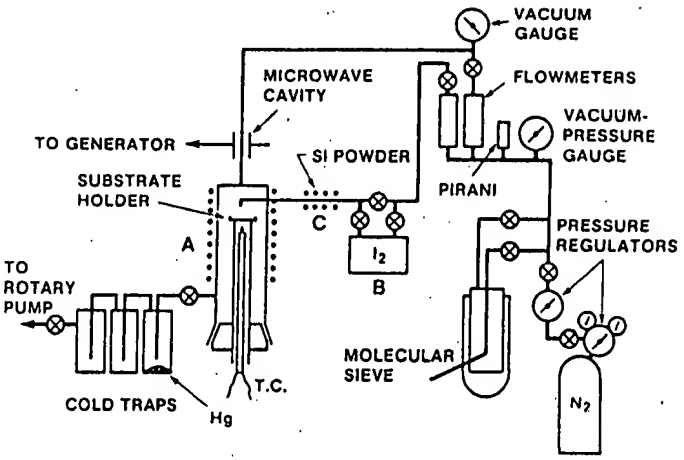

Fig. 3. Vertical tube reactor with microwave excitation of the plasma indirectly from the substrate location (Shiloh *et al.* [8] originally presented at the 152nd Fall Meeting of the Electrochemical Society, Inc., in Atlanta, Georgia).

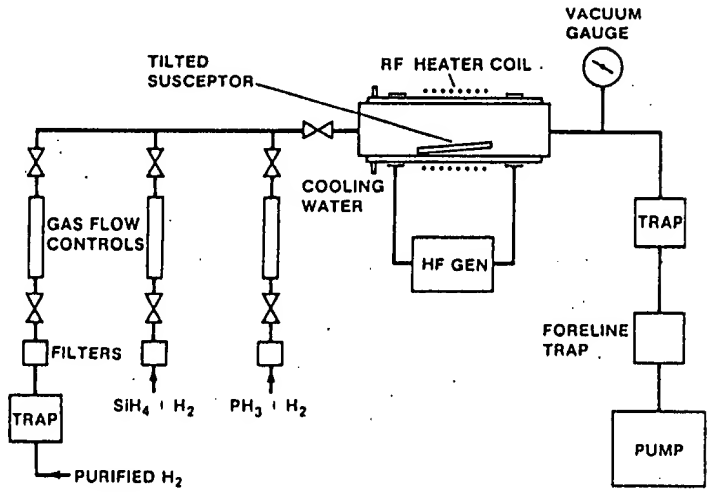

Fig. 4. Horizontal tube reactor around which an rf heater coil is placed. At either end of the coil are located electrode bands to provide the plasma throughout the reactor zone (after Townsend and Uddin [9], by permission of the publisher, Pergammon Press, Ltd.).

6. *Process Control*

The control of plasma-enhanced CVD processes is assuming increasing importance, especially with the advent of production-type reactors. Although very little has been published in this area specifically for plasma processes, process control should be achievable by the use of film thickness monitors, mass spectroscopy, and optical spectroscopy for detecting gas phase intermediate species and for monitoring their concentration. Measurement of film composition is another monitoring approach. For example, in the case of plasma "silicon nitride" films, correlation of optical absorption edges with composition in terms of Si/N ratios can be used [10]. A rapid optical inspection of the film produced after each deposition run provided better assurance that film qualities are within specification.

III. DEPOSITION OF THIN INORGANIC FILMS

A. Silicon Nitride

Plasma deposition of "silicon nitride" films from SiH_4, N_2, and/or NH_3 has been extensively studied and is now at the stage of production applications in semiconductor device manufacture, mainly for device final passivation. Films on the order of 3000–10,000 Å thickness are excellent

diffusion masks for alkali ion contaminants and other impurities. The recognition of the potential of low-temperature deposited nitrides to semiconductor applications is not new. The delay in the widespread use for this material has resulted, in part, not from an emphasis on competing technologies but, more particularly, from the lack of equipment adequate to the film uniformity and production requirements of the industry. The chemistry of plasma silicon nitride deposition is extremely complex and the detailed reaction kinetics are not understood, largely because such deposition reactions are difficult to probe diagnostically as opposed to processes taking place exclusively in the gas phase.

"Silicon nitride" produced via plasma is quite unlike silicon nitride produced by conventional chemical or physical vapor deposition techniques. In the latter case, the stoichiometry is virtually assured to be Si_3N_4, while in the former process the stoichiometry (Si/N ratio) can be controllably varied depending on ratios of entrant reactant gas flows, power level, substrate temperature during deposition, and reactor pressure.

1. *Film Deposition and Properties*

Amorphous silicon nitridelike films can be produced by reaction of nitrogen and/or ammonia with silane or other substituted silane or derivative reactants. Nitrogen atoms derived from ammonia may be more advantageous in reaction systems because of the lower ionization energy of NH_3 relative to N_2. The relevant appearance potentials (AP) are given in Table II [11].

If we assume a predominately silicon nitride phase in the solid material and propose kinetic pathways for the formation of Si—N, Si=N, or Si≡N bonds, we immediately arrive at an overwhelming number of reaction possibilities. This is because the gas phase dissociation of silane produces SiH_3, SiH_2, and SiH, and dissociation of nitrogen or ammonia produces N or NH_2 and NH.

Table II

Appearance Potentials for Nitrogen Containing Ions from NH_3 and N_2[a]

Parent molecule	NH_3			N_2	
Ion	NH_3^+	NH_2^+	NH^+	N_2^+	N^+
AP (eV)	10.5	15.8	19.5	15.6	24.3

[a] After Reinberg [11].

Such speculative intermediate reactions involving N or NH_2 species as

$$SiH_4 + N \rightarrow SiN + 2H_2$$
$$SiH_4 + NH_2 \rightarrow SiN + 3H_2$$
$$SiH_3 + N_2 \rightarrow SiN + NH_3$$
$$SiH_3 + NH_2 \rightarrow SiN + \tfrac{1}{2}H_2$$

may be important, but undoubtedly are oversimplifications of the true reaction processes. This is evidenced by the fact that plasma "silicon nitride" films can vary in stoichiometry, contain large amounts of hydrogen, and may incorporate impurity constituents, such as a few percent oxygen from the background gases or water and possible carbon content from background hydrocarbons (pump oil, for example). It is possible then that the "silicon nitride" film has a compositional nature of $Si_aN_bO_x$-H_yC_z, where indeed x, y, and z may be very small numbers and a and b are not necessarily 3 and 4, respectively. A similar argument for departure from ideal stoichiometry likely holds for plasma produced films in general.

In early studies in small laboratory reactors, usually of the tube type, reports on silicon nitride deposition described the macroscopic properties of the film material. Only recently have more detailed analyses of the films evolved along with an attempt to infer the chemistry of film formation from the gas phase. The number of published reports describing silicon nitride production is now steadily increasing.

The initial nitride deposition process is generally attributed to Sterling and Swann [12], who in 1965 reported on films of "silicon nitride" they had produced in a quartz tube by decomposition of SiH_4 and NH_3 gas mixtures in a 1-MHz rf discharge at 500 W and 0.1 Torr. Deposition rates of 500 Å/min were measured.

This initial work briefly presented macroscopic property measurements of plasma nitride as well as of plasma silicon oxide and was followed by an expanded report [13]. Additional detailed reports appeared [14–19] which reported laboratory studies in unique reactor designs.

It is not possible to compare all data on an absolute basis in these references from one reactor study to another because of differences in experimental design. The comparison of deposition data or plasma parameters becomes more meaningful with the advent of parallel plate reactors which have become reasonably standardized in production of films on a larger scale basis (see Section III.A.2). Although diverse reactors, plasma source frequencies, electrode configurations, power, pressure, and flow ranges have been investigated, some unmistakably consistent trends are evident in plasma nitride film properties. The refractive index can often serve as one criterion of film quality, and correlate with electrical properties (dielectric constant, breakdown strength, etc.), mechanical, and chemical properties, such as etch rate.

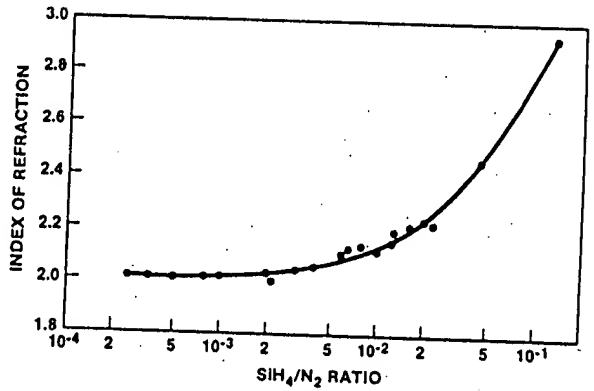

Fig. 5. Variation of the refractive index with the SiH_4/N_2 ratio (after Gereth and Scherber [16], by permission of the publisher, The Electrochemical Society, Inc.).

As representative examples [16], Fig. 5 shows the variation of refractive index with the SiH_4/N_2 ratios of the entrant gases. At higher SiH_4 flows, the films are becoming quite rich in silicon. Therefore, the SiH_4/N_2 ratio must be kept relatively low for the usually required refractive index range (2.0–2.1) to be achieved. The data of Fig. 5 were obtained from a quartz reactor 90-cm long and 7 cm in diameter. The plasma of 1–5% SiH_4 in N_2 was established at 500 kHz. Growth rates at a substrate temperature of 500°C up to 400 Å/min were measured.

Figure 6 shows the refractive index and deposition rate dependence on total pressure [20]. These data were obtained from a large 66-cm parallel plate reactor (to be described in detail in Section III.A.2). The refractive index is shown not to be very sensitive to total pressure. Figure 7 shows the index dependence on substrate (silicon wafer) temperature [20]. Above a temperature of 300°C, the index remains essentially constant, and a 50°C change in temperature causes only a 3% rate change.

Plasma silicon nitride invariably contains large amounts of hydrogen, which can be removed to some extent by annealing. The lower the deposition temperature, the greater will be the amount of entrained or bonded hydrogen, which has been correlated with a lowering of the index of refraction and an increase in etch rate [21].

The hydrogen appears to be largely bonded to Si entities in SiH_x groups where $x = 1, 2, 3$. In a detailed infrared spectroscopic study, evidence was presented that under preparative conditions where the films are Si rich, N–H infrared absorption bands appear [21]. Plasma nitride film density, composition, and refractive index have been correlated through the Lorentz–Lorenz relationship, as shown in Fig. 8 [22]. The information in Fig. 8 is helpful for correlating refractive index with density

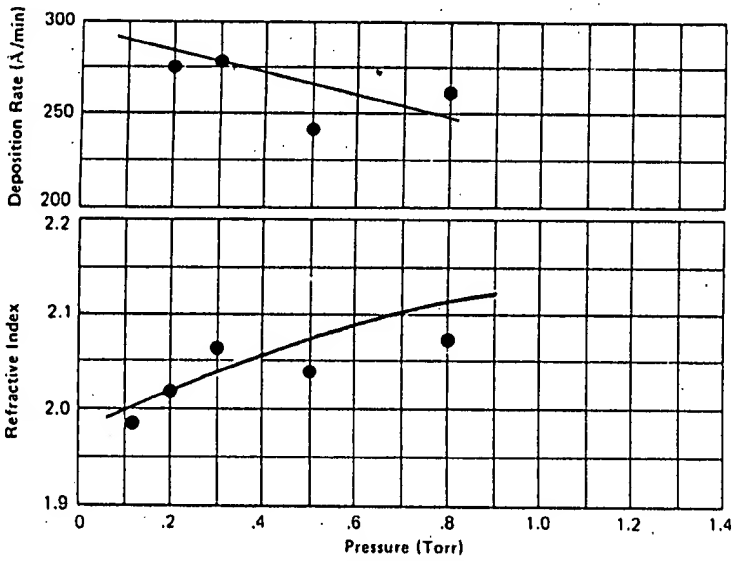

Fig. 6. Dependence of refractive index and deposition rate on total pressure (after Rosler *et al.* [20]).

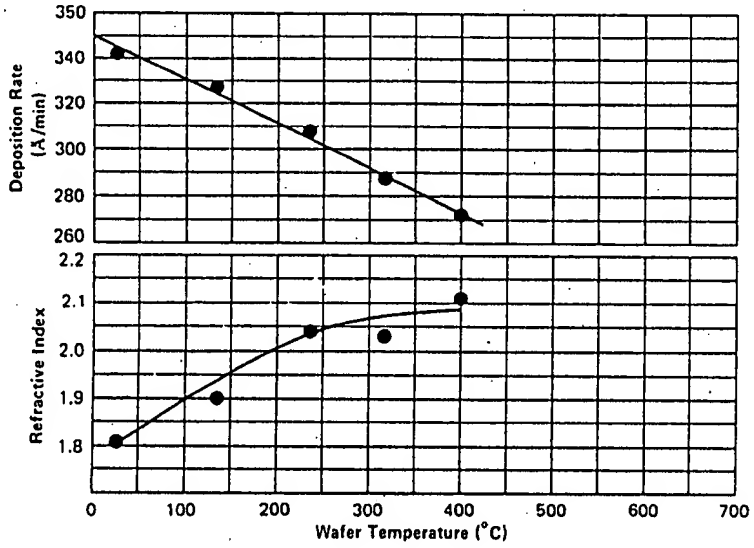

Fig. 7. Dependence of refractive index and deposition rate dependence on deposition temperature (after Rosler *et al.* [20]).

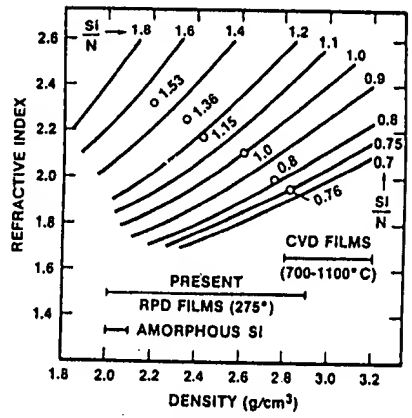

Fig. 8. Lorentz–Lorenz correlation curves for reactive plasma deposited (RPD) films of silicon nitride (after Sinha [22]).

for various Si/N ratios found in the film, which relates directly to the Si/N ratio of reactor entrant silicon and nitrogen containing gases.

Optical property studies of silicon nitride have shown [23] that different refractive indices and optical gaps can be obtained for the same film stoichiometry, depending upon the film densification. The influence of the reacting gas concentration and flow rate on the variation of the optical gap (3.5–4.9 eV) and the refractive index (1.8–2.1) is interpreted [24] in a detailed study as a variation of the stoichiometries of the deposited films. Therefore, it is necessary to separate out the substrate temperature effect from other plasma parameters (flow, pressure, and power) when considering optical properties of silicon nitride, and very likely plasma-produced thin films in general.

Electron spectroscopy for chemical analysis (ESCA) or Auger characterization [25] of substrate surfaces and plasma deposited films permits one to maintain better control of film growth which are affected by interfacial phenomena, background gas contaminants, and other sources of impurity incorporation. Since the density and optical properties can vary through the film, these surface limited analytical techniques become quite valuable and provide a true profile of film composition by repeated ion etching and ESCA or Auger analysis, provided that the results are interpreted to account for artifacts introduced in these measurements by the ion etching.

Silicon nitride films have also been prepared by reaction or active nitrogen and SiI_4 according to the overall representative reaction [8]

$$4N + 3SiI_4 \rightarrow Si_3N_4 + 6I_2,$$

which was found to be exothermic. The SiI_4 was prepared *in situ* outside the plasma region by passing I_2 vapor over heated silicon powder. The product then entered the reactor which contained a microwave excited nitrogen plasma. No provision was made to heat the substrate to elevated temperatures, and except for infrared spectra, no physical or chemical evaluation has yet been published on nitride prepared via this plasma process. Infrared spectra showed basically the same dominant Si–N absorption based centering at ~870 cm^{-1} that is found for CVD films produced from SiH_4–NH_3 and reactive sputtering of Si in N_2. Rather high rates of nitride film formation were observed (>3300 Å/min) to produce films of 1.4 to 2.0 index of refraction.

The deposition of silicon nitride from SiH_4 has been described [26] using a microwave excited plasma produced at some distance from the substrate, thus minimizing the direct field of excitation around the substrate. At 680 W, a substrate temperature of 350°C, and a SiH_4 concentration ranging from 1 to 20% in N_2, deposition rates approaching 400 Å/min were obtained. A maximum of 1.95 was found for the refractive index. The significance of these types of experimental arrangements is that the substrate is out of the field of direct plasma generation where this may be a problem for very radiation sensitive substrates.

A phenomenon of a weak visible luminescence appearing over the surface of silicon wafers was attributed to emissions from silicon and nitrogen atoms by correlation of the emission band frequencies with known values. If this is true, the following might be proposed:

$$\begin{aligned} SiH_4 &\rightarrow Si + 2H_2, \\ 2N &\rightarrow 2N \quad , \\ Si + N &\rightarrow SiN \quad , \\ SiH_4 + N &\rightarrow SiN + 2H_2, \quad \text{etc.} \end{aligned}$$

2. *Production Reactors*

The deposition of "silicon nitride" films has now been optimized for production reactors designed for multisubstrate throughput (e.g., silicon device wafers). Reinberg first announced the radial flow reactor design in 1973 [27]. A variation on this concept was later commercialized [20]. In the latter case, the reactor is a parallel plate system, as shown in cross-sectional form in Fig. 9.

The reactor, constructed largely of aluminum, contains two parallel 66-cm diameter electrodes separated by a distance of 5 cm. The high-voltage upper electrode is connected through a matching network to a 5 kW, 50 kHz power supply. The lower electrode, which serves as the substrate support, is grounded. A magnetic drive assembly permits rotation of this

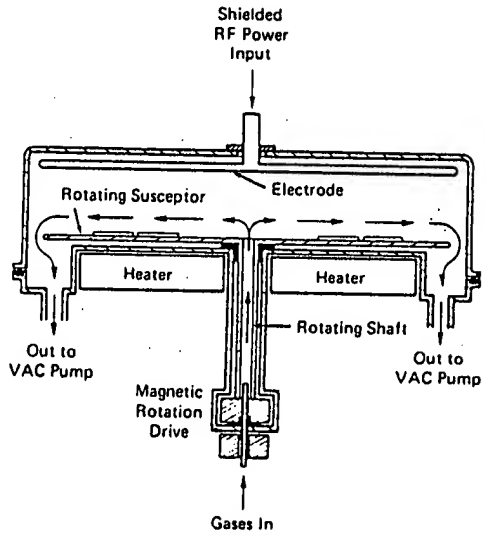

Fig. 9. Planar, radial flow reactor (after Rosler *et al.* [20]).

lower electrode to permit randomization of substrate position for maximum substrate-to-substrate uniformity. This electrode is typically heated to 300–325°C by an externally mounted three-zone heater.

The reactant gas mixture ($SiH_4/NH_3/N_2$) enters upward through the rotating central shaft and flows radially outward between the two electrodes. Reaction by-products and unreacted gases exhaust into a circumferential plenum below the outer edge of the grounded electrode and then through four uniformly spaced exhaust ports to the pumping system.

Depending on gas flow and composition, the deposition rate can be strongly dependent or independent of power level above a certain point. At higher SiH_4 flow rates, this relationship is linear within the range of the reported experimental conditions. At lower SiH_4 flows, particularly when combined with reduced total gas flow, the rate of film deposition tends toward an asymptotic value at higher power input levels. Reactor characterization for deposition of materials other than silicon nitride would have to take these possibilities into consideration. Under flow conditions that provide uniform deposition, the rate of film deposition can be controlled by variation in the input power without materially affecting the radial uniformity of deposition. The conditions of 600 cm^3/min N_2, 300 cm^3/min NH_3, and 150 cm^3/min SiH_4 at 500 W provides a ±1.6% film thickness uniformity in the deposition zone. Deposition rates of 300–350 Å/min can

Table IIIa

Physical Properties of Silicon Nitride Films from $SiH_4 + NH_3 + N_2$[a]

Property	Si_3N_4 HT-CVD-NP 900°C	$Si_xN_yH_z$ PE-CVD-LP 300°C
Density	2.8–3.1 g/cm³	2.5–2.8 g/cm³
Refractive index	2.0–2.1	2.0–2.1
Dielectric constant	6–7	6–9
Dielectric strength	1×10^7 V/cm	6×10^6 V/cm
Bulk resistivity	10^{15}–10^{17} Ω-cm	10^{15} Ω-cm
Surface resistivity	$>10^{13}$ Ω/sq	1×10^{13} Ω/sq
Stress at 23°C on Si	1.2–1.8×10^{10} dyn/cm² Tensile	1–8×10^9 dyn/cm² Compressive
Thermal expansion	4×10^{-6}/°C	$>4 < 7 \times 10^{-6}$/°C
Color, transmitted	None	Yellow
Step coverage	Fair	Conformal
H_2O permeability	Zero	Low–none
Thermal stability	Excellent	Variable >400°C

Table IIIb

Chemical Properties of Silicon Nitride Films from $SiH_4 + NH_3 + N_2$[a]

Property	HT-CVD-NP 900°C	PE-CVD-LP 300°C
Composition	Si_3N_4	$Si_xN_yH_z$
Si/N ratio	0.75	0.8–1.0
Solution etch rate		
HFB 20–25°C	10–15 Å/min	200–300 Å/min
49% HF 23°C	80 Å/min	1500–3000 Å/min
85% H_3PO_4 155°C	15 Å/min	100–200 Å/min
85% H_3PO_4 180°C	120 Å/min	600–1000 Å/min
Plasma etch rate		
70% CF_4/30% O_2, 150 W, 100°C	200 Å/min	500 Å/min
Na^+ penetration	<100 Å	<100 Å
Na^+ retained in top 100 Å	>99%	>99%
IR absorption		
Si–N max	~870 cm⁻¹	~830 cm⁻¹
Si–H minor	—	2180 cm⁻¹

[a] After Kern and Rosler [28].

be attained. A ±40% change in power level causes only a modest increase in the radial uniformity profile.

As the pressure in the reactor increases, the deposition rate decreases steadily over the range studied of 0.1–0.8 Torr. This general behavior is not necessarily common in plasma deposition. However, it can result from depletion and gas phase recombination at higher pressures, reducing the availability of reactive film-producing species. Typical chemical and physical properties of plasma deposited nitride produced in the planar reactor are listed in Tables IIIa and IIIb [28].

B. Silicon Oxide and Oxynitride

1. Silicon Oxide

Unless great care is taken with the vacuum and wall conditions during plasma deposition, most silicon oxides will contain a small, but measurable, amount of nitrogen derived from background sources. The reactive competition of oxygen for silane, however, is much greater than that of nitrogen. Although several publications describe the plasma deposition of "SiO_2," in many instances the true stoichiometry was never determined. As with the plasma nitride, an amount of hydrogen is certain to exist, with possible carbon content as well.

Silicon oxides may be prepared by:

(1) Coreaction of silane or silane derivatives with oxygen, N_2O, CO, or other sources of oxygen.

(2) Decomposition of an oxygenate, such as $Si(OR)_4$, where R is an organic alkyl group, such as $-C_2H_5$ or $-CH_3$.

(3) *In situ* film growth on the substrate, i.e., "plasma anodization."

The basic laboratory or production reactor design that has been described for the deposition of the plasma nitride in most cases is suitable for oxide deposition. Other than the gas composition, major plasma parameters (power, pressure, and total gas flows) may not vary appreciably from nitride deposition requirements for a given reactor configuration.

The reaction of nitrous oxide with silane in the overall reaction

$$SiH_4 + 2N_2O \rightarrow SiO_2 + 2N_2 + 2H_2$$

is among the earliest studied plasma reaction system to produce SiO_2 [12]. The possible mechanism for the reaction might be explained as follows, consistent with bond energy considerations. Nitrous oxide has two resonant electronic structures, $^-N{=}N^+{=}O$ and $N{\equiv}N^+{-}O^-$. The nitrogen–nitrogen bonds have a higher bond energy than nitrogen–oxygen or sili-

con–hydrogen bonds. If SiH_4 is predominantly dissociated in the plasma, SiH_2 or SiH radicals could form intermediate complexes of the types, as shown below, which decompose to SiO_2 and $N_2 + H_2$.

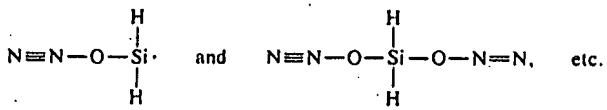

Nitrogen–oxygen single bond energies are low by a factor of 2 or 3 compared to Si–O bond energies so that Si–O bonds may form. What part the substrate surface versus the gas phase contributes to the process is unknown, at least in the published literature.

Radio frequency discharge of $N_2O + SiH_4$ [12] produced silicon oxide films readily up to 1.0 μm in thickness. Again, as the relative gas flow ratios are varied, the electrical and structural properties also vary. Dielectric constant values varied from 3.8 to 10 in the above referenced study for N_2O/SiH_4 ratios ranging from 1 : 1 to 10 : 1. Over a similar range of gas ratios, the refractive index varied from 1.46 to 1.9. Infrared studies [21] showed predominantly Si—O bonds at 9.3, 12.4, and 22 μm.

Silicon tetrachloride reacting with an oxygen plasma, which was sustained by a microwave discharge, produced glassy SiO_2 films up to several millimeters in thickness in small diameter quartz tubes at 950–1000°C deposition temperature [29] by the overall reaction

$$SiCl_4 + O_2 \rightarrow SiO_2 + 2Cl_2.$$

In an oxygen plasma, the primary reactive species is $O(^3P)$, and, in addition, a rather long lived excited molecular oxygen state exists [$O_2(^1\Delta_g)$, ~0.96 eV] in appreciable concentration [3]. This species has been termed "singlet" oxygen and undoubtedly also participates in the formation of oxide films, if oxygen plasmas are utilized.

If TEOS [tetraethoxy silane, $Si(OC_2H_5)_4$] is decomposed in the presence of an oxygen plasma amorphous silicon oxide films are formed [30–32]. Tetraethoxy silane is a liquid and must be transported by a carrier gas (O_2) into the reaction zone.

If TEOS is decomposed with argon as the carrier gas, organosilicon films are formed. A detailed infrared study [30] of films prepared at 1 MHz and 0.2 Torr total pressure in a vertical tube reactor showed evidence of CH_2, CH_3, Si–OH, Si–O–C_2H_5, and many other hydrocarbon moieties. The primary mechanism for deposition then appears to be based on an oxygen plasma combustion of the hydrocarbon part of the molecule to CO_2 and H_2O, with the remaining SiO_x fragments probably forming types of cluster complexes with adsorption and growth on the substrate surface. Excess TEOS vapor (that is, more than can be consumed by the oxidizing plasma) will lead to a hydrocarbon content in the film depending on the

substrate surface temperature. If the temperature is ~500°C, then simultaneous plasma decomposition and pyrolysis of the excess TEOS will occur, leading to a more nearly SiO_2 stoichiometry.

In a microwave discharge (2450 MHz) study [33], vapors of either TEOS or tetraethyl silane were decomposed in an oxygen plasma to produce films on substrates at 200°C. At 100 W and 0.24 Torr the deposition rates were rather low, about 10–80 Å/min. A bell jar apparatus was employed permitting the use of a quartz microbalance to measure film growth.

Oxide films prepared from $SiH_4 + N_2O$ under plasma conditions are reported [34] to be better suited for use in semiconductor fabrication than those deposited from TEOS. Hydrogen and hydrocarbon content is lower at a deposition temperature of 450°C, and the films are reportedly cleaner. By whatever preparative technique employed, SiO_x films do not exhibit the excellent alkali ion diffusion barrier properties displayed by the silicon nitride films.

2. *Silicon Oxynitride*

Nitrogen atoms may be included into an SiO_x network by such plasma processes as coreaction of $SiH_4 + NO + NH_3$, or reactively evaporating SiO with an ionized plasma of nitrogen [35]. This latter reaction produces a SiO_xN_y structure that has described [35] as a glassy mixture of elemental Si, N, and O, rather than a mixed phase of SiO_2 and Si_3N_4. As the amount of N is increased, infrared absorptions of Si–N appear while Si–O intensities decrease. Multiple internal infrared reflection measurements have shown [36] as much as 7% hydrogen concentrations. Hydrogen bound to silicon can be annealed out after annealing 1 hr at 900°C, with a 20% reduction in the N–H bond centers [36]. Thus, a very complex structure is being produced in the formation of oxynitrides.

The same general techniques to produce silicon nitride and oxide are appropriate for the oxynitride. In spite of the complexity of the resulting material, basic properties of the film are reproducible, if plasma conditions are carefully reproduced. The refractive index is claimed, for example, to be reproducible to ±0.01 over the range 1.5–2.0 [34]. In principle, by adjustment of gas composition and deposition temperature at given plasma conditions, one can tune in desirable electrical and chemical properties intermediate between all-oxide and all-nitride compositions.

C. Silicon Carbide

Amorphous SiC films can be readily prepared from silane and a volatile carbon containing coreactant, such as C_2H_4 [37], CH_4 [38], or CF_4

[39]. In these examples, the overall reactions may be written

$$2SiH_4 + C_2H_2 \rightarrow 2SiC + 5H_2$$

and

$$SiH_4 + CH_4 \text{ (or } CF_4) \rightarrow SiC + 2H_2 \text{ (or 4HF)}.$$

The variations of the SiC optical gap $\mathscr{E}_g$ and the refractive index were correlated with pressure, gas flow rates, power, and substrate temperature. In a detailed reactor performance and materials study [38], $\mathscr{E}_g$ decreased from 2.5 to 2.1 eV and the refractive index increased from 1.9 to 2.1 as the SiH_4/CH_4 ratio increased from 0.24 to 0.80. Typical optimum deposition conditions in the 7-cm diameter × 40-cm length cylindrical reactor were 0.2 Torr pressure, 100 W power (5 MHz), 40 cm³/min (STP) total flow, and a 200°C substrate temperature. It is interesting that if the pressure is above 1.0 Torr, a fine brownish powder is deposited along with the film. Rapid gas phase polymerization with nucleation of particles is occurring, similar to the case found in the plasma deposition with ethylene, where different plasma regimes would produce films, particles, or oils [40].

The optical properties of plasma SiC have been considered in some detail [37]. A general conclusion is that amorphous plasma produced thin films of SiC have an appreciably lower overall density of gap states compared to sputtered or pyrolytically deposited material. The optical gap was found to reach a maximum at a film composition of $Si_{0.32}C_{0.68}$ at deposition temperatures of 225 and 525°C.

D. Silicon and Germanium

Amorphous silicon or germanium are the simplest materials that can be produced in a plasma of their respective hydrides. Mass spectrometric fragmentation patterns reveal that the primary product ion is SiH_2^+; thus, the term "polysilane" might be appropriate for films containing large amounts of hydrogen where SiH, SiH_2, and terminal SiH_3 are certain to exist [40]. Films of low hydrogen content can be viewed as a random three-dimensional matrix of tetrahedrally bonded silicon atoms with an occasional hydrogen atom or atoms at a silicon bond site. Large amounts of hydrogen will be retained at lower deposition temperature higher-pressure regimes, while at higher temperatures and lower pressures, the amount retained is much less. For example, the atomic fraction of hydrogen in films prepared at 250°C and 0.1 Torr is 0.14 (0.7×10^{22} atoms/cm³), while at 25°C and 1.0 Torr the atomic fraction is 0.35 (1.7×10^{22} atoms/cm³).

The amount of hydrogen contained in amorphous silicon has been analytically followed by infrared spectroscopy, and also by the nuclear resonance reaction $^{15}N + {}^1H + {}^{13}C = {}^4HC + \gamma$, microprobe, and mass spectrographic methods of analysis [41]. Doping of amorphous silicon with phosphine or diborane was achieved [42, 43] by the plasma decomposition of silane with these dopants (5×10^{-6} PH_3 and 10^{-2} B_2H_6 per unit volume SiH_4). The substrate temperature was held at 250°C and the total plasma pressure at 0.8 Torr, which produced a relatively low 50 Å/min deposition rate. An amorphous silicon *p-n* junction was finally fabricated whose rectification and photovoltaic responses were qualitatively similar to those of a crystalline *p-n* junction.

Epitaxial silicon has been grown from SiH_4 in H_2 in the presence of an electric discharge (350 W at ~27 MHz) at 0.2–0.6 Torr in the apparatus discussed in Fig. 4 [9]. Epitaxial silicon can be produced, of course, in such an apparatus without an electric discharge at 1050–1200°C at 1 atm. However, when the deposition occurred in the presence of the plasma, temperatures could be reduced to as low as 800°C, while still maintaining good epitaxial growth for both doped and undoped *N*-type layers. That good films can be grown at 800°C was augmented by the marked reduction in stacking fault density (~20% of the process without glow discharge), and improvement in surface quality of the epitaxial silicon layers was observed. The main advantage of the discharge was thought to be the continuous cleanup of the substrate provided during deposition. In addition, however, there may be energy transfer processes available not possible at 1 atm that produce films of better integrity at low pressure.

E. Other Oxides

1. Aluminum Oxide

Amorphous films of Al_2O_3 have been formed by vaporizing $AlCl_3$ into an oxygen plasma [44]. The pressure of the discharge and the $AlCl_3$ vaporization rate greatly affected the rate of film formation, which varied from 70 to 500 Å/min, and was linearly dependent on rf power over the range studied. Adherent films up to thicknesses of several microns were prepared at the optimum substrate temperature of 480°C. The Al–Al_2O_3–Si structures were characterized as having large positive flat band voltage shifts of up to 40 V, under negative bias at elevated temperature. This implies these films will show high resistance to Na^+ ion diffusion, unlike SiO_2. Other film properties such as resistivity and dielectric constant and strength were acceptable or compared well with oxide prepared from thermal decomposition of aluminum triethoxide.

2. *Oxides of Ge, B, Ti, and Sn*

Clear, crystalline, and glassy films of several oxides were prepared by microwave discharge decomposition of the corresponding alkyls or alkoxides [32]. Films were produced typically at 0.24 Torr on NaCl substrates (for infrared spectroscopic studies) at 200°C. Growth rates were very low, about 20 Å/min. Table IV summarizes the M–O band infrared absorption and index of refraction measurements. Thus, these oxides were formed with indices (and presumably densities) very close to their thermal counterparts.

3. *Plasma Oxides by Anodization*

Plasma anodization is the formation of thin oxide films by placing the metal or semiconductor substrate under bias in the field of an oxygen plasma. Thus, plasma anodization is not a deposition process but rather an *in situ* film growth process. A positive bias of a few to several hundred volts is placed on the sample to affect film growth. Ions in the discharge are now more actively participating in the film growth, in contrast to much less participation by ions on floating or grounded substrates. Reviews of plasma anodization have summarized a good deal of this work [45, 46] to which the reader is referred.

Table IV

Comparison of the Optical Properties of Plasma-Deposited and Glassy or Crystalline Oxide Films[a]

	Material	Principal infrared frequency (cm^{-1})	Index of refraction
GeO_2	Plasma-formed film	850	1.582 ± 0.002
	Fusion-formed glass	850	1.534–1.607
B_2O_3	Plasma-formed film	1350	1.470 ± 0.002
	Fusion-formed glass	1350	1.464(3)
Ti_xO_y	Plasma-formed film	950–700	1.7
TiO_2	Anatase	1200–500	1.7
Sn_xO_y	Plasma-formed film	1425	1.536 ± 0.002
SnO_2	Cassiterite	850–500	1.7
SiO_2	Plasma-formed film	1045; 800	1.458 ± 0.002
	Fusion-formed glass	1080; 800	1.458 ± 0.002

[a] After Secrist and Mac Kenzie [32].

F. Miscellaneous Films

1. *Boron Nitride*

Boron nitride thin films have been prepared by reacting B_2H_6 and NH_3 in a plasma at 1000°C on various substrates lying flat on a graphite susceptor in a horizontal tube reactor [47]. Only 4 W rf power at 13.56 MHz were required. Pressures ranged from 0.3 to 1.0 Torr. Transmission and reflection electron diffraction revealed that some crystallites exist within the film. The films were smooth and transparent, and exhibited better crystalline quality than BN films obtained from the same reagents by high-temperature CVD. At a $NH_3:B_2H_6$ ratio of 8.1:1 nearly stoichiometric but slightly boron-rich BN was found by electron microprobe analysis. At a projected gas ratio of 7.1:1, stoichiometric BN should be obtained.

2. *Phosphorus Nitride*

By directly vaporizing elemental phosphorus in a nitrogen plasma, transparent glasslike films of P_3N_5 ranging from 0.5 to 10 μm in thickness were produced on a variety of metal and glass substrates [48]. Conditions of film formation were as follows: horizontal tube; pressure, 1.0 Torr; power, to 500 W; frequency, 25 MHz; deposition temperatures, 265°C. Electrical properties were evaluated, and permittivity at room temperature was found to be 4.4, independent of frequency. Dielectric strength values between 0.3 and 0.5 × 10^7 V/cm were found for samples which had been cycled through temperature extremes of − 196 to 230°C.

IV. CONCLUSIONS, APPLICATIONS, AND PROSPECTS

The foregoing examples indicate the diversity of thin film processes obtainable under low temperature plasma conditions. By adjusting gas flows, their ratios, power, and pressure of the plasma, one can, in principle, alter and optimize film properties at will. A major limitation today is the transition from laboratory R&D efforts to production-type or standardized reactors. While this has been accomplished for silicon nitride, many other materials which have been qualified as useful structural or functional thin films require the scaled up processor to be able to produce them in practice economically.

The major reason for the acceleration of interest in plasma processing and production-type reactors has been for the use of plasma silicon nitride films as a final device passivation overcoat. Because these nitride films

are a significant improvement over doped or undoped SiO_2 films, their use is now rapidly becoming the standard within the semiconductor industry.

Description of the superior passivating properties of plasma nitride with actual devices shows that its use as an overcoating of trimetal devices has eliminated electroplating between closely spaced oppositely biased conductors [49], and that it has improved the lifetime by a factor of 3 as an overcoat for plastic encapsulated nichrome link PROMS [50]. The use of plasma nitride as an excellent interlevel dielectric has been described [51, 52]. This application, if high speed (and thus a smaller dielectric constant) is desired, may be better filled by plasma silicon dioxide, provided its step coverage, pinhole density, and adhesion are comparable to plasma nitride.

Plasma nitride films have potential uses as an antireflection coating over solar cells, LED's or LCD's, or optics lenses, as an implantation annealing barrier, as III–V structure diffusion masks, and as a photomask coating for scratch protection and sticking reduction.

Plasma deposited amorphous silicon has potential as a material for low cost solar cells [53] and for the thermal growth of thin epitaxial layers of Si on Si from the amorphous phase.

There are many film materials that may yet be synthesized via plasma processes. Virtually all the refractory compounds of carbides, phosphides, silicides, borides, and sulfides can be considered via various reaction pathways.

Even more complex is the prospect of mixed or ternary element films. Silicon oxynitride has already been discussed. There are possible films of oxycarbides, sulfides, silicides, borides, etc., or other mixed, nonoxy, ternary systems. Additionally, the inclusion by vaporization of metal atoms or dopant atoms into the films certainly exists, leading to semiconducting films or films with other unusual electrical properties [54]. The number and types of films that can be produced in a low temperature plasma with their as yet unevaluated mechanical, electrical, and optical properties offer the materials scientist new dimensions of research and development.

REFERENCES

1. F. Kaufman, *Adv. Chem. Ser.* No. 80, p. 29 (1969).
2. F. K. McTaggart, "Plasma Chemistry in Electrical Discharges." Elsevier, Amsterdam, 1967.
3. "Techniques and Applications of Plasma Chemistry" (J. R. Hollahan and A. T. Bell, eds.). Wiley (Interscience), New York, 1974.

3a. M. Hudis, unpublished summary, NASA–Ames Research Center, Moffett Field, California.

4. E. O. Degenkolb, C. J. Mogab, M. R. Goldrick, and J. E. Griffiths, *Appl. Spectrosc.* 30, 520 (1976).
5. R. Kumar, C. Ladas, and G. Hudson, *Solid State Technol.* 19(10), 54 (1976).
6. H. Yasuda and T. Hsu, *J. Polym. Sci., Polym. Chem. Ed.* 15, 81 (1977).
7. M. J. Helix, K. V. Vaidyanathan, and B. G. Streetman, *Electrochem. Soc. Extend. Abstr.* No. 77-2 (1977).
8. M. Shiloh, B. Gayer, and F. E. Brinckman, *J. Electrochem. Soc.* 124, 295 (1977).
9. W. G. Townsend and M. E. Uddin, *Solid-State Electron.* 16, 39 (1973).
10. M. J. Rand and D. R. Wonsidler, *Electrochem. Soc. Extend. Abstr.* No. 77-2 (1977).
11. A. R. Reinberg, *Int. Round Table Surf. Treat. Plasma Polymer., IUPAC, Limoges, Fr.,* (1977).
12. H. F. Sterling and R. C. G. Swann, *Solid-State Electron.* 8, 653 (1965).
13. R. C. G. Swann, R. R. Mehta, and T. P. Cauge, *J. Electrochem. Soc.* 114, 713 (1967).
14. Y. Kuwano, *Jpn. J. Appl. Phys.* 8, 876 (1969).
15. Y. Kuwano, *Jpn. J. Appl. Phys.* 7, 88 (1968).
16. R. Gereth and W. Scherber, *J. Electrochem. Soc.* 119, 1248 (1972).
17. R. Kirk and I. I. Gurev, *Symp. Appl. Electr. Discharge Chem., Am. Inst. Chem. Eng., Annu. Meet. 64th, 1971.*
18. C. R. Barnes and C. R. Geesner, *J. Electrochem. Soc.* 107, 98 (1960).
19. A. W. Horsley, *Electronics* January 20, p. 3 (1969).
20. R. S. Rosler, W. C. Benzing, and J. Baldo, *Solid State Technol.* 19(6), 45 (1976).
21. E. A. Taft, *J. Electrochem. Soc.* 118, 1341 (1971).
22. A. K. Sinha, *Electrochem. Soc. Extend Abstr.* No. 76-2, p. 625 (1976).
23. A. K. Sinha, *J. Electrochem. Soc.* 123, 262 (1976); *J. Electron. Mater.* 5, 441 (1976).
24. Y. Catherine and G. Turban, *Int. Round Table Surf. Treat. Plasma Polymer., 3rd, IUPAC, Limoges, Fr., 1977.*
25. P. H. Holloway and H. J. Stein, *Electrochem. Soc. Extend. Abstr.* No. 75-2, p. 218 (1975).
26. M. Shibagaki, Y. Horuke, T. Yamazaki, and M. Kashiwagi, *Electrochem. Soc. Extend. Abstr.* No. 77-2, Abstr. 152 (1977).
27. A. R. Reinberg, *Electrochem. Soc. Extend. Abstr.* No. 74-1, p. 4 (1974); U.S. Patent 3,757,733 (1973).
28. W. Kern and R. S. Rosler, *J. Vac. Sci. Technol.* 14, 1082 (1977).
29. D. Kuppers, J. Koenings, and H. Wilson, *J. Electrochem. Soc.* 123, 1079 (1976).
30. S. P. Mukherjee and P. E. Evans, *Thin Solid Films* 14, 105 (1972).
31 S. W. Ing and W. Davern, *J. Electrochem. Soc.* 111, 120 (1964).
32. D. R. Secrist and J. D. MacKenzie, *J. Electrochem. Soc.* 113, 914 (1966).
33. D. R. Secrist, *Adv. Chem. Ser.* No. 80, p. 242 (1969).
34. R. Kirk, *in* "Techniques and Applications of Plasma Chemistry" (J. R. Hollahan and A. T. Bell, eds.), Ch. 9, Wiley (Interscience), New York, 1974.
35. M. Mashita and K. Matsushima, *Jpn. J. Appl. Phys., Suppl.* 2, Part 1, p. 761 (1974).
36. H. J. Stein, *J. Electron. Mater.* 5, 161 (1976).
37. D. A. Anderson and W. E. Spear, *Philos. Mag.* 35 1A (1976).
38. Y. Catherine and G. Turban, *Int. Round Table, 3rd Symp. Plasma Chem., IUPAC, Limoges, Fr.* Pap. RT2 (1977).
39. J. R. Hollahan, unpublished results (1977).
40. H. Kobayashi, A. T. Bell, and M. Shen, *J. Appl. Polym. Sci.* 17, 885 (1973).
41. M. H. Brodsky, M. A. Frisch, and J. F. Ziegler, *Appl. Phys. Lett.* 30, 561 (1977).
42. W. E. Spear, P. G. LeComber, S. Kinmond, and M. H. Brodsky, *Appl. Phys. Lett.* 28, 105 (1976).
43. W. E. Spear and P. G. LeComber, *Philos. Mag.* 33, 935 (1976).

44. H. Katto and Y. Koga, *J. Electrochem. Soc.* 118, 1619 (1971).
45. S. B. Hyder and T. O. Yep, *J. Electrochem. Soc.* 123, 1721 (1976).
46. J. F. O'Hanlon, *J. Vac. Sci. Technol.* 7, 330 (1970).
47. C. J. Dell'Oca, D. L. Pulfrey, and L. Young, *in* "Physics of Thin Films" (M. H. Francombe and R. W. Hoffman, eds.), Vol. 6, p. 1. Academic Press, New York, 1971.
48. S. Veprek and J. Roos, *J. Phys. Chem. Solids* 37, 554 (1976).
49. H. Khajezadeh and A. S. Rose, *Annu. Proc. Reliab. Phys. [Symp.], 15th* p. 244 (1977).
50. J. A. Ferro, *Annu. Proc. Reliab. Phys. [Symp.] 15th* p. 125 (1977).
51. F. W. Hewlett, Jr. and W. D. Ryden, *Int. Electron. Devices Meet., Washington, D.C.* pp. 304–307 (1976).
52. W. D. Ryden, E. F. Sabuda, and W. van Gelder, *Int. Electron. Devices Meet., Washington, D.C.* pp. 597–600 (1976).
53. D. E. Carlson and C. R. Wronski, *Appl. Phys. Lett.* 28, 671 (1976).
54. V. M. Kolotyrkin, A. B. Gilman, and A. K. Tsapuk, *Russ. Chem. Rev.* 36, 579 (1967).

IV-2

Glow Discharge Polymerization

H. YASUDA

Department of Chemical Engineering
University of Missouri–Rolla, Rolla, Missouri

I. INTRODUCTION

When an organic vapor is injected into a glow discharge of an inert gas such as argon, or when a glow discharge of a pure organic vapor is created, the deposition of polymeric films onto an exposed surface is

ISBN 0-12-728250-5.

often observed. Polymer formation that occurs in such a process is generally referred to as plasma polymerization or glow discharge polymerization.

The recognition of thin film formation by glow discharge polymerization can be traced back to 1874 [1, 2]. However, in most cases the polymers were considered as by-products of an electric discharge [3–9] and, consequently, little attention was paid either to the properties of those polymers (undesirable by-products) or to the process as a means of forming polymers.

Only in relatively recent years (about the 1950s) has glow discharge been utilized in a practical way to make a special coating on metals. Once some of the advantageous features of plasma coating (e.g., flawless thin coatings, good adhesion to the substrate, chemical inertness, and low dielectric constant) were recognized, much applied research on the use of the process was done. The literature cited here [10–63] represents only some of the early investigations.

In this chapter, the significance of glow discharge polymerization as a process for forming thin films is discussed. The emphasis is placed on the process aspect, but not on reactions or mechanisms of polymerization. For details of general chemical reactions in plasma and the fundamental aspects of plasma or glow discharge, the reader is advised to consult the general references cited in Baddour and Timmins [64], McTaggert [65], Gould [66], Venugopalan [67], Hollahan and Bell [68], and Shen [69].

In order to distinguish the term *plasma polymerization*, which is used to describe a special kind of polymer formation mechanism in glow discharge, the term *glow discharge polymerization* is used in this chapter to refer to plasma polymerization in the wider meaning. Therefore, in the context used in this chapter, *plasma polymerization* refers to polymerization mechanisms that constitute a portion of the glow discharge polymerization.

II. CHARACTERISTIC ASPECTS OF GLOW DISCHARGE POLYMERIZATION

A. Glow Discharge Polymerization

Although the phenomenon of polymer formation in a glow discharge is referred to as *glow discharge polymerization*, the terminology of *polymerization* may not represent the actual process of forming a polymer, or the word "polymerization" may even be misleading. The conventional meaning of *polymerization* is that the molecular units (monomers) are linked

together by the *polymerization* process. Therefore, the resultant polymer is conventionally named by "poly + (the monomer)". For instance, the polymer formed by the polymerization of styrene is named *polystyrene*. In this conventional context, polymerization refers to molecular polymerization—i.e., the process of linking molecules of a monomer.

In a strict sense, polymerization in the conventional context does not represent the process of polymer formation that occurs in a glow discharge—although such polymerization may play a role, depending on the chemical structure of a monomer and also on the conditions of the glow discharge.

In contrast to conventional polymerization—i.e., molecular polymerization—polymer formation in glow discharge may be characterized as elemental or atomic polymerization. That is, in glow discharge polymerization, the molecular structure of a monomer is not retained, and the original monomer molecules serve as the source of elements which will be used in the construction of large molecules. Therefore, glow discharge polymerized styrene is not polystyrene. Also, glow discharge polymerized benzene is not polybenzene, but glow discharge polymers of styrene and of benzene are very much alike.

Because of this characteristic nature of the polymer formation process, the starting compound cannot be considered to be the monomer in the conventional context used in relation to the corresponding polymer. A compound used in glow discharge polymerization is merely a starting material in the process.

A polymer formed by glow discharge polymerization cannot be identified by the starting material since the molecular structure of the starting material is not retained in the polymer structure. This leads to another important point—the glow discharge polymerization or polymers formed by glow discharge of a starting material are highly dependent on the system or conditions under which the polymer is formed.

In other words, glow discharge polymerized styrene is not polystyrene, and there is no material that can be fully identified as *glow discharge polymerized styrene*. Not enough emphasis has been placed on the latter aspect, perhaps due to the somewhat misleading use of the word *polymerization*, and also due to an a priori concept of *polymerization* and lack of the distinction mentioned above.

It should be noted here that a polymer similar to polystyrene can be formed by using an electric discharge process if conditions are chosen to favor conventional polymerization of styrene. Even in such a case, the polymer that is formed is generally not quite equivalent to the conventional polystyrene because polymer formation that is characterized by atomic polymerization usually occurs simultaneously. The balance be-

tween different polymer formation mechanisms is indeed an important factor which contributes to the system-dependent nature of glow discharge polymerization.

B. Overall Mechanism of Polymer Formation in a Glow Discharge

The individual steps or reactions that are involved in the process of polymer formation in a glow discharge are extremely complex; however, several important types of phenomena can be identified in order to construct a general picture of glow discharge polymerization. The process involved can be represented schematically, as in Fig. 1 [70]. Glow discharge polymerization can be considered to consist of two major types of polymerization mechanisms. The direct route is *plasma-induced polymerization* and another is *plasma polymerization*. Plasma-induced polymerization is essentially the conventional (molecular) polymerization triggered by a reactive species that is created in an electric discharge. In order to form polymers by plasma-induced polymerization, the starting material must contain polymerizable structures such as olefinic double bonds, triple bonds, or cyclic structures.

Plasma (atomic) polymerization is a unique process which occurs only in a plasma state. This polymerization can be represented by:

initiation or reinitiation

$$M_i \rightarrow M_i^*$$
$$M_k \rightarrow M_k^*$$

propagation and termination

$$M_i^* + M_k^* \rightarrow M_i - M_k$$
$$M_i^* + M_k \rightarrow M_i - M_k,$$

where i and k are the numbers of repeating units (i.e., $i = k = 1$ for the starting material) and M* represents reactive species which can be an ion of either charge, an excited molecule, or a free radical, produced from M but not necessarily retaining the molecular structure of the starting material (i.e., M can be a fragment, or even an atom detached from the original starting material).

In *plasma polymerization*, the polymer is formed by the repeated stepwise reaction described above. It should be noted that *plasma-induced polymerization* does not produce a gas phase by-product, since the polymerization proceeds via utilization of polymerizable structure. Plasma-induced polymerization may be schematically represented by a chain propagation mechanism as follows:

$$M^* + M \rightarrow MM^*$$
$$M_i^* + M \rightarrow M_i^* + 1 \quad \text{propagation}$$
$$M_i^* + M_k^* \rightarrow M_i - M_k \quad \text{termination.}$$

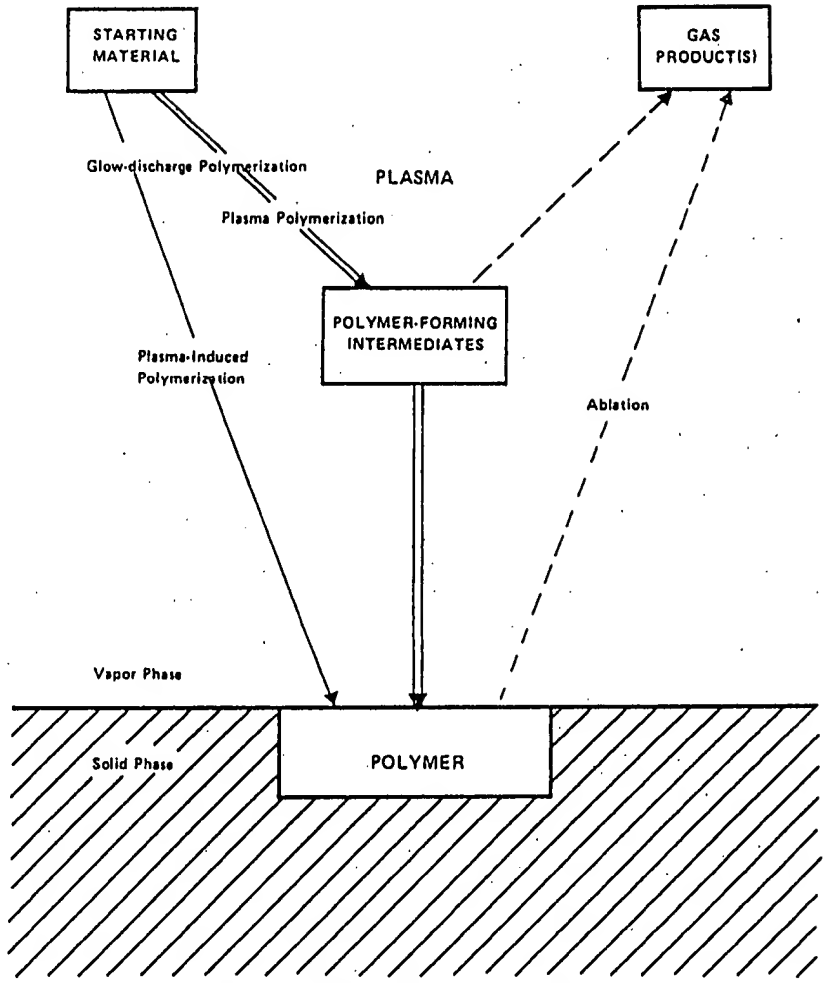

Fig. 1. Overall mechanism of glow discharge polymerization.

It should be emphasized that general polymerization in a glow discharge consists of both *plasma-induced polymerization* and *plasma polymerization*. Which one of these two polymerization mechanisms plays the predominant role in the polymer formation in a glow discharge is dependent not only on the chemical structure of the starting materials, but also on the conditions of the discharge.

Nonpolymer-forming gas products are produced in the process of forming reactive (polymer-forming) intermediates and also in the process

of decomposition (etching) of the polymer deposit or of the substrate material. Since polymer-forming species do not stay in the gas (plasma) phase long enough, the major portion of the gas phase of a polymer-forming glow discharge consists of the product gas when a high conversion ratio of a starting material to a polymer is obtained. This is an extremely important factor; however, it has been dealt with lightly or has been completely neglected in most work appearing in the literature.

The characteristics of the product-gas plasma play the predominant factor in determining the extent of the ablation process, which is shown in Fig. 1. Since the majority of work on glow discharge polymerization appearing in the literature is with hydrocarbons—which produce hydrogen as the product gas—the effect of ablation happened not to be great. Consequently, the complete neglect of ablation did not make a significant difference in the overall picture of glow discharge polymerization. However, when a fluorine- or oxygen-containing compound is used as the starting material, the image of glow discharge polymerization that is built around that of hydrocarbons is completely shattered. With such a compound as the starting material, the extent of ablation becomes the predominant factor, and the extent of polymer formation is entirely dependent on the extent of the product-gas formation.

Perhaps, the most dramatic demonstration of the ablation effect has been recently shown by Kay [71] for glow discharge polymerization of CF_4. It had been thought that CF_4 was one of the very few organic compounds that does not polymerize in glow discharge. On the other hand, CF_4 has been used as one of the most effective gases in plasma etching. Kay has observed that no polymer deposition occurs under normal conditions in spite of the fact that C—F bonds are broken in the glow discharge, which is confirmed by mass-spectroscopic analysis of the gas phase. However, when a small amount of hydrogen is introduced into the discharge, deposition of polymer is observed. When the hydrogen flow is stopped, ablation of the polymer deposit occurs.

The situation observed in the above example may be visualized by the comparison of bond energies shown in Table I. It should be noted that the energy level involved in a glow discharge is high enough to break any

Table I

Comparison of Bond Energies

Bond	Energy, kcal/mole	Bond	Energy, kcal/mole
C—C	80	C—F	102
C=C	142	H—H	104
C≡C	186	F—F	37
C—H	99	H—F	135

bond [72, 73] (i.e., C—F is also broken although C—F is stronger than C—H). The important point is the stability of the product gas. The bond energy for F—F is only 37 kcal/mole, whereas H—F is 135 kcal/mole, which is higher than 102 kcal/mole for the C—F bond. The introduction of H_2 into the monomer flow evidently produces HF and removes F from the discharge system, thus reducing the etching effect by F_2 plasma. Although the term F_2 plasma is used to describe the effect of detached F in plasma, F_2 is not detected in the plasma state, perhaps due to its extremely high reactivity [74].

It is interesting to note that F and O are two elements which reduce the rate of polymer formation from compounds that contain one of these elements. These two elements are the two most electronegative elements among all elements. Of course, the bond energy itself is not a measure of the etching effect of plasma. For instance, the N—N bond is only 32 kcal/mole. However, N_2 plasma does not etch polymer surfaces; instead, the incorporation of N into the surface predominates [75]. Nevertheless, the importance of the ablation process shown in Fig. 1 seems to be well demonstrated by the poor polymer formation in glow discharge polymerization of CF_4 and oxygen-containing compounds [76].

The polymer formation and properties of polymers formed by glow discharge polymerization are controlled by the balance among *plasma-induced polymerization*, *plasma polymerization*, and ablation; i.e., polymer formation is a part of the competitive ablation and polymerization (CAP) scheme shown in Fig. 1. The kind of conditions that affect these balances will be explained in the following section. Because of this CAP scheme of glow discharge polymerization, gas evolved from substrate materials also plays an important role, particularly at the early stage of coating.

III. PROCESSING FACTORS OF GLOW DISCHARGE POLYMERIZATION

It is extremely important to recognize the difference between polymer-forming and nonpolymer-forming plasmas in order to understand the true meaning of the processing factors of glow discharge polymerization. Not all glow discharges yield polymer deposition. For instance, plasmas of Ar, Ne, O_2, N_2, and air are typical nonpolymer-forming plasma. The significance of polymer-forming plasmas, such as glow discharges of acetylene, ethylene, styrene, benzene, etc., is that a considerable portion or the majority of molecules of starting material leave the gas (plasma) phase and deposit as a solid polymer.

In contrast to polymer-forming plasmas, the total number of gas phase molecules in nonpolymer-forming plasmas do not change. Only a portion

of gas molecules are repeating the process of being ionized, excited, and quenched. However, the total number of gas molecules remains constant. This situation can be visualized by the pressure change that occurs before, during, and after the glow discharge. In the case of a nonpolymer-forming plasma, no pressure change is observed unless a material which reacts with excited species of plasma is placed in the discharge system [77, 78]. The system pressure of a polymer-forming plasma changes as soon as discharge is initiated. The pressure change is dependent on the characteristic nature of the starting material, which is related to the product-gas formation described in the previous section. With starting materials that yield very little product gas (e.g., acetylene, benzene, styrene), the system pressure drops to nearly zero when a high polymerization yield is obtained. In other words, an efficient plasma polymerization is an excellent vacuum pump, whereas a nonpolymer-forming plasma has no characteristic of this nature.

Unfortunately, most fundamental work on the plasma state was done with nonpolymer-forming plasmas, and the concept of the operational parameters used in such studies cannot be applied directly to polymer-forming plasmas.

Characteristic polymer deposition by glow discharge polymerization occurs onto surfaces exposed to (directly contacting) the glow. Some deposition of polymer occurs on surfaces in nonglow regions (but the deposition rate is orders of magnitude smaller). The surface on which a polymer deposits could be an electrode surface, a wall surface, or a substrate surface suspended in the glow region. Another important factor that must be considered in dealing with operational factors of glow discharge polymerization is that glow discharge polymerization is system dependent. Consequently, polymer deposition rates are dependent on the ratio of surface to volume of glow. Therefore, other operational parameters such as flow rate, system pressure, and discharge power are insufficient parameters for the complete description of glow discharge polymerization. Such parameters serve as empirical means of describing operational conditions of glow discharge polymerization in a particular system, but they should not be taken beyond this limitation.

The following operational factors are important; however, all factors influence glow discharge polymerization in an interrelated manner. Therefore, any single factor cannot be taken as an independent variable of the process.

A. Modes of Electric Discharge

Electric power sources with frequencies in the 0 (dc) to gigahertz (microwave) range can be used for glow discharge polymerization. The use of

a low frequency electric power source (up to about the audio frequency range) requires internal electrodes. With higher frequencies, external electrodes or a coil also can be used. Typical combinations of discharge modes and reactor design are shown schematically in Fig. 2.

The use of internal electrodes has the advantage that any frequency can be used. The glow discharge is more or less restricted to the space between electrodes. The best glow discharge is obtained with internal electrodes at a relatively high pressure (>0.1 Torr). At lower pressure, the glow discharge expands beyond the space between electrodes. At low pressure (<0.02 Torr), the glow occurs mainly in the space outside of the gap between the electrodes, and the system becomes inefficient for glow discharge polymerization. In order to restrict the glow to the space between the electrodes in the low pressure range, it is necessary to employ magnetic enhancement. Under typical conditions, polymer deposition occurs mainly onto the electrode surface. With a high frequency (rf range)

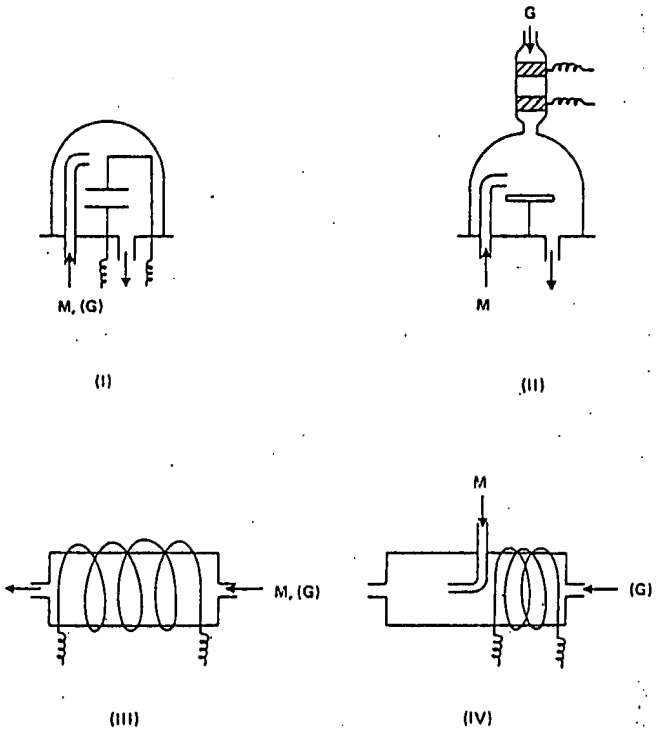

Fig. 2. Schematic representation of some typical arrangements of electric discharge, flow of starting material M, (and carrier gas G), and the location of polymer deposition.

power source, the glow tends to stray away from the space between the electrodes; however, because of this tendency, polymer deposition onto a substrate surface placed in between the electrodes increases [79].

The systems that employ external electrodes or a coil are suited for large volume glow discharges. They are particularly suited for the utilization of the tail-flame portion of the glow discharge. The tailflame refers to the glow discharge away from the energy input region (under external electrodes or coil).

Whether a substrate is placed in the energy input region or placed in the tail flame—or in the case of an internal electrodes system, whether a substrate is placed directly onto the electrode surface or placed in between electrodes—plays an important role in the properties of the polymer formed [70, 80–82]. The relative location of the energy input and the polymer deposition is an important factor to be considered in view of the CAP scheme of glow discharge polymerization (Fig. 1) in which the substrate material also plays an important role in glow discharge polymerization.

B. Flow Rate

The flow rate in most cases of glow discharge polymerization simply refers to the feeding-in rate of the starting materials into the total vacuum system, and it does not necessarily mean the rate at which the starting material is fed to the region of the system where polymerization occurs.

It should be pointed out also that flow rates of a gas in a vacuum system merely represent the total flux of gas but do not represent the velocity of molecules as visualized in the flow of a liquid. The parameter F/p (where F is flow in cubic centimeters (STP) per minute and p the system pressure in atmospheres) is proportional to the velocity of gas molecules in a given flow rate F at pressure p.

C. System Pressure

The system pressure is perhaps the most misunderstood and ill-treated parameter of glow discharge polymerization. This misunderstanding or mistreatment largely stems from the lack of distinction between nonpolymer-forming and polymer-forming plasmas. As mentioned earlier, efficient glow discharge polymerization is an excellent pump. Consequently, the polymerization itself changes the system pressure. Another factor contributing to the misunderstanding is the failure to recognize the effect of product gas. In many cases, the system pressure observed before glow discharge p_0 is cited as though it represents the system pressure during

glow discharge polymerization p_g. Some authors claim that p_g is adjusted to p_0 by controlling the pumping rate. Since p_g is dependent on the production rate of product gas, such an operation is not always possible. Furthermore, in view of the ablation process, which is highly dependent on the amount of product gas, such an operation does not seem to have any advantages or significance in controlling the process.

The following points may clarify the meaning of system pressure in glow discharge polymerization:

(1) The system pressure before glow discharge p_0 at a given flow rate is entirely dependent on the pumping rate [83]; the higher the pumping rate, the lower is the value of p_0.

(2) The pumping rate of a system is dependent on the nature of the gas and is particularly important when a liquid nitrogen trap or a turbomolecular pump is employed in a vacuum system, as shown in Fig. 3. These are excellent pumps for most organic vapors (starting material of glow dis-

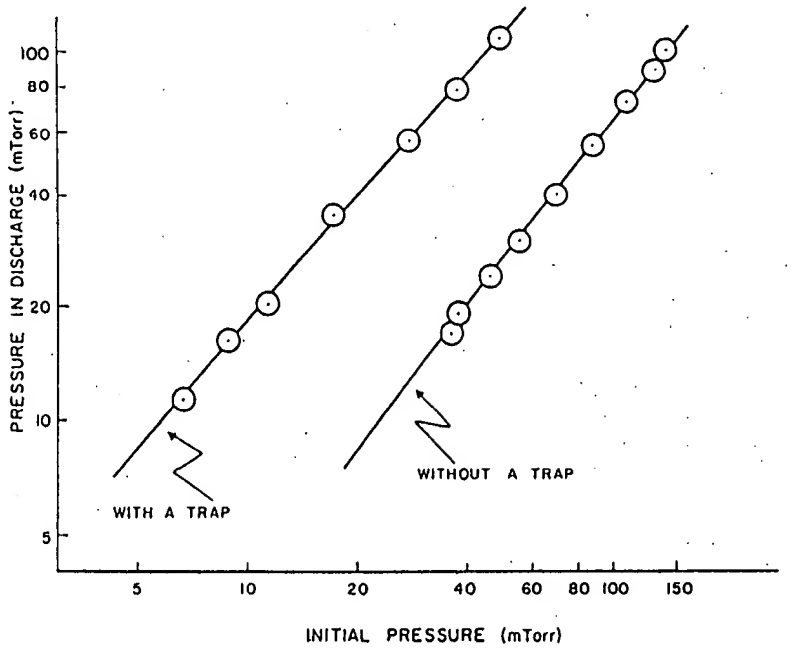

Fig. 3. The dependence of system pressure in the discharge p_g on the initial system pressure p_0, for glow discharge polymerization of ethylene. The initial pressure at a given flow rate is dependent on the pumping rate of the system as shown by the two lines representing systems with and without liquid nitrogen traps.

charge polymerization) and some gases; however, they offer virtually no pumping action for H_2, which is the main product gas when hydrogen-containing compounds are used as the starting material.

(3) As far as the gas phase is concerned, glow discharge polymerization acts as an additional pump.

(4) Glow discharge polymerization changes the gas phase from the starting material to the product gas.

(5) Consequently, the system pressure with the glow discharge on, p_g, is largely determined by the pumping efficiency of the product gas, the efficiency of the polymerization, and the production rate of gas.

(6) Therefore, there is no unique relationship between p_0 and p_g.

In a system where the polymerization yield is maintained at nearly 100%, p_g is determined by the flow rate but not by the value of p_0, as shown in Fig. 4.

Since the velocity of gas molecules is dependent on pressure, the value of p_g (but not p_0) is important in controlling the distribution of polymer deposition and the properties of polymers formed in glow discharge

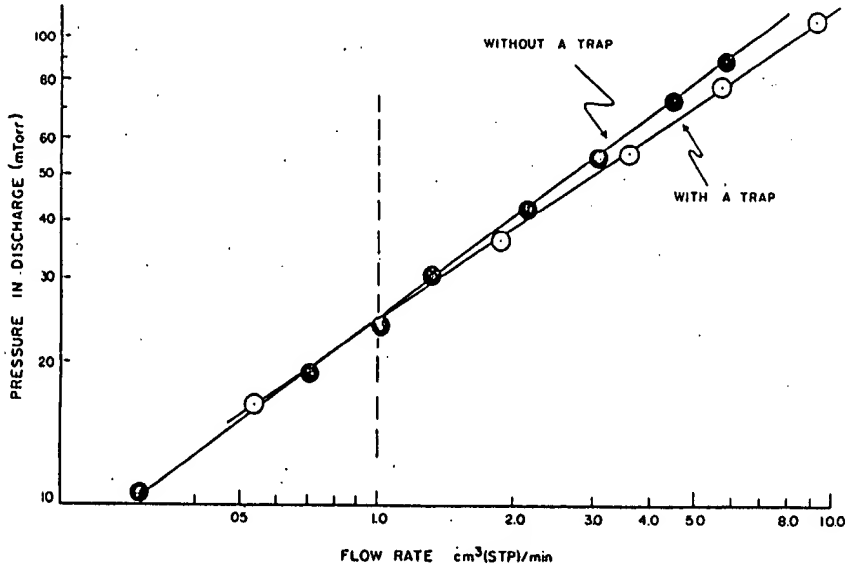

Fig. 4. The dependence of system pressure during the discharge p_g on the flow rate of starting material (ethylene). Despite the difference in p_0's for systems with or without a liquid nitrogen trap, p_g is mainly dependent on the flow rate, indicating that the production rate of the product gas (H_2) and the pumping rate of a system for the product gas determine the value of p_g.

polymerization; however, p_g cannot be considered as a manipulatable processing factor. The value of p_g can be manipulated to a certain extent, but it is largely determined by the nature of the starting material (i.e., gas production rate).

D. Discharge Power

The significance of discharge power in glow discharge polymerization is quite different from that for nonpolymer-forming plasmas. In essence, (the absolute value of) discharge power itself cannot be considered as an independent variable of the operation, since a certain level of discharge power (e.g., 60 W) in a given set of discharge conditions for one starting material (e.g., ethylene) could not even initiate a glow discharge with another starting material (e.g., *n*-hexane) under otherwise identical conditions. In other words, a relative level of discharge power which varies according to the characteristics of starting materials is needed to describe the discharge power for glow discharge polymerization.

In order to understand the importance of the discharge power parameter for glow discharge polymerization, it is very important to recognize the following characteristics of glow discharge polymerization: (1) the starting material is in the gas phase, but the main product is in the solid phase; (2) glow discharge polymerization occurs mainly in the glow region of a reactor; and (3) the glow region of the gas phase is not a simple plasma of the starting material but contains significant amounts of nonpolymer-forming gas product(s). Therefore, in order to describe the discharge power of glow discharge polymerization, it is necessary to express the characteristic power density in the glow volume of a flow system. Consequently, the discharge power level to describe glow discharge polymerization is a system-dependent parameter, not simply the power input into the system.

For instance, the discharge power necessary for glow discharge polymerization (based on the maximum change which occurs in gas phase [84]) of various hydrocarbons is shown in Figs. 5 and 6 as a function of flow rate of the starting material. As seen in these figures, the discharge power necessary for glow discharge polymerization depends on both the molecular weight and chemical structure of the compounds.

The best first-order approach to dealing with this situation is to use the parameter given by W/FM, where W is the power input, F the flow rate given in cubic centimeters (STP) per minute, and M the molecular weight of the starting material [84]. The parameter W/FM represents the power input per unit mass of the starting material. The parameter W/FM does not contain terms that describe the geometric factor of and flow pattern

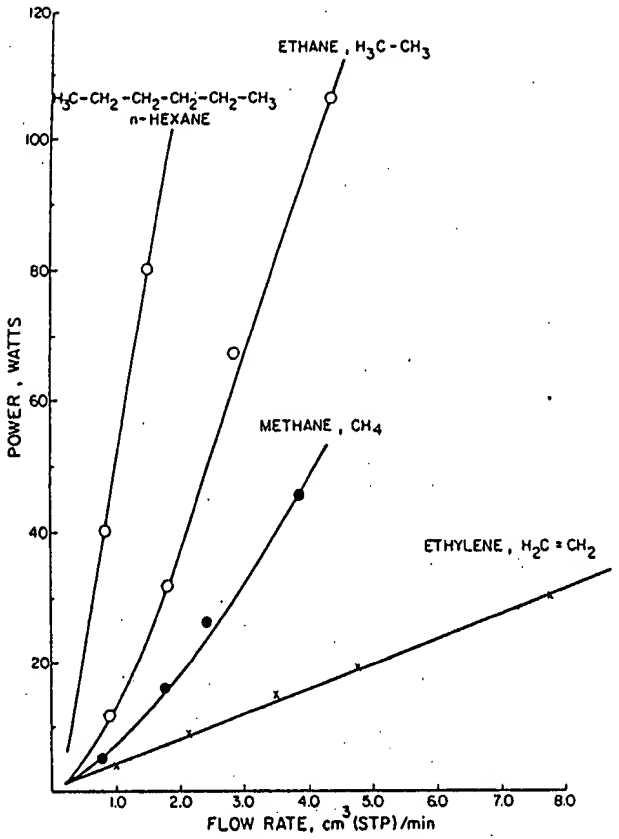

Fig. 5. The dependence of discharge power to obtain a comparable level of glow discharge polymerization on the flow rates of starting materials. The discharge power is greatly dependent on the molecular weights of the starting materials.

within a reactor, and consequently, the absolute value cannot be used in general cases. However, it is a useful parameter to describe glow discharge polymerization of different starting materials in a polymerization reactor.

The wide spread of discharge power shown in Figs. 5 and 6 for various compounds becomes roughly comparable values when $(W/FM)_c$ is plotted against F, as shown in Figs. 7 and 8. The parameter $(W/FM)_c$ represents the values of W/FM given by lines shown in Figs. 5 and 6. The values $[(W/FM)_c]_{F\to 0}$ for various hydrocarbons are nearly constant, dependent only on structures of starting materials. It is worth noting here that the slope observed in the plots of $(W/FM)_c$ versus F is proportional to the

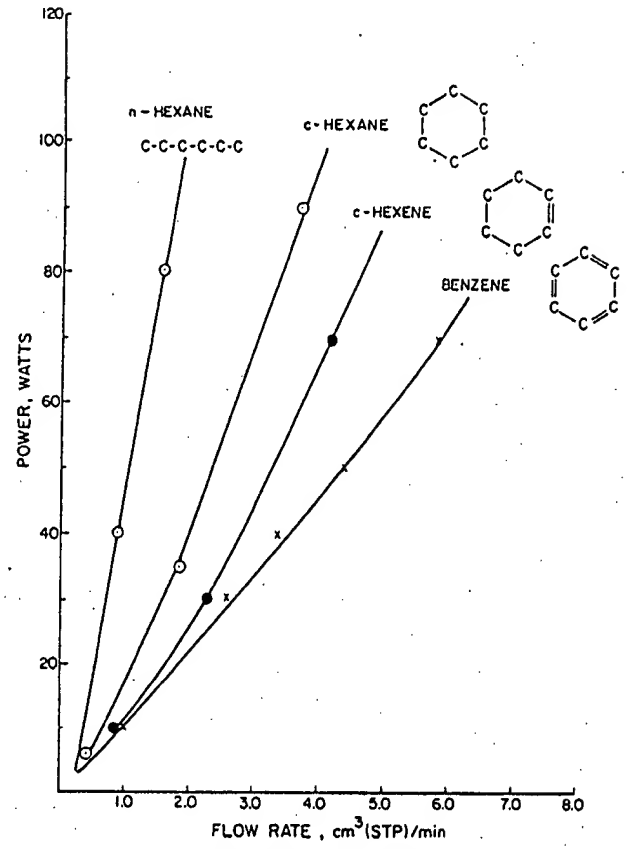

Fig. 6. The dependence of discharge power to obtain a comparable level of glow discharge polymerization on the flow rates of the starting materials for hydrocarbons containing six carbons. The discharge power is also dependent on the structures of starting materials.

hydrogen yield of compounds, as shown in Fig. 9. In order to obtain comparable glow discharge polymerization, the discharge power must be selected according to F and M.

E. Geometrical Factor of Reactor

1. Bypass Ratio of Flow

Not all starting materials fed into a glow discharge polymerization reactor are utilized in the polymer formation. The bypass ratio represents the portion of flow which does not contribute to glow discharge polymer-

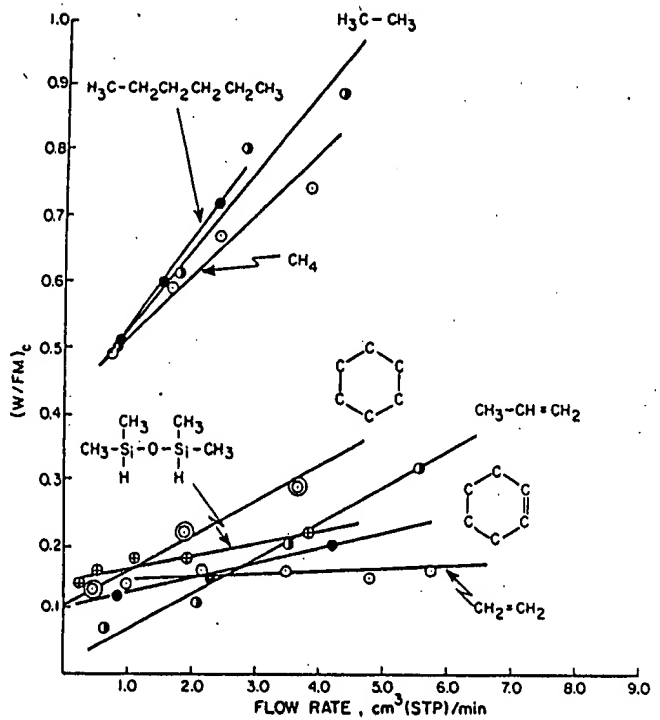

Fig. 7. Plots of $(W/FM)_c$ against the flow rate for various compounds, where W is the discharge power for glow discharge polymerization, F the flow rate, and M the molecular weight of the starting material, and $(W/FM)_c$ represents the values of W/FM given by lines shown in Figs. 5 and 6.

ization. Consequently, the higher the bypass ratio of a reactor is, the lower the conversion of the starting material to the polymer. Clearly, this ratio depends on the ratio of the volume occupied by discharge to the total volume.

2. *Relative Position of Energy-Input and Polymer Deposition*

In glow discharge polymerization which utilizes internal electrodes, either the substrate is placed directly on an electrode surface or in the space between the electrodes.

With external electrodes or a coil, the location of the substrate can be chosen in a variety of ways. Since the polymer properties and the deposition rate are dependent on the location within a reactor, this is an extremely important factor in practical applications. The relative position is further complicated by the factor described below.

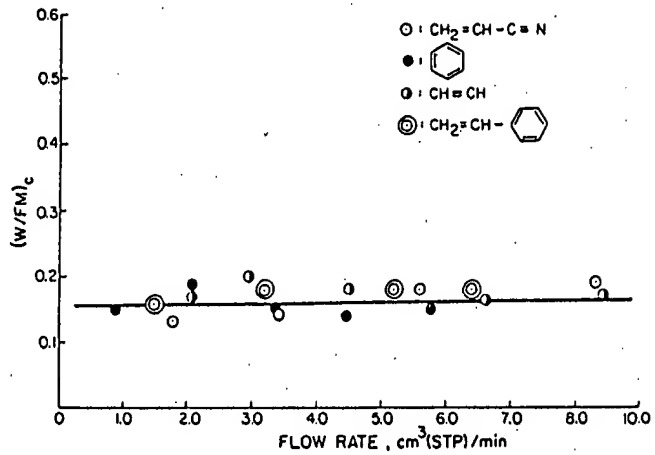

Fig. 8. Plots of $(W/FM)_c$ versus the flow rate of compounds which contain triple bonds and/or aromatic structures. $(W/FM)_c$ is nearly independent of the flow rate for these compounds (see Fig. 7 caption for letter definitions).

3. *Relative Location of the Feed-In of the Starting Material and Flow Pattern*

The location where the starting material is introduced is very important for polymer deposition. The importance of flow pattern with respect to the location of energy input and of polymer deposition can be visualized in an example of glow discharge polymerization in a straight tube reactor with an external coil placed in the middle portion of the tube. In such a system, the volume of glow discharge is generally much larger than the volume of the portion of tube which is directly under the coil. Consequently, polymer deposition occurs even at the upstream side of the coil. The flow can best be established by avoiding all starting materials passing through the energy-input region, as seen in the examples shown in I, II, and IV of Fig. 2. This factor is less obvious in a system with internal electrodes (e.g., in a bell jar).

IV. ORGANIC COMPOUNDS FOR GLOW DISCHARGE POLYMERIZATION

As mentioned in the introduction, nearly all organic compounds can be polymerized by glow discharge polymerization; however, the starting material should not be considered as the monomer (the starting material of polymerization in the conventional concept) of a polymerization process.

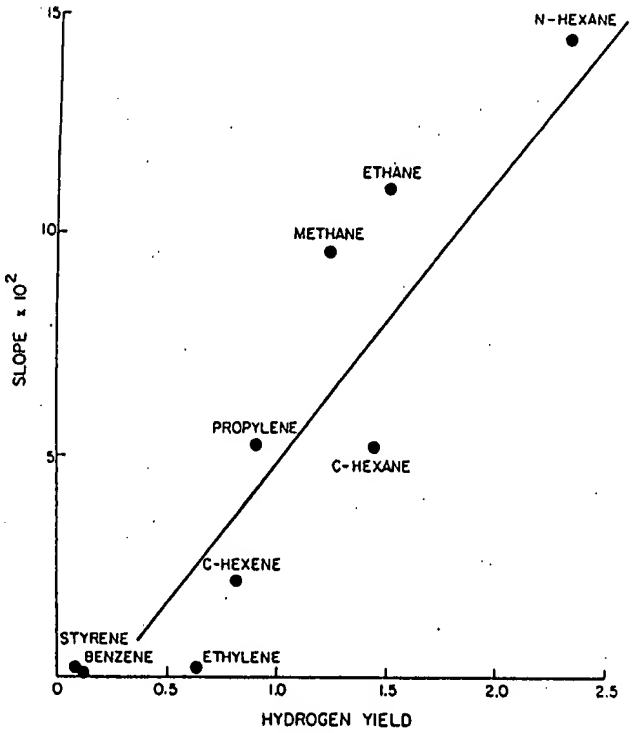

Fig. 9. The dependence of the slopes of $(W/FM)_c$ versus F plots on the hydrogen yield of compounds. The hydrogen yield is the number of hydrogen molecules evolved when a molecule of starting material is incorporated into the glow discharge polymer.

Since glow discharge polymerization can be characterized best as elemental or atomic polymerization, organic compounds can be classified based on elements contained in organic compounds.

A. Hydrocarbons

Hydrocarbons produce H and H_2 as the major nonpolymer-forming gas products. Since H and H_2 plasmas have little etching effect on polymers formed by glow discharge polymerization, the process of forming polymer is least affected by ablation.

Hydrocarbons can be grouped, according to their behavior in glow discharge polymerization, into the following three major groups [85, 86]:

Group I. Triple-bond-containing and aromatic compounds,
Group II. Double-bond-containing and cyclic compounds, and
Group III. Compounds without the above-mentioned structures.

Group I compounds form polymers by utilizing the opening of triple bonds or aromatic structures with the least evolution of hydrogen.

Group II compounds form polymers via both the opening of double bonds or cyclic structures and hydrogen abstraction. Production of hydrogen is considerably higher than in group I compounds.

Group III compounds polymerize primarily by *plasma polymerization* based on hydrogen abstraction. Consequently, hydrogen production is much higher than in those for group II compounds.

Hydrogen production per mole of starting material for typical hydrocarbons is shown in Fig. 10. The discharge power necessary for glow discharge polymerization of hydrocarbons is also dependent on the types of compound. The same groupings mentioned above apply [84]. Groups I and II compounds require approximately the same energy input. However, the dependence on flow rate is nearly zero for group I compounds, but an appreciable increase in the required energy input is observed for group II compounds for increasing flow. Group III compounds require the highest energy input and their dependence on flow rate is much greater than that for group II compounds (see Figs. 7 and 8).

B. Nitrogen-Containing Compounds

Results obtained with various amines and nitriles indicate that N remains in the polymer (nitrogen does not evolve as the nonpolymer-forming product gas) [86]. This tendency is in accordance with another trend that N_2 gas used in a glow discharge is easily incorportated into either glow discharge polymers or polymers used as substrates [75].

C. Fluorine-Containing Compounds

Glow discharge polymerization of fluorine-containing compounds, particularly of perfluoro compounds, is very sensitive to the conditions of polymerization. The use of a relatively low discharge power level is an extremely important factor for obtaining polymers from fluorine-containing compounds. High discharge power causes the detachment of F and enhances ablation. Consequently, it is often observed that no polymer is formed when glow discharge polymerization is carried out at a high discharge power, while the same compound yields polymers at a low discharge power [88]. In order to obtain a polymer by glow discharge poly-

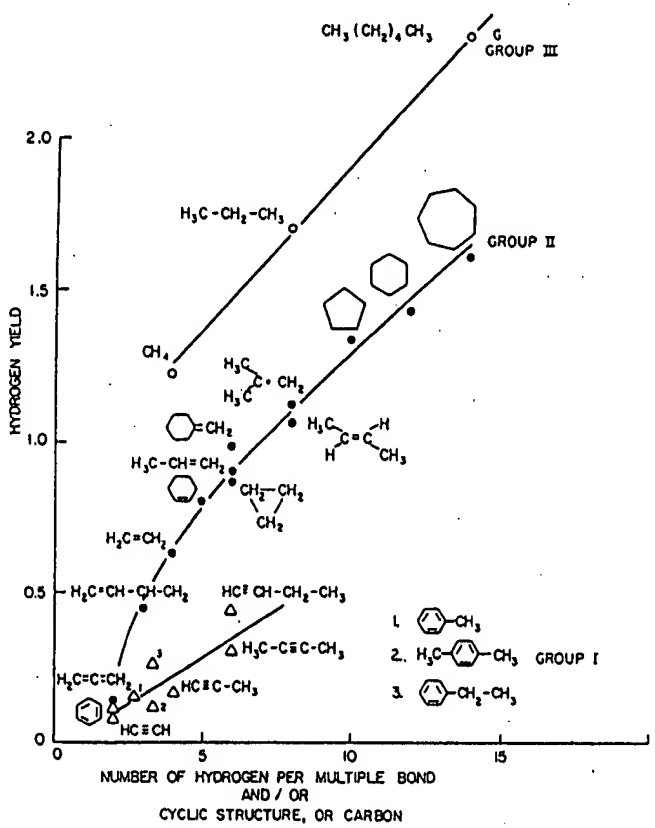

Fig. 10. Number of hydrogen molecules evolved per molecule of starting material when hydrocarbons polymerize (hydrogen yield) as a function of chemical structure.

merization of fluorine-containing compounds, it is advantageous to use compounds which belong to groups I and II mentioned above for hydrocarbons [89], and/or to employ techniques that suppress the etching effect of the detached fluorine (plasma), such as the addition of a small amount of H_2 [71] or hydrogen-producing compounds [90], and use of pulsed or intermittent discharges [89].

D. Oxygen-Containing Compounds

Oxygen is another of two elements (i.e., F and O) that tend to be evolved from either the starting material or substrate material, causing

significant ablation of organic materials. Consequently, oxygen-containing compounds are generally poor starting materials for glow discharge polymerization. The deposition rate of polymers is generally much smaller than that of nonoxygen-containing compounds of similar molecular weight [76]. When oxygen is incorporated in chemical structures mentioned in groups I and II for hydrocarbons (i.e., easily polymerizable structures), glow discharge polymerization proceeds with ease [59, 60].

E. Si-Containing Compounds

Silicon is one of the elements that has a high tendency to stay in the solid phase; therefore, glow discharge polymerization of Si-containing compounds, such as silanes and siloxanes, proceeds extremely well [49, 50, 60]. This, together with the additional factors of relatively high molecular weight and relatively high vapor pressure of silicon-containing compounds, leads to the deposition rate obtainable from silicon-containing compounds being perhaps the highest among a variety of starting materials [60].

F. Compounds Containing Other Elements

Although not enough data are available to judge behavior of compounds that contain other elements in glow discharge polymerization, a simple rule of thumb may be drawn from the CAP scheme of glow discharge polymerization. Elements which are reactive and exist in the gas phase in the normal temperature range favor the ablation process and do not contribute to polymer formation. However, it is possible that many unusual elements which are not incorporated in conventional polymers could be incorporated into thin films formed by glow discharge polymerization.

V. DEPENDENCE OF GLOW DISCHARGE POLYMERIZATION ON PROCESSING FACTORS

In glow discharge polymerization as a means of thin film formation, the following aspects and their dependence upon the operational or processing factors seem to be of utmost practical importance. As mentioned earlier, however, many operational factors affect glow discharge polymerization in a complexly interrelated manner, and none of them can be singled out as being an independent variable or the most important factor of the process. It should also be kept in mind that glow discharge polymer-

ization is system dependent, and consequently, the trends or conclusion based on data obtained in a particular system may not be extended to another system.

A. Rate of Polymer Deposition

In the practical sense, the rate at which a polymer deposits is an extremely important aspect of the process. The rate of polymer deposition can be increased by increasing the characteristic rate of polymer formation (often called polymerization rate), or by increasing the yield of polymer formation (reducing the amount of starting material that leaves the system without being polymerized). Unfortunately, the terms "polymer deposition rate" and "polymerization rate" are often used synonymously.

1. Discharge Power

The polymer deposition rate generally increases with discharge power in more or less linear fashion in a certian range of discharge power, and reaches a plateau, as shown in Fig. 11. Further increase of discharge power often decreases the polymer deposition rate.

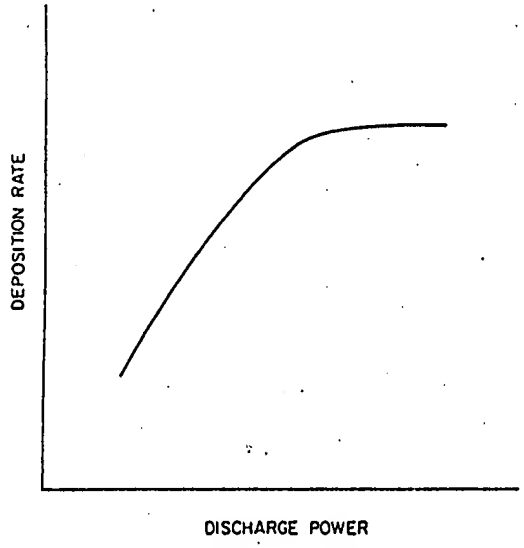

Fig. 11. Schematic representation of the dependence of polymer deposition rate on discharge power when a constant flow rate is employed.

2. Flow Rate

The polymer deposition rate increases linearly with the flow rate of a starting material under ideal conditions where the conversion ratio of starting material to polymer is high or remains at a constant level. However, the change of flow rate is often associated with changes in flow pattern (affecting the yield of polymer formation or bypass ratio of the flow) and/or the efficiency of discharge power input. Therefore, the apparent dependence of the polymer deposition rate on flow rate is often characterized by a decrease of the polymer deposition rate after passing a maximum or a narrow plateau, as shown in Fig. 12.

3. W/FM Parameter

As mentioned earlier, the effect of W or F cannot be determined independently since glow discharge polymerization is dependent on the combined parameter of W/FM. As long as the W/FM value remains above a critical level $(W/FM)_c$ where energy input is sufficient for polymerization, the major effect of increasing the flow rate is to increase the feed-in rate,

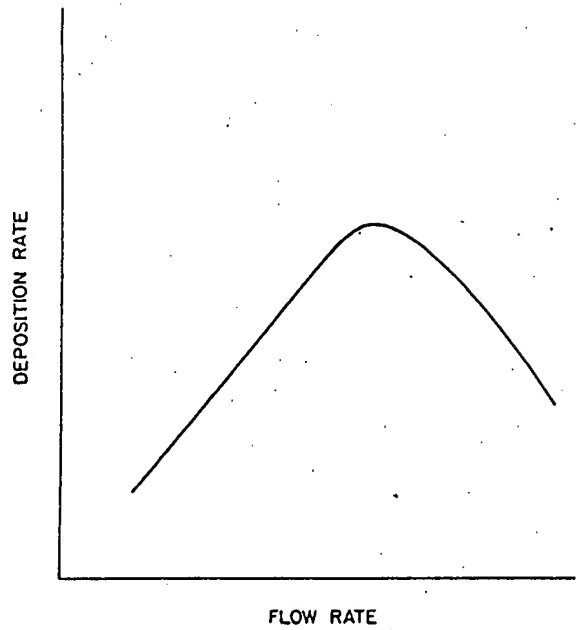

Fig. 12. Schematic representation of the dependence of polymer deposition rate on flow rate of a starting material when a constant discharge power is employed.

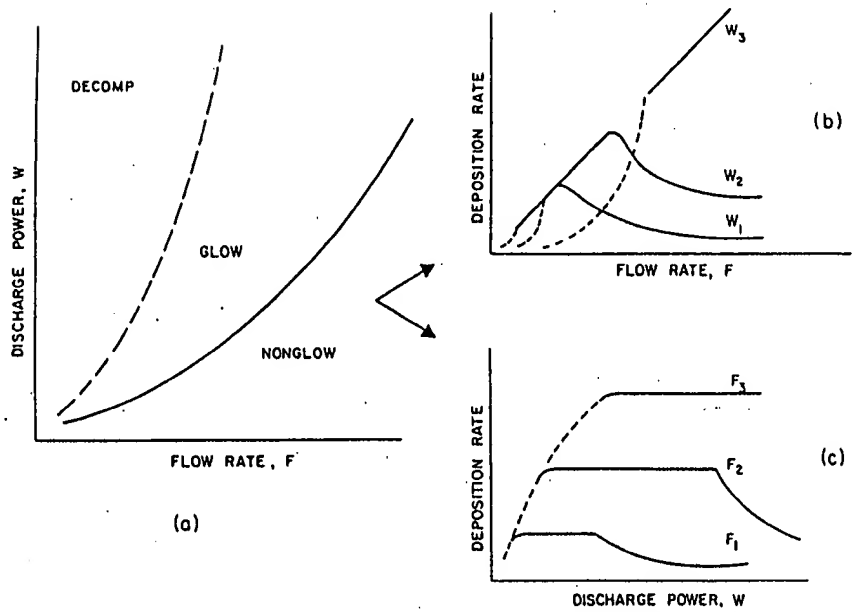

Fig. 13. Schematic representation of the interrelationship of polymer deposition rate with flow rate and discharge power. (a) Indicates the power-flow domains of decomposition (poor polymer deposition due to predominanting ablation process), normal glow where glow discharge polymerization occurs, and nonglow region. (b) and (c) At a fixed level of W or F, change of F or W crosses the domain shown in (a), and consequently, the apparent dependence of polymer deposition rate on either F or W is determined by where the change of domain occurs.

which increases the polymer deposition rate. However, if the W/FM level drops to a certain level as F increases at a constant W, where the discharge power is not sufficient to polymerize all starting materials coming into the reaction system, the polymerization mechanism itself changes. Consequently, the polymer deposition rate decreases despite the fact that more starting materials are supplied to the reaction system. The general situation is shown in the schematic diagrams given in Fig. 13.

According to the W/FM parameter, the discharge power W must be increased as the flow rate of starting materials increases, and/or as the molecular weight of the starting materials increases.

B. Distribution of Polymer Deposition

The distribution of polymer deposition is directly related to the uniformity of the thin film formed by glow discharge polymerization. Distribution

of polymer deposition is dependent on (1) the geometrical arrangement of inlet of starting material, outlet of the system, and region of energy input; (2) the operating pressure of the discharge (not the initial pressure); and (3) the reactivity of a starting material to form polymers. The effects of these factors on the distribution of polymer deposition may be visualized from the data shown in Figs. 14–19 obtained from an rf (inductively coupled) discharge [91–93]. The general trends are as follows:

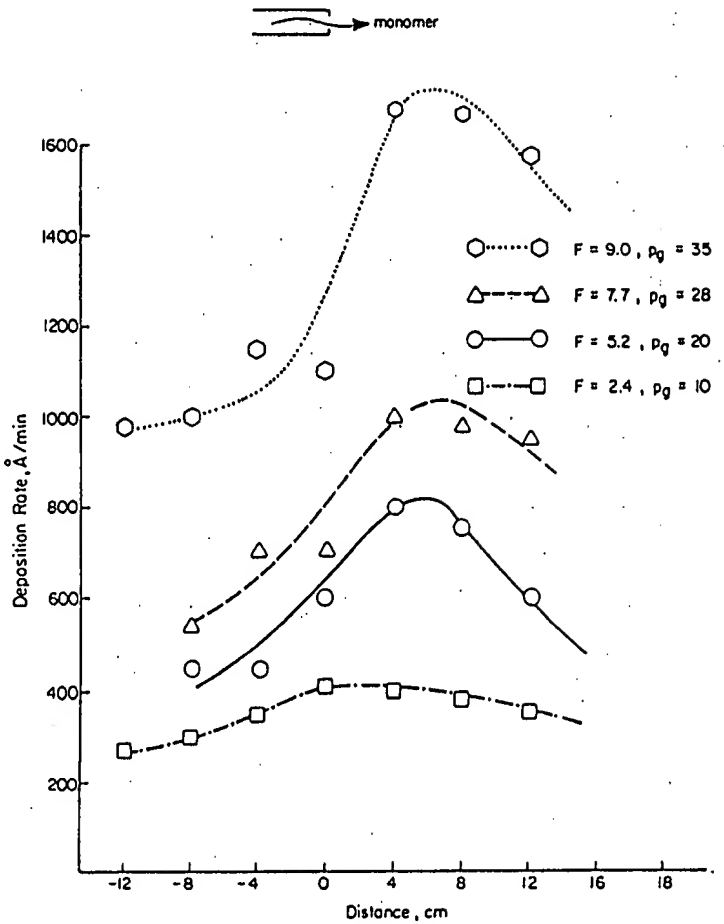

Fig. 14. Distribution of polymer deposition in glow discharge polymerization of acetylene at various flow rates. The letter F denotes flow rate in cm³(STP)/min, and p_g the system pressure in the glow discharge given in mTorr. The distance is taken from the point of the starting material inlet in the direction of flow (see Yasuda and Hirotsu [91] for details of the reactor).

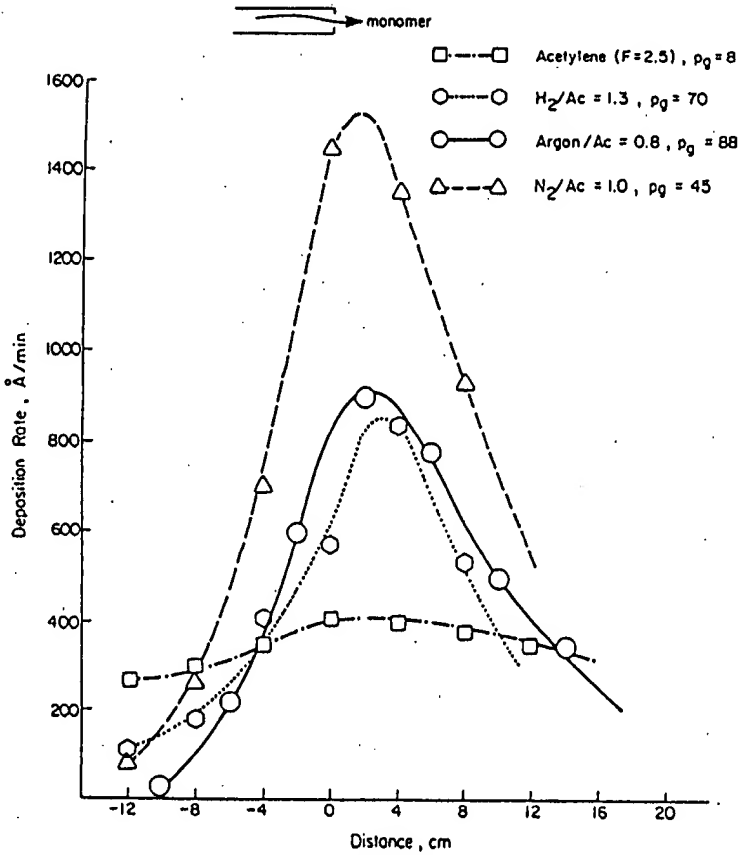

Fig. 15. Distribution of polymer deposition in glow discharge polymerization of acetylene with the addition of a carrier gas. H_2/Ac, Argon/Ac, and N_2/Ac denote the mole ratios of carrier gas to acetylene. The flow rate of acetylene is maintained constant in all cases. Other notation and units are the same as those in Fig. 14.

(1) The lower the discharge pressure, the wider is the distribution of polymer deposition. The lower the pressure, the larger is the mean free path of gas molecules and the diffusional displacement becomes more efficient. Therefore, the polymer formation is not localized at either the region of excitation or site of introduction of the starting material.

(2) The higher the reactivity of the starting material (to form polymer), the narrower is the distribution curve of polymer deposition, which has the maximum in the vicinity of the starting material inlet.

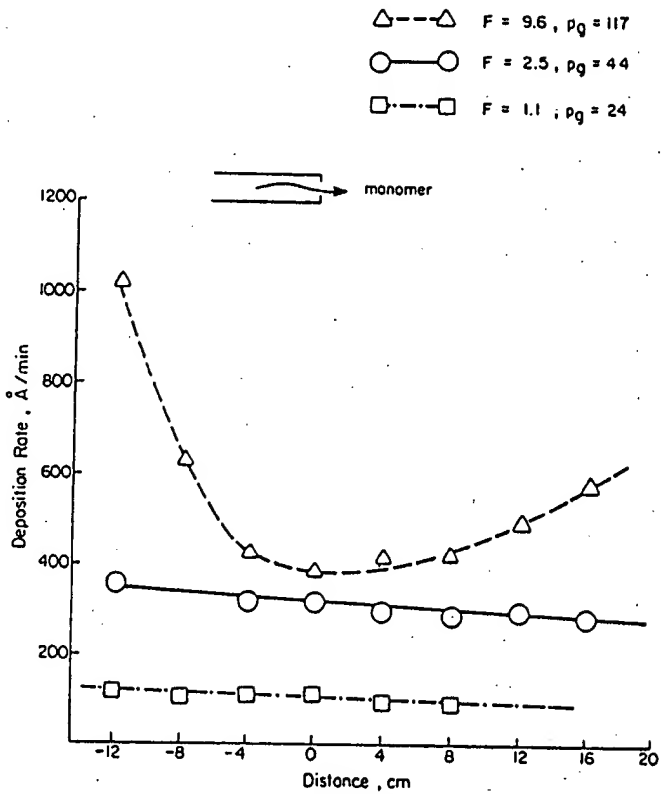

Fig. 16. Distribution of polymer deposition in the glow discharge polymerization of ethylene. All notation and units are the same as those in Fig. 14. Ethylene is a less reactive material than acetylene, as far as glow discharge polymerization is concerned. The increase of flow rate yields a maximum of deposition in the downstream side of the inlet, consequently, the apparent minimum is observed near the inlet.

(3) With starting materials that have low reactivity, the maximum peak is shifted towards the downstream side of the inlet. Consequently, the minimum (rather than the maximum) in the distribution curve is often observed at the vicinity of the inlet.

(4) Addition of nonpolymer-forming gas (e.g., Ar) tends to narrow the distribution curve.

The distribution of polymer deposition onto the surface of internal electrodes is generally very smooth, unless the starting material inlet is placed too close to the electrodes or too small an electrode gap (in relation

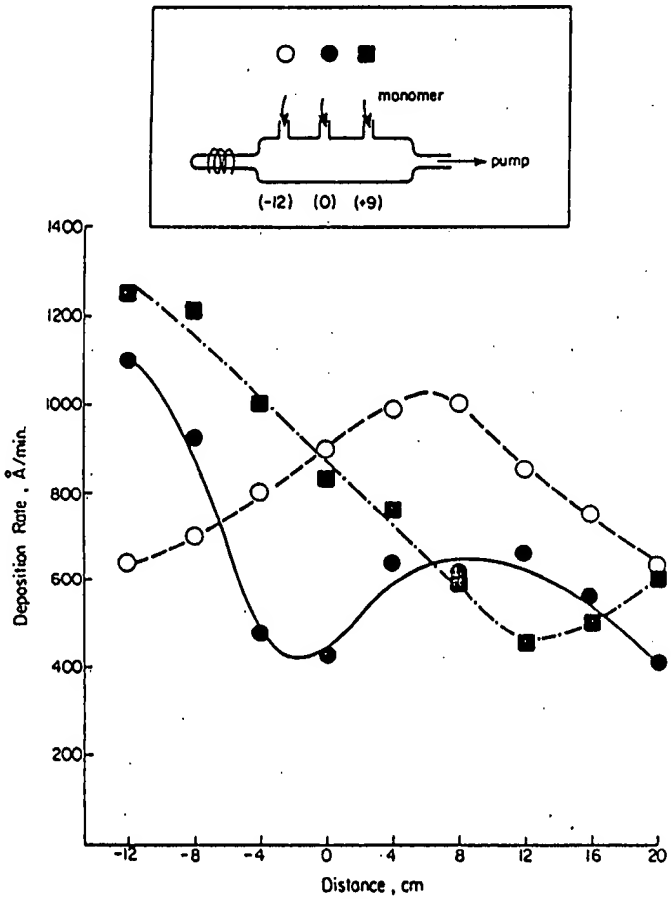

Fig. 17. The effect of location of the starting material (ethylene) inlet on the distribution of polymer deposition. The location of the inlet is shown in the insert. The flow rate of ethylene is maintained constant (F = 9.8 cm³(STP)/min) in all cases.

to the mean free path of gases) is employed. The effect of inlet–outlet locations in a bell-jar-type reactor is shown in Fig. 20 [94].

Regardless of the mode of electric discharge or type of reactor, the region where glow discharge polymerization occurs is located in the direct or tortuous pathway of the starting material from the inlet to the outlet. On this pathway, starting material is consumed to form a polymer, and simultaneously the gas phase changes from the starting material to the gas

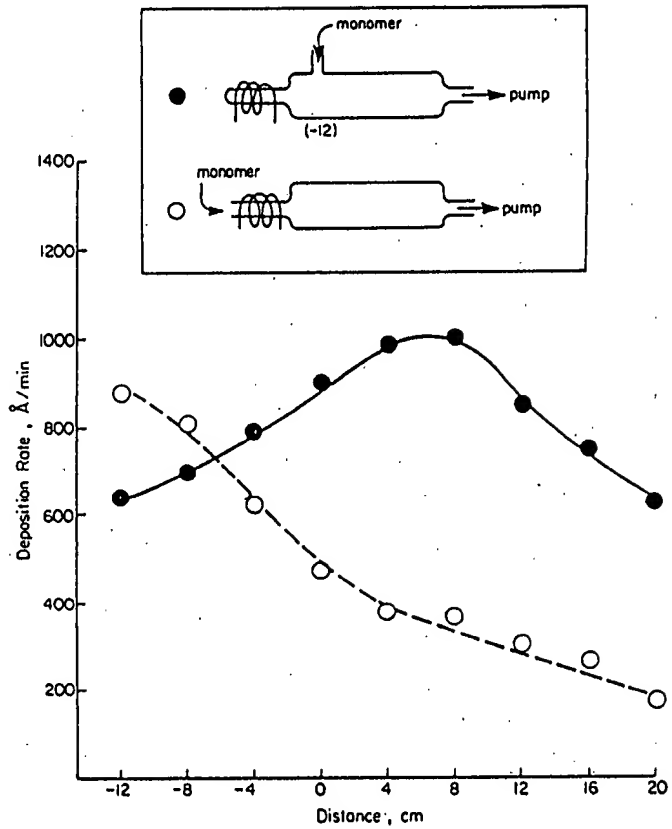

Fig. 18. The effect of flow passing through the rf coil (energy input region) on the distribution of polymer deposition in glow discharge polymerization of ethylene. F = 9.8 cm³(STP)/min for both cases.

product as polymerization proceeds. Therefore, an uneven distribution always exists if the polymer is collected on a stationary substrate surface. A moving substrate will average out this inherent uneven distribution of polymer deposition, and provide a practical means of yielding a uniform coating.

The distribution of polymer deposition should be taken into consideration when the polymer formation is monitored at a fixed location. The shift of the distribution curve due to changes in operational factors could be misinterpreted as a change in the polymer deposition rate itself.

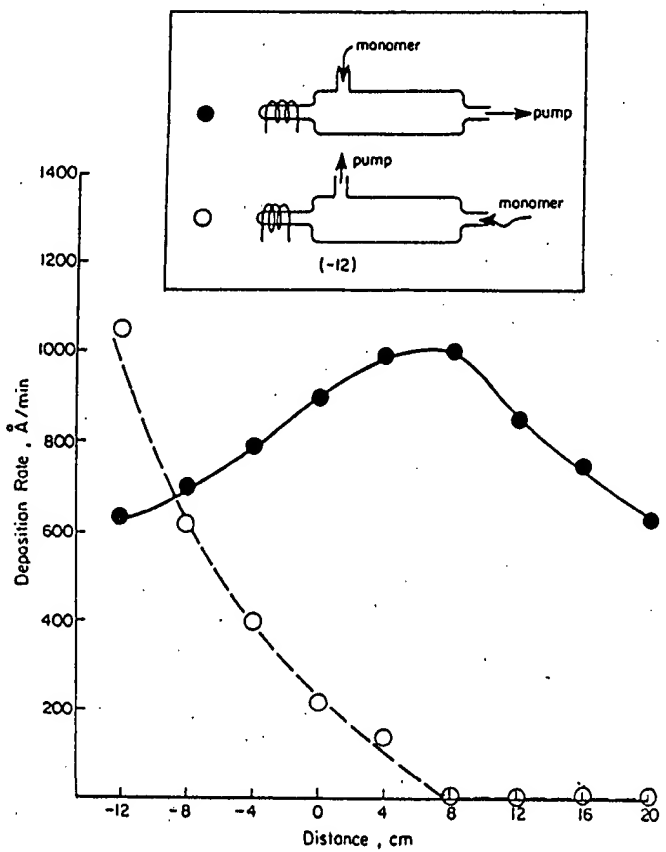

Fig. 19. The effect of direction of flow in relation to the rf coil (energy input region) on the distribution of polymer deposition in glow discharge polymerization of ethylene. All other conditions are maintained constant for both cases.

C. Properties of Polymers

Since glow discharge polymerization is system dependent, the properties of polymers formed by glow discharge polymerization are also dependent on the conditions of the process. The properties of polymers are dependent not only on the kind of reactor used but also on the location within a reactor where polymer deposition occurs.

The diagrams presented in Fig. 21 [95] show what kinds of polymers are formed from a given starting material, depending upon the apparent operational factors described. Because the strict meaning of parameters,

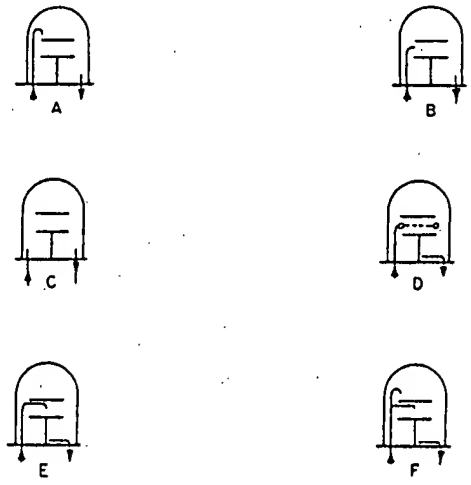

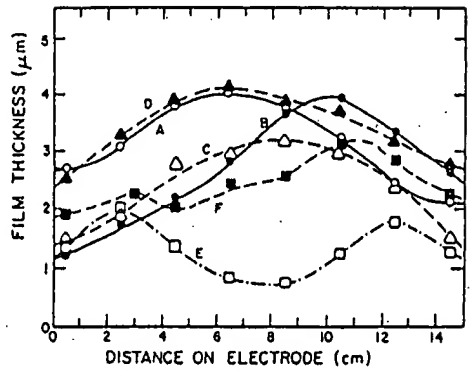

Fig. 20. Effect of relative location of starting material inlet, outlet, and electrodes on the distribution of polymer deposition onto electrode surfaces. p, 2 Torr; P, 100W; F, 80cm³/min (see Kobayashi *et al.* [97] for details of conditions).

such as flow rate and pressure, depends on the geometrical factors of a reactor and the type of starting material, generalization of trends should not be made from such a diagram. However, it clearly shows the important fact that the properties of polymers formed by glow discharge polymerization are entirely dependent on how the polymerization is carried out.

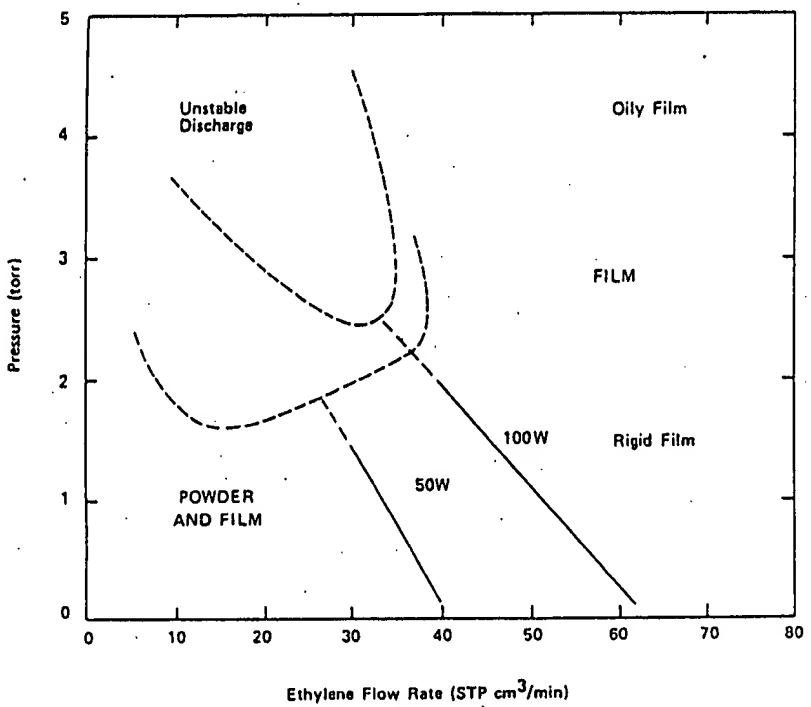

Fig. 21. An example of the dependence of the type of polymer formed on the apparent operational factors of power, pressure, and flow rate.

Analysis of polymers collected in different sections of a system, and of polymers formed by different electric discharges, also shows considerable differences in their properties [96, 97].

A study of the properties of polymers formed from tetrafluoroethylene by glow discharge polymerization and investigated by electron spectroscopy for chemical analysis (ESCA) [98] provides further evidence of the importance of processing factors. Tetrafluoroethylene is an ideal starting material to illustrate the CAP scheme of glow discharge polymerization. Therefore, some results are shown in Figs. 22–24.

The ESCA C1s spectrum of conventionally prepared polytetrafluoroethylene shows a single intense peak at 292 eV corresponding to the $—CF_2—$ carbon bond. The peaks at binding energy levels of less than 291 eV represent the presence of cross-links (>CF—, >CC<) and carbons bonded to other substituents, including nitrogen- and oxygen-containing groups.

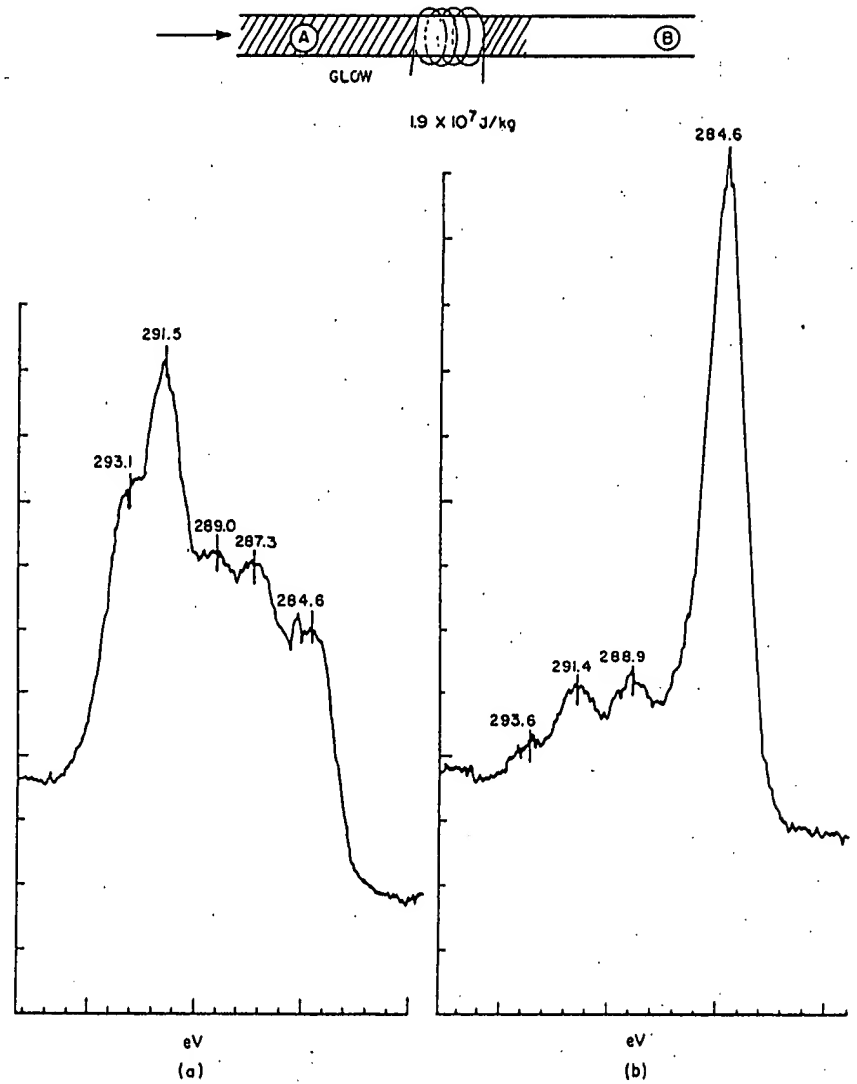

Fig. 22. Dependence of the ESCA C1's peaks of glow discharge polymers of tetrafluoroethylene on discharge conditions and the location of polymer deposition. Polymer deposit occurred at two locations (a) before the rf coil and (b) after rf coil. Discharge power level is 1.9×10^7 J/kg.

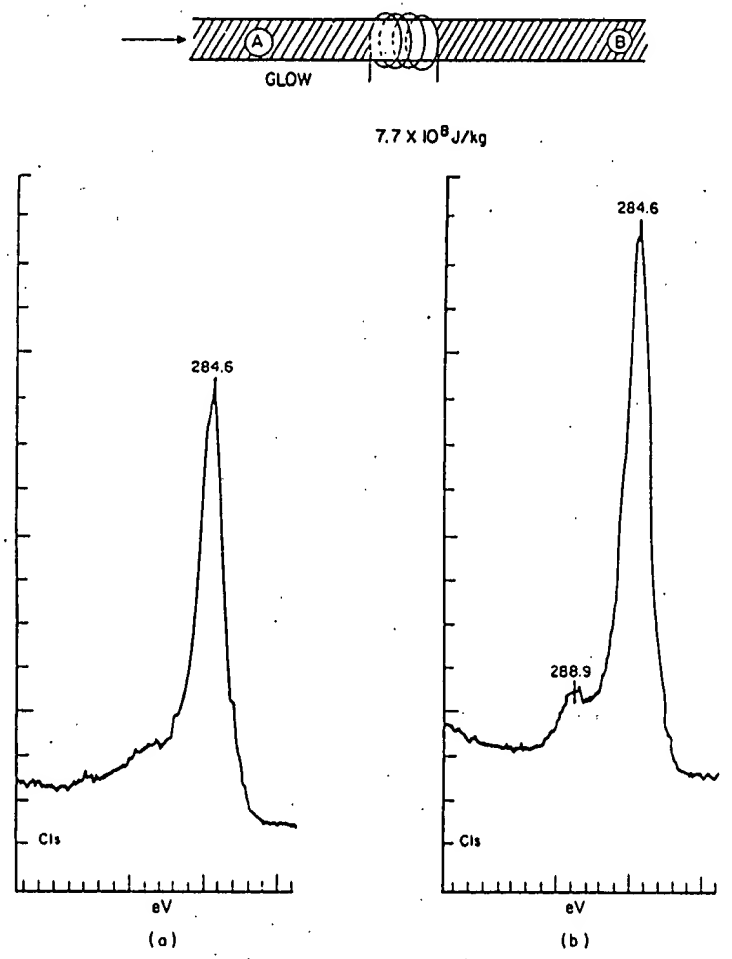

Fig. 23. Electron spectroscopy for chemical analysis C1's peaks of glow discharge polymers of tetrafluoroethylene in the same reactor shown in Fig. 22, but at the higher discharge power level of 7.7 × 10⁸ J/kg.

Characteristic shapes of the C1s peaks shown in Fig. 22 indicate that polymers that are formed at locations on the upstream and downstream sides of the rf coil are quite different when a relatively low discharge power is used. The polymer formed in the upstream side contains considerable amounts of CF_3 and CF besides the expected CF_2. This is undoubtedly due to the elemental or atomic nature of glow discharge polymerization rather than conventional molecular polymerization.

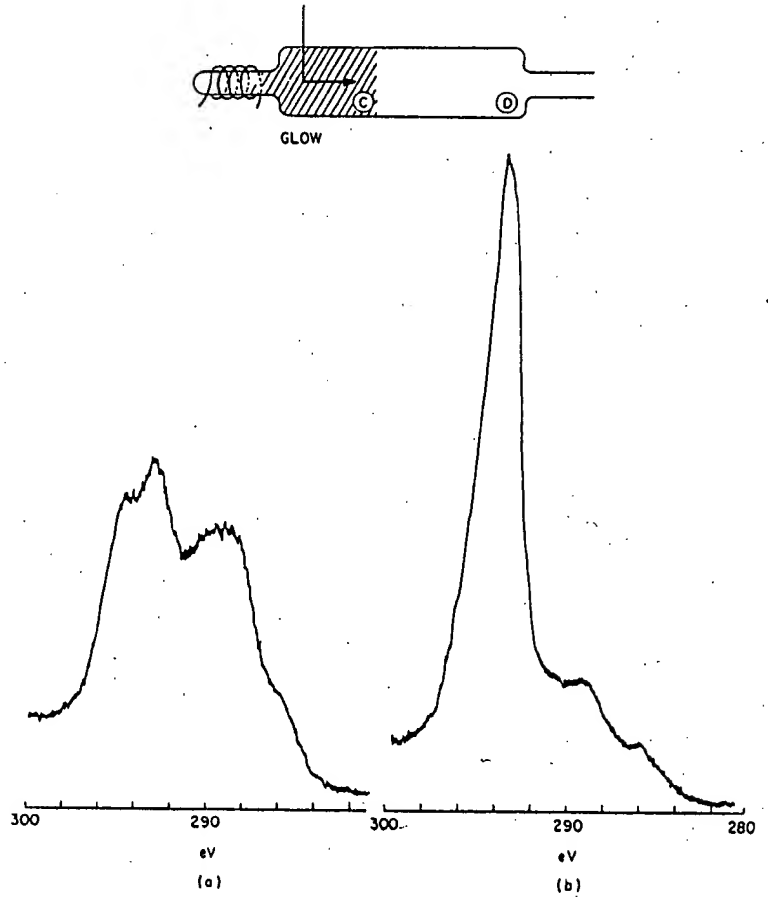

Fig. 24. Electron spectroscopy for chemical analysis C1's peaks of glow discharge polymers of tetrafluoroethylene prepared in a reactor shown in the insert: (a) at the end of the glow region and (b) at the end of the tube in the nonglow region.

The polymer formed in the downstream side of the rf coil at this low discharge power contains much less F (i.e., much smaller peaks for higher binding energy), and the peak at 284.6 eV becomes the major peak. This is a dramatic display of the effect of the energy input zone (i.e., tube directly under rf coil) on the properties of glow discharge polymers. As the discharge power is increased, this severe effect of the energy input zone expands eventually to the entire length of the tube and at a high discharge power, the polymer formed in the upstream side of the rf coil becomes similar to the polymer formed in the downstream side, as seen in Fig. 23.

When a system in which the flow does not pass through the energy input zone is used and glow discharge polymerization is carried out in the tail-flame portion of the glow discharge, the polymer formed at the downstream end of a reactor is not necessarily the same as that formed at the downstream end of a straight tube. Results given in Fig. 24 show that the polymer formed in the nonglow region, although it is located at the downstream end of a reactor, is nearly identical to the conventional polytetrafluoroethylene. This means that polymers formed under such conditions are formed mainly by *plasma-induced polymerization*.

As mentioned earlier, tetrafluoroethylene is a special starting material which reflects the effects of operationl factors in a very sensitive manner. Therefore, some effects (e.g., the increase of ablation by the increase of discharge power and by the location within a reactor) might be much smaller with other starting materials. However, the important aspects of (1) elemental or atomic polymerization and (2) system dependent polymerization, would be undoubtedly applicable to many other starting materials. These effects should be taken into consideration in designing the reactor, during processing, and in interpretation of results.

REFERENCES

1. P. de Wilde, *Ber. Dtsch. Chem. Ges.* 7, 4658 (1874).
2. A. Thenard, *C. R. Acad. Sci.* 78, 219 (1874).
3. C. S. Schoepfle and L. H. Connell, *Ind. Eng. Chem.* 21, 529 (1929).
4. J. B. Austin and I. A. Black, *J. Am. Chem. Soc.* 52, 4552 (1930).
5. E. G. Linder and A. P. Davis, *J. Phys. Chem.* 35, 3649 (1931).
6. W. D. Harkins and J. M. Jackson, *J. Chem. Phys.* 1, 37 (1933).
7. H. Koenig and G. Helwig, *Z. Phys.* 129, 491 (1951).
8. K. Otazai, S. Kume, S. Nagai, T. Yamamoto, and S. Fukushima, *Bull. Chem. Soc. Jpn.* 27, 476 (1954).
9. P. B. Weisz, *J. Phys. Chem.* 59, 464 (1955).
10. J. Goodman, *J. Polym. Sci.* 44, 551 (1960).
11. G. J. Argnette, U.S. Patent 3,061,458 (1962).
12. J. H. Coleman, U.S. Patent 3,068,510 (1962).
13. M. Stuart, *Nature (London* 199, 59 (1963).
14. A. Bradley and J. P. Hammes, *J. Electrochem. Soc.* 110, 15 (1963).
15. P. L. Kronick and K. F. Jesch, *J. Polym. Sci., Part A* 1, 767 (1963).
16. F. J. Vastola and J. P. Wightman, *J. Appl. Chem.* 14, 69 (1964).
17. E. M. DaSilva and R. E. Miller, *Electrochem. Technol.* 2, 147 (1964).
18. N. M. Bashara and C. T. Doyty, *J. Appl. Phys.* 35, 3498 (1964).
19. R. A. Connell and L. V. Gregor, *J. Electrochem. Soc.* 112, 1198 (1965).
20. T. Williams and M. W. Hayes, *Nature (London)* 209, 769 (1966).
21. R. M. Brick and J. R. Knox, *Mod. Packag.* January, p. 123 (1965).
22. K. Jesch, J. E. Bloor, and P. L. Kronick, *J. Polym. Sci., Part A-1* 4, 1487 (1966).
23. T. Willams and M. W. Hayes, *Nature (London)* 216, 614 (1967).
24. S. Tsuda, *Kobunshi* 16, 937 (1967).

25. T. Hirai and O. Nakada, *Jpn. J. Appl. Phys.* 7, 112 (1968).
26. I. Sakurada, *Macromolecules* 1, 265 (1968).
27. P. L. Kronick, *J. Appl. Phys.* 39, 5806 (1968).
28. A. T. Denaro, P. A. Owens, and A. Crawshaw, *Eur. Polym. J.* 4, 93 (1968).
29. A. R. Denaro, P. A. Owens, and A. Crawshaw, *Eur. Polym. J.* 5, 471 (1969).
30. P. L. Kronick, K. Jesch, and J. E. Bloor, *J. Polym. Sci. Part A-1* 7, 767 (1969).
31. J. R. Hollahan and R. P. McKeever, *Adv. Chem. Ser.* No. 80, p. 272 (1969).
32. M. W. Ranney and W. F. O'Connor, *Adv. Chem. Ser.* No. 80, p. 297 (1969).
33. D. D. Neiswender, *Adv. Chem. Ser.* No. 80, p. 338 (1969).
34. P. M. Hay, *Adv. Chem. Ser.* No. 80, p. 350 (1969).
35. C. Simionescu, N. Asandei, F. Dénes, M. Sandulovici, and G. Popa, *Eur. Polym. J.* 5, 427 (1969).
36. A. R. Denaro, P. A. Owens, and A. Crawshaw, *Eur. Polym. J.* 6, 487 (1970).
37. F. Dénes, C. Ungurenasu, and I. Haidue, *Eur. Polym. J.* 6, 1155 (1970).
38. K. R. Buck and V. K. Davor, *Br. Polym. J.* 2, 238 (1970).
39. J. R. Hollahan and C. F. Emanuel, *Biochim. Biophy. Acta* 208, 317 (1970).
40. A. R. Westwood, *Eur. Polym. J.* 7, 363 (1971).
41. A. R. Westwood, *Eur. Polym. J.* 7, 377 (1971).
42. R. Liepins and J. Kearney, *J. Appl. Polym. Sci.* 15, 1307 (1971).
43. H. Yasuda and C. E. Lamaze, *J. Appl. Polym. Sci.* 15, 2277 (1971).
44. S. Morita, T. Mizntani, and M. Leda, *Jpn. J. Appl. Phys.* 10, 1275 (1971).
45. R. Liepins and H. Yasuda, *J. Appl. Polym. Sci.* 15, 2957 (1971).
46. J. R. Hollahan, *Makromol. Chem.* 154, 303 (1972).
47. L. F. Thompson and G. Smolinsky, *J. Appl. Polym. Sci.* 16, 1179 (1972).
48. A. F. Stancell and A. T. Spencer, *J. Appl. Polym. Sci.* 16, 1505 (1972).
49. M. J. Vasile and G. Smolinsky, *J. Electrochem. Soc.* 119, 451 (1972).
50. L. F. Thompson and K. G. Mayhan, *J. Appl. Polym. Sci.* 16, 2291 (1972).
51. L. F. Thompson and K. G. Mayhan, *J. Appl. Polym. Sci.* 16, 2317 (1972).
52. C. T. Wendel and M. H. Wiley, *J. Polym. Sci., Part A-1* 10, 1069 (1972).
53. P. K. Tien, G. Smolinsky, and R. J. Martin, *Appl. Opt.* 11, 637 (1972).
54. R. Liepins and K. Sakaoku, *J. Appl. Polym Sci.* 16, 2633 (1972).
55. H. Yasuda, C. E. Lamaze, and K. Sakaoku, *J. Appl. Polym. Sci.* 17, 137 (1973).
56. H. Yasuda and C. E. Lamaze, *J. Appl. Polym. Sci.* 17, 201 (1973).
57. M. Duval and A. Theoret, *J. Appl. Polym. Sci.* 17, 527 (1973).
58. H. Kobayashi, A. T. Bell, and M. Shen, *J. Appl. Polym. Sci.* 17, 885 (1973).
59. H. Yasuda and C. E. Lamaze, *J. Appl. Polym. Sci.* 17, 1519 (1973).
60. H. Yasuda and C. E. Lamaze, *J. Appl. Polym.* Sci. 17, 1533 (1973).
61. M. M. Millard, J. J. Windle, and A. E. Pavlath, *J. Appl. Polym. Sci.* 17, 2501 (1973).
62. H. Yasuda, *Appl. Polym. Symp.* No. 22, p. 241 (1973).
63. J. R. Hollahan and T. Wydeven, *Science* 179, 500 (1973).
64. R. F. Baddour and R. S. Timmins, eds., "The Application of Plasmas to Chemical Processing." MIT Press, Cambridge, Massachusetts, 1967.
65. F. K. McTaggart, "Plasma Chemistry in Electrical Discharges." Elsevier, Amsterdam, 1967.
66. R. F. Gould, ed., *Adv. Chem. Ser.* No. 80 (1969).
67. M. Venugopalan, ed., "Reactions Under Plasma Conditions," Wiley (Interscience), New York, 1971.
68. J. H. Hollahan and A. T. Bell, eds., "Techniques and Application of Plasma Chemistry." Wiley, New York, 1974.
69. M. Shen, ed., "Plasma Chemistry of Polymers." Dekker, New York, 1976.
70. H. Yasuda and T. Hsu, *Surf. Sci.* 76, 232 (1978).